Understanding potential reservoir interconnectivity between two contemporaneous volcanoes during the onset of cone-building activity, Middle Sister and South Sister, Central Oregon

Undergraduate Thesis
By
Emma Calvert
June 2023

Abstract

Klah Klanee (Three Points) is located in the central Cascades near Bend, Oregon. The Three Sisters Volcanic Complex (TSVC) lies at a tectonically complex intersection of the Cascade Subduction Zone, the Basin and Range Province, and the High Lava Plains. The TSVC is a compositionally diverse volcanic field consisting of four stratovolcanoes and numerous periphery cones and vents. Middle Sister and South Sister are the youngest of the stratovolcanoes and they share a largely contemporaneous and semi-alternating episodic eruptive history. These parallel histories could indicate a complex, interconnected magmatic root system within the crust below the TSVC and the surrounding area.

To determine the extent of interconnectivity between these two peaks, whole rock chemistry, mineral chemistry, and petrography were utilized to compare two temporally related andesites on the west flanks of Middle Sister and South Sister. The andesites, andesite of Lost Creek Glacier (alg) and andesite of Linton Creek (alc), erupted ca. 27 ka and have nearly identical whole rock chemistry, mineral types, and mineral abundances. Origins of these andesites were determined using mineral populations based on mineral textures and chemistry. South Sister unit alg contains three plagioclase populations, four clinopyroxene populations, five orthopyroxene populations, and one olivine population. Middle Sister unit alc contains two plagioclase populations, three clinopyroxene populations, three orthopyroxene populations, and two different types of enclaves. The enclaves identified consist of an olivine and plagioclase-bearing type and orthopyroxene and plagioclase bearing-type. Each of these types carries its own unique crystal cargo not found in the host, alc. Therefore, the enclaves were determined to be lithic fragments incorporated during the final stages before eruption. The andesites, alc and alg, appear to share two plagioclase populations, two clinopyroxene populations, and two orthopyroxene populations. Several mineral populations found in alg commonly have fine reaction rims that are not present in the equivalent alc populations, although other than this slight variation, these populations are interpreted to be the same.

Plagioclase mineral chemistry suggest that the andesites erupted on the west flanks of these two volcanoes share two sources, one at depth (higher An plagioclase, populations 1a and 1b) and a second, shallower source (moderate An plagioclase, population 2). Pyroxene mineral populations failed to clearly constrain potential sourcing due to significant overlap in compositions; further trace element analysis is required. Overall, alg and alc contain many of the same populations with similar chemistry and textures, indicating these magmas likely share a magmatic source(s). However, unit alg contains a much more complicated crystal cargo with more complex clots and increased mineral populations across every phase. It is likely that prior to eruption alg interacted with an additional magma reservoir(s) (e.g., mush) that alc did not encounter.

Acknowledgements

I would like to acknowledge that the work shown in this report is based on a collection of samples from Klah Klahnee, the "Three Points", or Three Sisters, Oregon, with a particular focus on Middle Sister and South Sister. Klah Klahnee are located on the ancestral homelands of the Confederated Tribes of Warm Springs, which includes the Wascoes (Chinookan-speaking), Warm Springs (Sahaptin-speaking), and Paiutes (Shoshonean-speaking), who have lived in and around this area from time immemorial. Please join me in expressing our deepest respect and gratitude for our indigenous neighbors, thank them for their stewardship of the beautiful land that we are fortunate to study and for their enduring care and protection of our shared lands and waterways.

This project would not have been possible without funding from the Jack Kleinman Memorial Fund for Volcano Research, Central Oregon Geoscience Society Grant, Western Washington University Advance for Research, and Western Washington University Research and Sponsored Programs Grants. I would like to extend my deepest appreciation to the organizations supporting this project and my continued growth in the scientific community.

I would especially like to thank my advisor Dr. Mai Sas whose guidance and support throughout this process has fostered immense growth and development of my scientific and critical thinking skills. Throughout my time on this project, you have shown great humility, patience, and insight into what it means to be an advisor, educator, academic, and person. Your hard work, selflessness, and persistence has made you into a role model in the eyes of many. I am extremely fortunate to have you as an advisor and I cannot help but express my deepest gratitude.

To my fellow colleagues- James Peale, Sean Halstead, Alex Newsom, and Madelyn Cook it has been a pleasure learning alongside you. I look forward to seeing what you all accomplish in your future pursuits.

Special thanks go out to Dr. Kristina Walowski, Dr. Nathan Anderson, and the ERVPT group for creating a space for me to further my academic growth and providing me with much-needed guidance.

Finally, thank you to all my friends and family for supporting me throughout this process. I could not have done it without you.

Table of Contents

Table of Figures

1. Introduction

The Three Sisters Volcanic Complex (TSVC) consists of an intricate network of eruptive products. These products are a likely indication of the much more complex magmatic root system within the crust below the TSVC and the surrounding area. This magmatic root system is made up of a series of magma bodies throughout the crust with varying depths and compositions, and each of these magma bodies have their own distinct crystal cargo and chemical composition (Cashman et al. 2017). These traits allow the ability to retrace specific crystal's eruptive history (Cashman et al. 2017). This is particularly important because many intermediate magmas are often thought to be the product of magma mixing and hybridization (Kent 2014). The wide range of eruptive products at the TSVC create an ideal environment to investigate magma origins, mixing, and differentiation processes that can then be applied to similar volcanic systems worldwide.

The major recreation and population center of Bend, Oregon lies at the feet of these volcanic giants, creating a greater need for better hazard assessments in this area. This complex contains a wide range of magma compositions, which leads large discrepancies in eruption styles and eruption related hazards. The TSVC is a complex area of study with four stratovolcanoes, North Sister, Middle Sister, South Sister, and Broken Top, all residing within the main reaches of the complex in Three Sisters Wilderness area. Of the four stratovolcanoes, Middle Sister and South Sister, which are the youngest, share an episodic and interconnected history (Calvert et al., 2018; Fierstein et al., 2011; Hildreth et al., 2012).

This project focuses on two intermediate lava units, the Andesite of Linton Creek (alc) from Middle Sister and the Andesite of Lost Creek Glacier (alg) from South Sister (Hildreth et al., 2012), to determine (1) which magmatic processes, mixing or fractional crystallization, dominated the formation of each lava, and (2) how similar the two units may be, which can have implications for how the two volcanoes might be connected at depth during early stages of cone-building volcanic activity. The two andesites were chosen because they are temporally related (ca. 27 ka), both erupted west of their respective volcanic edifice, and share similar whole rock chemistry (Calvert et al., 2018; Fierstein et al., 2011; Hildreth et al., 2012). Importantly, these eruptions occurred at a period where eruptive activity significantly increased at Middle Sister and South Sister. During this time, these two peaks saw a compositional shift to more mafic lavas.

2. Geologic Setting

2.1. Tectonic Setting

The TSVC lies at a tectonically complex intersection of the Cascade Arc, the Basin and Range extensional province, and the High Lava Plains (Fig. 1). The Cascade volcanic arc is a 1,300 km long stretch in western North America, consisting of many notable peaks such as Tahoma (Mount Rainier), Wy'East (Mount Hood), Loowit (Mount St. Helens), and many others. The Pacific Northwest is well known for subduction related magmatism that produced these notable peaks. The present-day arc is the result of the accretion of the Siletzia oceanic plateau, the remains of which comprise a significant amount of the Oregon-Washington coast ranges, likely with some remains below the subsurface (Leeman, 2020). Slab seismicity occurs predominantly in the northern and southern parts of the arc, with the down-going slab at a depth of ~100 km (Weaver and Baker, 1988). The Nootka and Blanco Fracture Zones separate the subducting Explorer, Juan de Fuca, and Gorda microplates, subducting under the North American Plate at a rate ranging from 30 mm/yr at the southern end and 45 mm/yr at the northern end (Wilson, 1993). The arc is also one of the warmest modern subduction zones, with accelerated slab dehydration and low flux of slab derived fluids (Leeman, 2020). The resulting volcanic activity for this arc creates a near linear belt of stratovolcanoes that extends from northern California up through Canada.

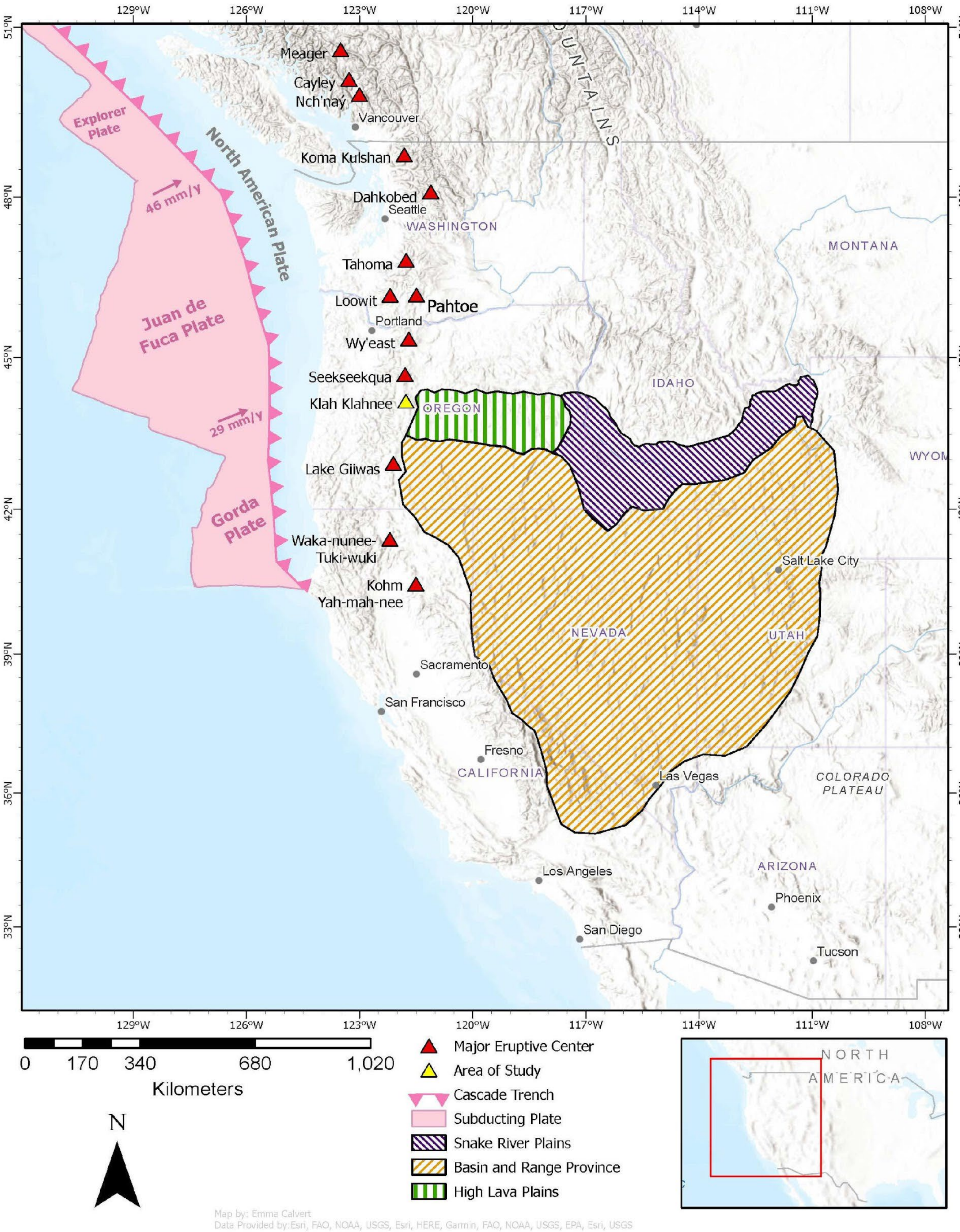

Figure 1. Terrain map of northern México through southern Canada, displaying regional tectonic influence in the TSVC area. Pink region shows the oceanic plates subduction beneath the North America Plate. The Basin and Range Extensional Province is shown in yellow; the High Lava Plains are shown in green, and the Snake River Plain is shown in purple. Triangles indicate locations of major Cascade volcanoes, with the TSVC highlighted in blue. The volcanoes from north to south are: Mount Meager, Mount Cayley, Nch'naý (Mount Garibaldi), Koma Kulshan (Mount Baker), Dhakobed (Glacier Peak), Tahoma (Mount Rainier), Pahtoe (Mount Adams), Loowit (Mount St. Helens), Wy'east (Mount Hood), Seekseekqua (Mount Jefferson), Klah Klahnee (Three Sisters), Lake Giiwas (Crater Lake), Waka-nunee-Tuki-wuki (Mount Shasta), Kohm Yah-mah-nee (Mount Lassen). Subduction rates are from Wilson (1993*). Physiographic provinces adapted after MacLeod et al. (1995) and Shoemaker and Hart (2002).*

The Basin and Range Extensional Province and the High Lava Plains are a prime example of the tectonic complexity of this region. The Basin and Range physiographic region is an extensional province encompassing much of eastern Oregon, Nevada, and western Utah. This extensional province is defined by a series of normal faults creating an alternating sequence of narrow mountains ranges and low basins or valleys (Eaton, 1982). The central Oregon region consists of multiple episodes of Oligocene and younger volcanism, which has produced a westward trend in bimodal silicic-mafic volcanism separate from the Yellowstone-Snake River Plain provinces, known as the High Lava Plains (Jordan et al., 2004). The High Lava Plains consists of Late Miocene and younger volcanics and is approximately 90 km wide and 275 km long (Ford et al., 2013). The High Lava Plains are situated just east of the TSVC in the backarc region of the Cascade arc, and is thought to be affected by slab rollback, steepening, and backarc extension (Fitton et al., 1991; Carlson and Hart, 1987). This region is bordered by the Cascade arc and the extensional Basin and Range province, and consists of ignimbrites, volcaniclastic sediment, and basalt flats (Jordan et al., 2004).

2.2. The Three Sisters Volcanic Complex (TSVC)

The central reach of the Cascade arc contains at least 466 Quaternary volcanoes (Hildreth et al., 2012), several of which are located in the TSVC. Volcanic structures within the mapped complex consist of three stratovolcanoes, eroded mafic shields, and flank volcanoes (Calvert et al., 2018). The main feature within the TSVC is a series of north-south trending, glaciated stratovolcanoes that dominate a 20-km stretch of the central Cascades near Bend, Oregon (Fig. 2). Additional notable volcanic structures dot the horizon to the south and southwest, consisting of Broken Top, Mount Bachelor and Newberry Volcano. Although only a handful of active glaciers remain today, the Three Sisters themselves have been revenged by glaciers several times since the Pleistocene, and there is evidence of a broad mountain ice sheet covering this region of the Cascade crest (Calvert et al., 2018). Evidence of glaciation lies within the deep cirques on North Sister and intricate moraine systems within the complex (Fig. 3). Glaciers within the TSVC have retreated up these peaks, revealing eruptive units that exhibit interaction with ice, which is indicated by glassy and quenched margins and flows confined to ridges between glaciated valleys (Hildreth et al., 2012, Calvert et al., 2018).

While similar in appearance and elevation, the main stratovolcanoes, North Sister, Middle Sister, and South Sister, are compositionally diverse, containing populations of basaltic andesite, andesite, dacite, and rhyolite lavas (Hildreth et al., 2012). North Sister (10,085 ft; 3,074 m) is an older, predominantly mafic edifice that has been heavily deformed by glaciers dating back to the Pleistocene (Hildreth et al., 2012). In contrast, Middle Sister and South Sister are younger and largely contemporaneous and were rapidly built during the same eruptive period mostly from ca. 37-14 ka (Calvert et al., 2018).

Middle Sister (10,047 ft; 3,157 m) is the central peak of the three siblings (Fig. 4) and is also the youngest cone; the current peak was built mainly between 25 and 18 ka, but cone building lasted at least from 48 to 14 ka (Hildreth et al., 2012). This edifice has erupted a range of compositions from basaltic-andesite, to andesite, to dacite, and even one rhyolite, from its central edifice and flank vents (Hildreth et al., 2012). Many of the andesite-dacite lavas met glaciated centers in the Middle Pleistocene (Hildreth et al., 2012). There was a long period of inactivity from ca. 37 to 27.5 ka prior to the modern growth of Middle Sister (Hildreth et al., 2012). This modern period of growth largely began with andesitic eruptions and shifted to basaltic-andesite and dacite bimodalism around 21.5 ka (Calvert et al. 2018). The unit of study from Middle Sister is the andesite of Linton Creek (alc) (Fig. 4).

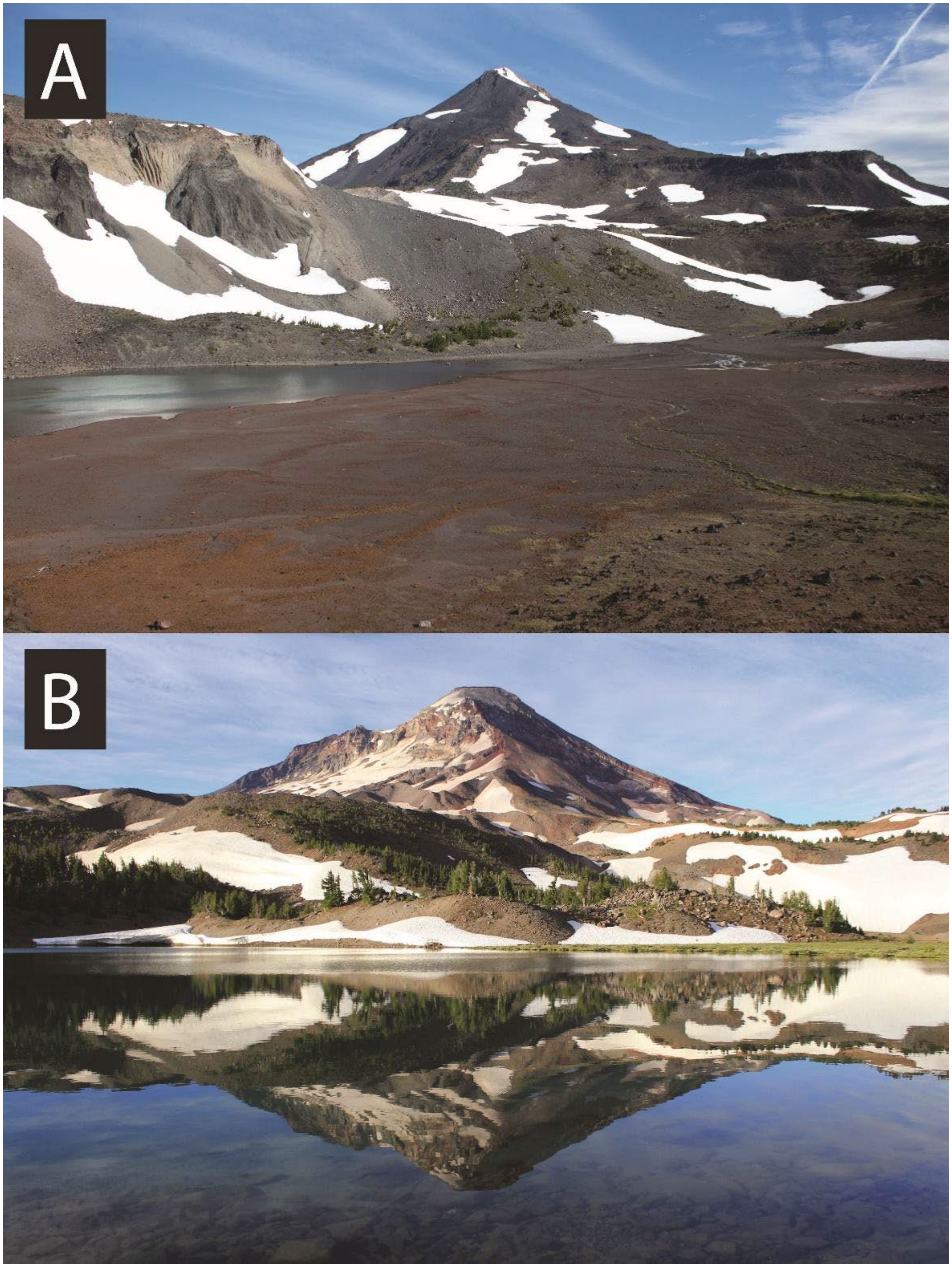

Figure 2. (A) South face of Middle Sister summit. Photo taken from saddle between Middle Sister and South Sister summits. (B) North Face of South Sister summit. Image taken from Camp Lake.

South Sister is the highest (10,358 ft; 3,062 m) and southernmost peak of the Three Sisters (Fig.4). Previously believed to be the youngest, South Sister is currently believed to be largely contemporaneous with Middle Sister. Between 50 to 30 ka, eruptions from South Sister were predominantly high silica, with rhyolitic lava flows and domes (Hildreth et al., 2012). South Sister experienced an increase in intermediate magmatism from 35 to 23 ka, and this period saw dacites and rhyodacites, as well as the construction of an andesitic cone (Hildreth et al., 2012). This eruptive period culminated at 22 ka with the building of a steeply dipping summit cone and a final basaltic-andesite flow draping the crater (Hildreth et al., 2012). More recent eruptions exhibit a compositional reversal with two flank rhyolitic eruptions at 2.2 and 2.0 ka (Hildreth et al., 2012). The unit of study from South Sister is the andesite of Lost Creek Glacier (alg) (Fig. 4).

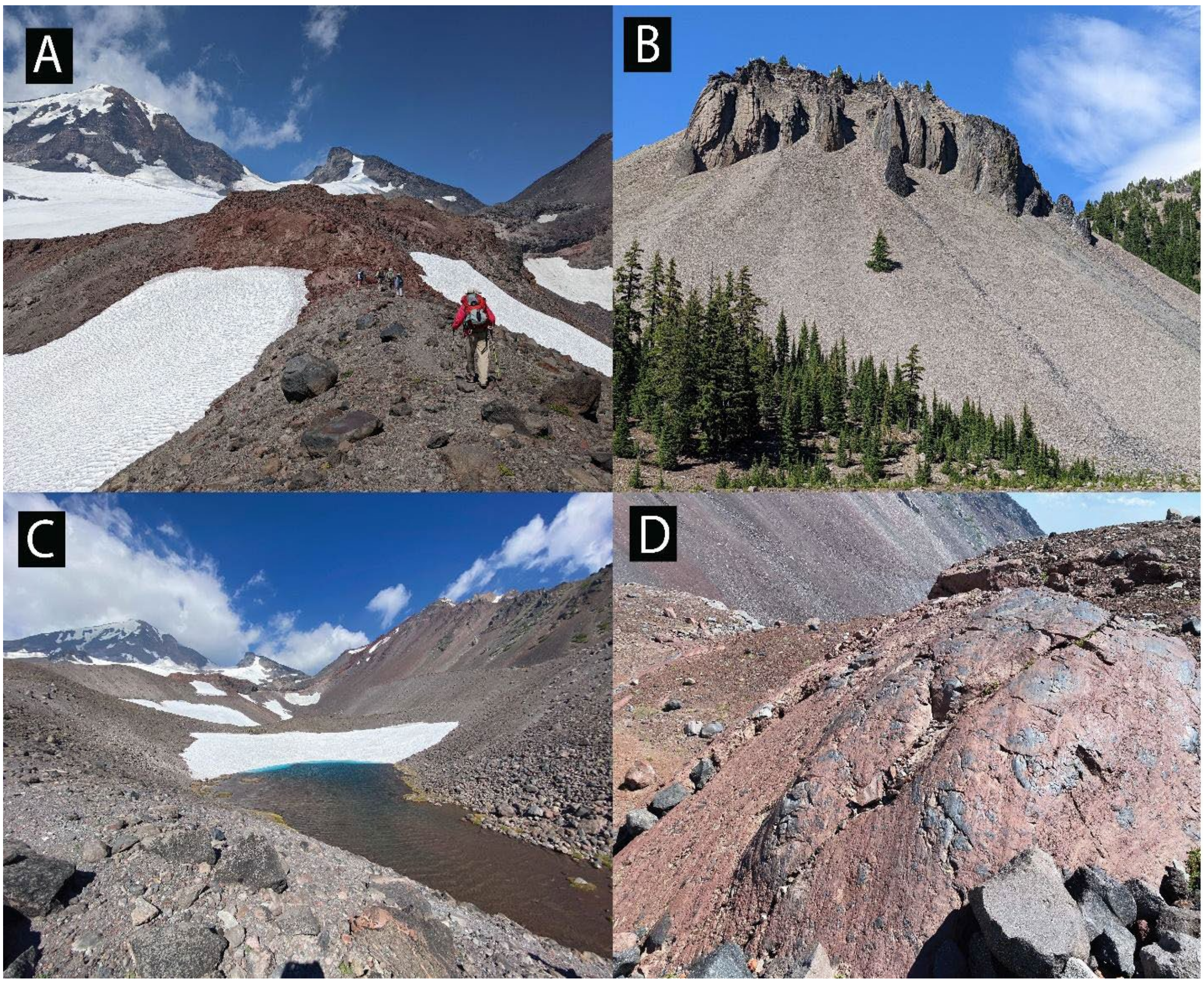

Figure 3. (A) In the foreground are multiple lava units disrupted by glacial activity and a colleague walking along the ridge of a glacial moraine. In the background is the current extent of Hayden Glacier. In the distance is the Middle Sister summit to the left and Black Hump in the middle. (B) Quenched margin displaying ice interactions. (C) U-shaped valley between moraines as one approaches the Hayden Glacier. (D) Striations on small outcrop east of the Hayden Glacier.

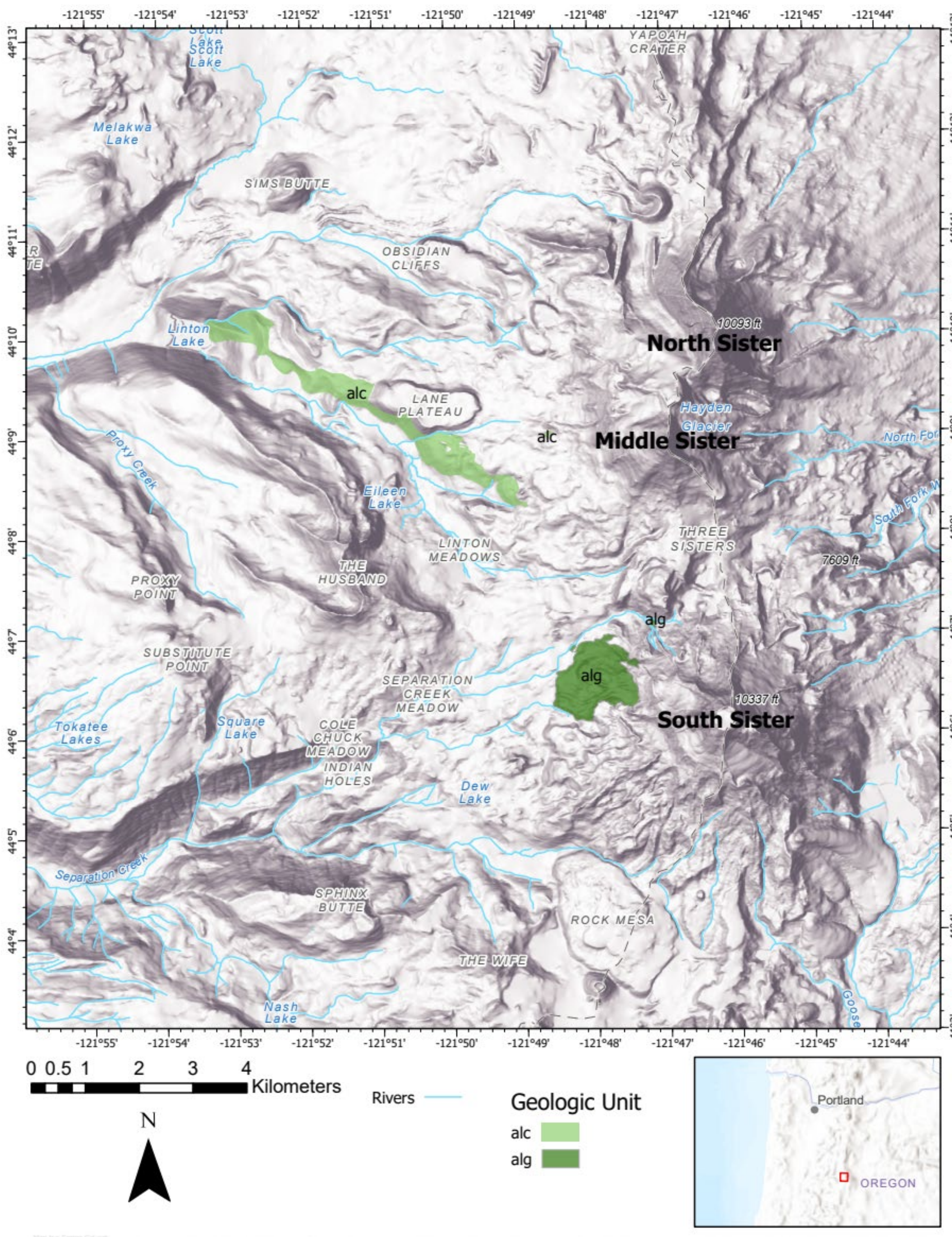

Figure 4. Terrain map of the TSVC area. The names of the three main stratovolcanoes, North Sister, Middle Sister, and South Sister are aligned with their respective peaks. Unit alg (Andesite of Lost Creek Glacier) is shown in green, and unit alc (Andesite of Linton Creek) is shown in orange. Data are from Hildreth et al. (2012).

3. Methods

3.1. Sample prep

Samples were collected between the summers of 2021-2022. Sample names and locations can be found in Table 1. First, samples were cut into billets and sent to Burnham Petrographic and Wagner Petrographic to be made into thin and (30 µm) and thick (100 µm) sections, respectively. Thin sections were used for sample characterization based on petrographic observations while thick sections were used for sample characterization and geochemical analysis. To easily navigate around the samples, all sample slides were scanned.

Table 1. Sample location, date, ID, and unit name of each newly collected sample considered in this study.

Sample ID	Unit	lat	long	elev	Date
TSO-029	alc	44.13794	-121.81899	1953	24-Jul-21
TSO-030	alc	44.14020	-121.82087	1954	24-Jul-21
TSO-032	alg	44.11558	-121.79956	2049	24-Jul-21
TSO-075.1	alc	44.13778	-121.81731	1991	7-Aug-22
TSO-076	alc	44.14027	-121.82048	1973	7-Aug-22
TSO-077	alc	44.13967	-121.82094	1972	7-Aug-22

3.2. Whole Rock Geochemistry

Whole rock major, minor, and some trace element analyses were performed by Hamilton Analytical Lab at Hamilton College, Clinton, New York. Analyses were completed using a Thermo ARL Perform'X X-ray fluorescence spectrometer (XRF) with an accelerating voltage of 45 kV. Samples were chipped and ground into a powder (~3.5 gm in diameter) using a tungsten carbide or alumina ring mill. Next, the powder was blended with Li-tetraborate flux (Merck Spectromelt A-10) in a vortex mixer and fused with graphite (Mersen grade UF-4S) at 1000°C to produce pellets. The pellets were cleaned, reground, and refused, then cleaned with ethanol.

Additional trace element concentrations were obtained on micro-polished chips cut from the pellets using laser ablation inductively-coupled plasma mass spectrometry (LA-ICP-MS) on a Photon Machines Analyte 193 laser ablation system coupled to a Varain 820 ICP-MS. Analytical settings followed the methods of Conrey et al. (2019). Whole rock data are listed in Table A1.

3.3. Petrography and SEM

A Leica DM750P microscope at Western Washington University (WWU) was used to complete petrographic characterization and identify textural populations. The scanning electron microscope (SEM) was used for additional sample characterization, as well as identification of ideal and representative minerals for geochemical analysis. The SEM used is a JEOL JSM-7200F Field Emission SEM at WWU. This SEM is equipped with a Schottky Field Emission detector, a 150 mm2 Oxford X-Max energy dispersive X-ray spectroscopy (EDS) detector, and a retractable backscatter electron (BSE) detector. This instrument was used with a working distance of 10 mm and an accelerating voltage of 12 (kV). A summary of sample petrography is included in Table A2.

3.4. EMPA

The Cameca SX-100 electron microprobe (EMPA) at Oregon State University was utilized for major and minor element analysis. This EMPA is equipped with spectrometers, five of which are wavelength dispersive and one energy dispersive. Plagioclase was analyzed with an accelerating voltage of 15 kV, a beam size of 5 µm, and a current of 30 nA. In plagioclase Si, Al, Na, and Ca were analyzed for 10 seconds, K and Ti for 30 seconds, and Mg and Fe were analyzed for 60 seconds each. Olivine was analyzed with an accelerating voltage of 15 kV, beam size of 1 µm, and current of 50 nA. In olivine Si, Mg, Fe, and Na were analyzed for 10 seconds, Mn was analyzed for 20 seconds, and Ca, Ni, Cr, and Al were analyzed for 60 seconds each. Clinopyroxene and orthopyroxene were analyzed with an accelerating voltage of 15 kV, beam size of 1 µm, and current of 30 nA. In pyroxene, Si was analyzed for 10 seconds, Fe, Na, Mg were analyzed for 20 seconds, and Al, K, Mn, Ti, Cr, and Ca were analyzed for 30 seconds each. Calibration standards and their measured concentrations are included in Tables A3-A6.

4. Results

4.1. Sample Descriptions

4.1.1. Andesite of Lost Creek Glacier (alg), South Sister

The andesite west of Lost Creek Glacier (alg) is a tree covered unit on the west flank of South Sister (Fig. 4). This unit is situated approximately 1-3 km from the summit of South Sister, cropping from neoglacial moraines of Lost Creek Glacier down to Separation Creek (Hildreth et al., 2012). The flows are 2-10 m thick and have been glacially eroded into stairstep benches that display a blocky to platy breakage pattern. Weathered surfaces of this unit are reddish brown to tan color, while fresh surfaces are light to medium grey. The sampled outcrop is approximately 8 m high and 10 m across (Fig. 5). In hand sample, alg is medium to light grey with 15-20% phenocrysts.

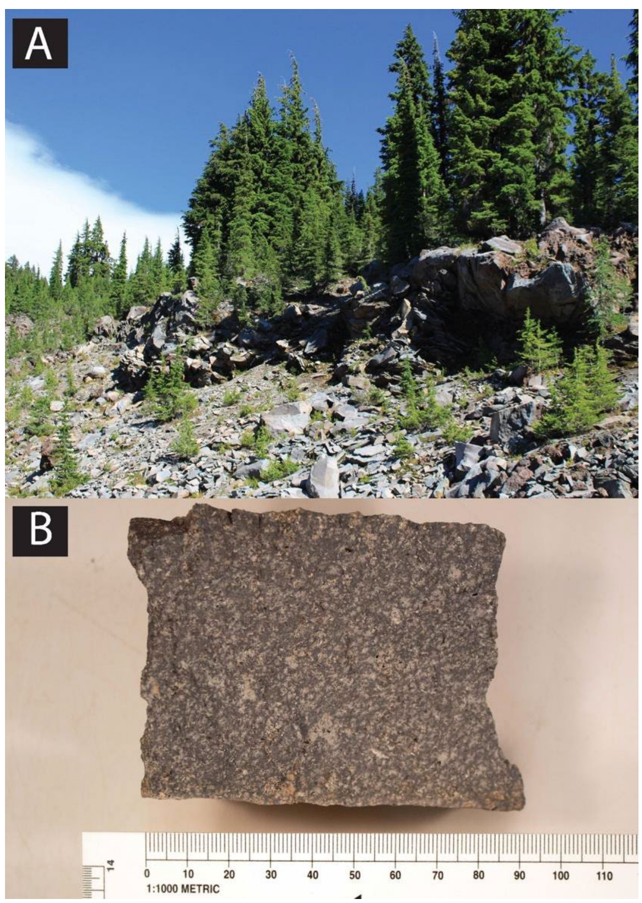

Figure 5. (A) Alg on the west face of South Sister displaying stairstep to blocky topographic breakage patterns. (B) Light grey hand sample of alg approximately 90 mm across and 60 mm in length.

Phenocrysts in alg consist of roughly ~9% plagioclase, ~2.5% clinopyroxene, 1% orthopyroxene, and ~2.5% oxides, both as single crystals and in clots (Fig. 6). Two types of clots were identified: (1) plagioclase, clinopyroxene, orthopyroxene, and oxides (≤4.5 mm in diameter), and (2) the more common plagioclase and oxides (≤2.5 mm in diameter). Plagioclase phenocrysts are 0.25-2.5 mm in diameter, predominantly tabular but some are bladed and randomly oriented. Plagioclase is commonly found in clots with other plagioclase and oxides or in clots with plagioclase, clinopyroxene, orthopyroxene, and oxides, but single phenocrysts are also present. Individual crystals are euhedral but in clots, they are subhedral to euhedral. Oscillatory zoning, polysynthetic twins, and no sieving to coarse sieving are all present in individual crystals and crystals found in clots. Clinopyroxene phenocrysts are 0.25-1 mm in diameter, euhedral to subhedral, equant to blocky, randomly oriented, and unzoned. Clinopyroxene crystals commonly have polysynthetic twinning and no sieving. Clinopyroxene is mostly found in clots with plagioclase, clinopyroxene, orthopyroxene, and oxides, but some crystals are found as single phenocrysts. Orthopyroxene phenocrysts are 0.25-0.75 mm in diameter, blocky to equant, euhedral to anhedral, and exhibit no zoning or twining. Orthopyroxene crystals range from unsieved to very coarsely sieved. Most commonly, orthopyroxene is present in plagioclase, clinopyroxene, and orthopyroxene clots, although a few single phenocrysts are present. Oxides are 0.25-0.75 mm in diameter, equant, subhedral, and are commonly present in clots with plagioclase, clinopyroxene, orthopyroxene, and other oxides, or in clots with plagioclase and other oxides, although there are as individual crystals as well, and some are crystals found as inclusions in pyroxene. The matrix of this unit is holocrystalline, and out of the visible crystals, approximately 90% are euhedral plagioclase that are narrow elongate crystals and are locally oriented. Approximately 9% are subhedral oxides that are equant and rounded. The remaining approximately 1% are anhedral pyroxenes that are rounded. There was no twinning or zoning identified in any groundmass crystals.

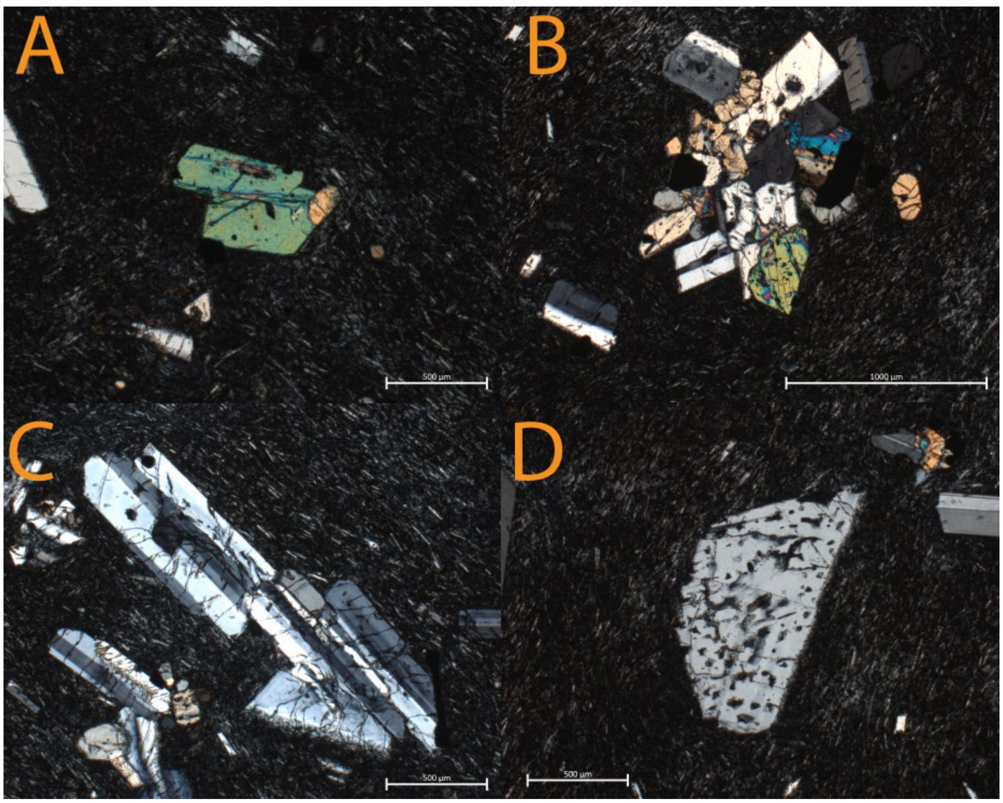

Figure 6. Petrographic images of alg. (A) Solitary clinopyroxene. (B) Representative clot with plagioclase, clinopyroxene, and orthopyroxene. (C) Representative plagioclase clot. (D) Large, sieved plagioclase.

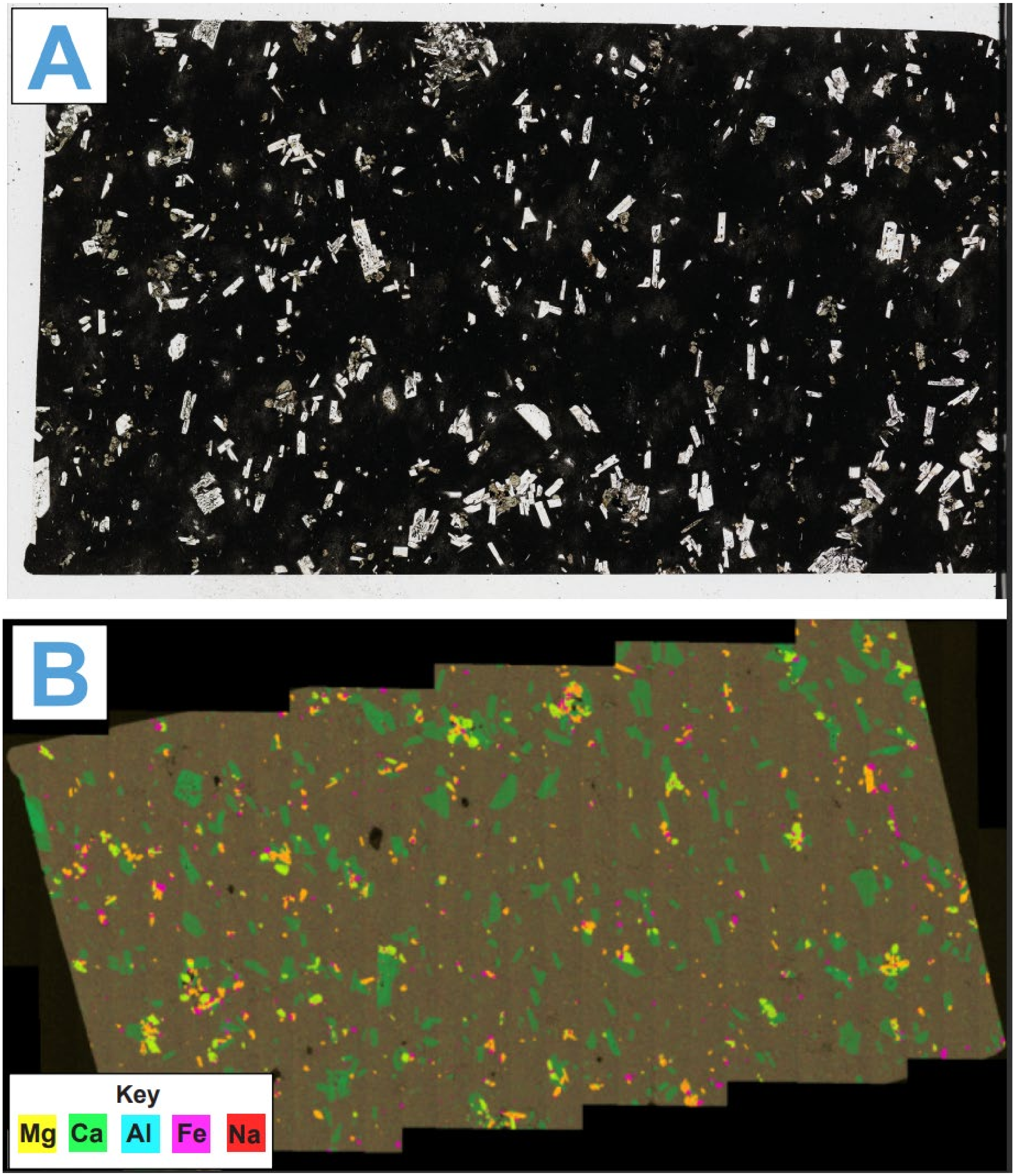

Figure 7. (A) Plain light scan of 032A (alg) thick section. (B) EDS Map of 032A (alg) thick section.

4.1.2. Andesite of Linton Creek (alc), Middle Sister

The andesite of Linton Creek (alc) is a tree covered unit that is approximately 2 km west from the Middle Sister summit at its highest point (Fig. 4) (Hildreth et al., 2012). This unit displays stairstep topography and margins with many chunk jointing or columnar jointing that are suggestive of direct ice contact during emplacement (Hildreth et al., 2012). The upper portion of outcrop, where samples were collected, is a boulder field that is split by a creek and is approximately 20-30 m in height, but the irregular topography and tree cover make it difficult to determine the full extent of the outcrop (Fig. 8). This outcrop weathers reddish brown and has medium to dark grey fresh surfaces. This unit contains enclaves, which appear in higher abundance north of the creek. The enclaves are described in detail in Section 4.1.3. This outcrop weathers dark grey to black, displays a chuck jointing pattern, and appears to have a quenched matrix. In the quenched outcrop there is less variation in size and types of enclaves, but enclaves are still present. In hand sample, alc is dark grey to black with 15-20% phenocrysts.

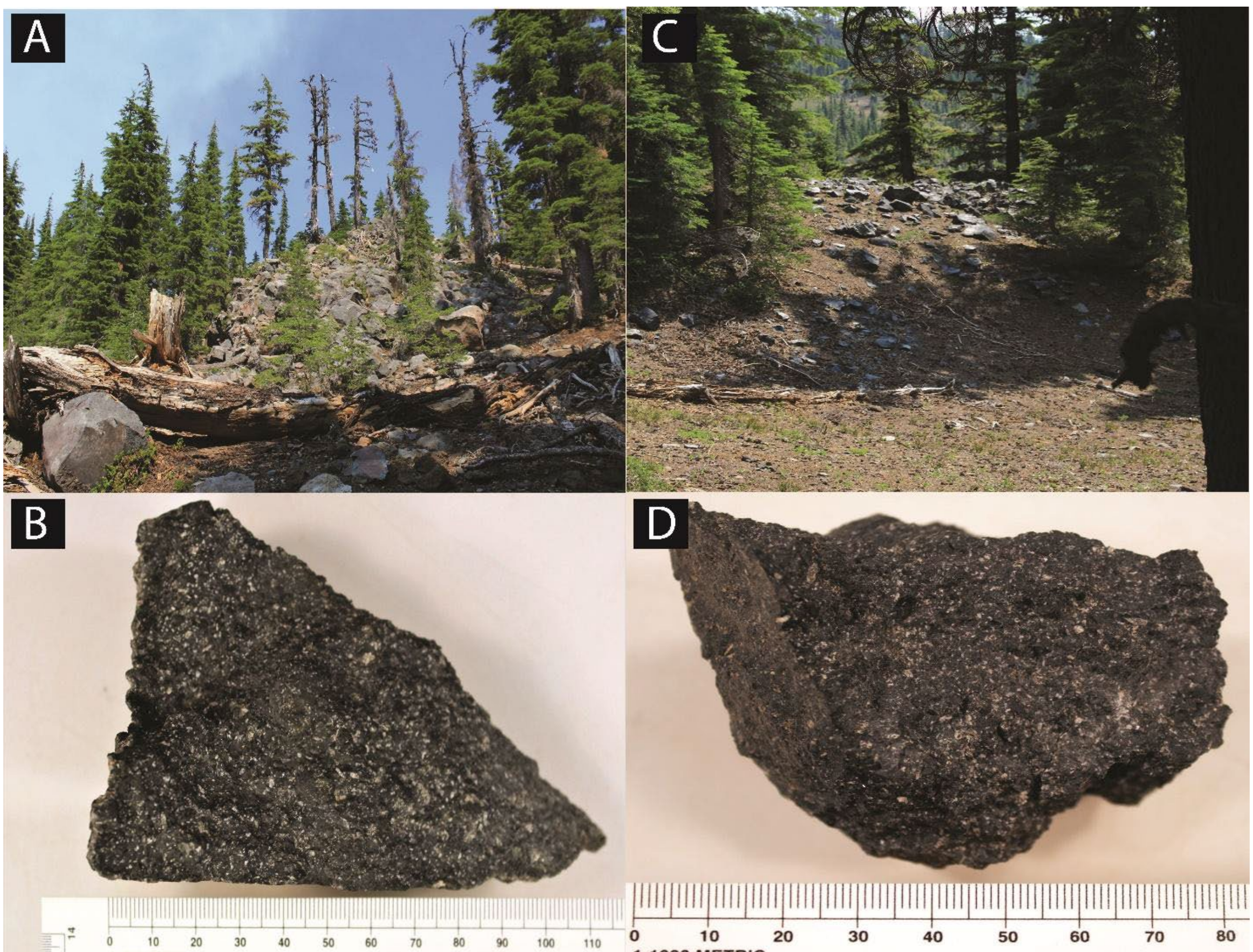

Figure 8. (A) Displays west facing upper portion of alc outcrop where abundant enclaves were noted. (B) Corresponding hand sample from upper outcrop. Hand sample is dark grey to black approximately 110 mm across and 70 mm in length. (C) Displays west facing lower portion of alc. This outcrop represents the quenched margin of this unit indicating ice interactions. (D) Quenched hand sample from lower outcrop. Dark grey to black approximately 80 mm in length and 60 mm across.

Phenocrysts are ~9% plagioclase, ~3% clinopyroxene, ~2% oxides, and ~1% orthopyroxene (Fig. 9). Four types of clots were identified: (1) plagioclase, clinopyroxene, orthopyroxene, and oxides (≤3.5 mm in diameter), (2) plagioclase and oxides (≤2 mm in diameter), (3) plagioclase, clinopyroxene, and oxides (≤2.5mm in diameter), and (4) clinopyroxene, orthopyroxene, and oxides (≤2 mm in diameter). Plagioclase phenocrysts are 0.25-4 mm in diameter, euhedral, tabular to equant to elongate, and randomly oriented. Plagioclase phenocrysts have polysynthetic twinning and oscillatory zoning, which are found in both individual crystals and in clot crystals. Most plagioclase crystals are unsieved, although some individual crystals are coarsely sieved. Plagioclase is commonly found as single phenocrysts or plagioclase and oxides clots, and sometimes can be found in plagioclase, clinopyroxene, orthopyroxene, and oxides clots. Clinopyroxene phenocrysts are 0.25-1 mm in diameter, euhedral, equant to blocky, and randomly oriented. Some clinopyroxene crystals have slight zones but are otherwise not twinned or sieved. Clinopyroxene crystals are most commonly found in clots with plagioclase and other clinopyroxene, and some can also be found in clinopyroxene, orthopyroxene, plagioclase, and oxides clots. Some single phenocrysts of clinopyroxene are present. Orthopyroxene phenocrysts are 0.25-0.5 mm in diameter, euhedral to subhedral, and blocky. Orthopyroxene crystals are also unzoned, unsieved, and untwinned. Orthopyroxene is most commonly found in orthopyroxene, clinopyroxene, and oxides clots, as well as in orthopyroxene, plagioclase, clinopyroxene, and oxides clots. Some sparse single phenocrysts of orthopyroxene are also present. Oxides are 0.25-0.5 mm in diameter, subhedral, equant to blocky, and most commonly present as single phenocrysts. However, they are also commonly found in plagioclase, orthopyroxene, and oxides clots, in plagioclase, orthopyroxene, and oxides clots, and in clinopyroxene, orthopyroxene, and oxides clots. The matrix is ~70% cryptocrystalline and ~30% holocrystalline; out of the visible crystals, ~95% are euhedral, narrow, elongate plagioclase crystals that are locally oriented. Approximately 4% subhedral, equant, rounded, oxides. The remaining ~1% are anhedral, rounded mafic minerals. No twinning or zoning was identified in any groundmass crystals.

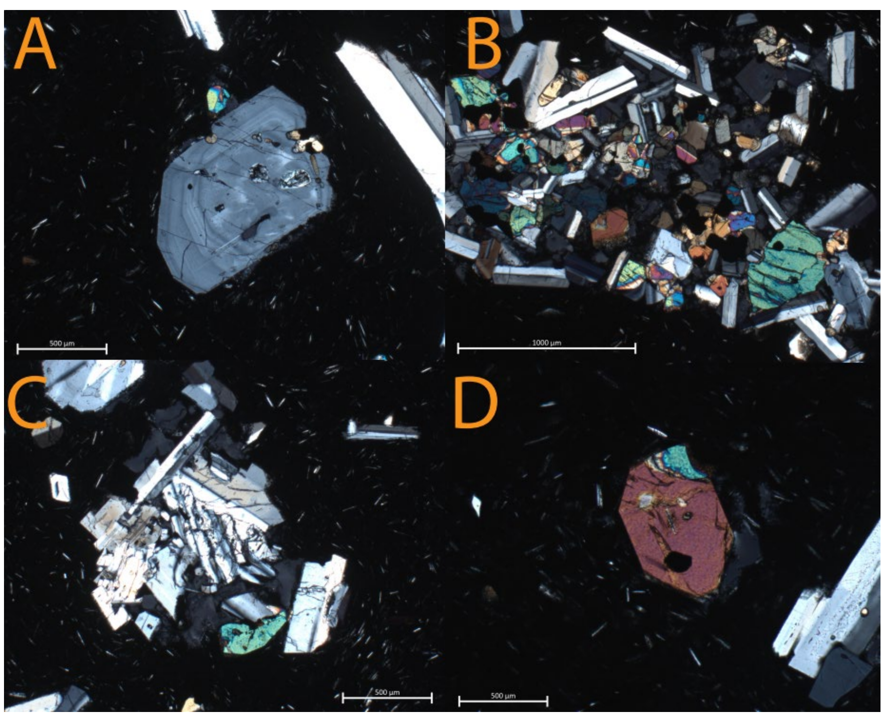

Figure 9. Displays petrographic images of alc. (A) Large solo plagioclase displaying patchy zoning. (B) Large representative clot with plagioclase, orthopyroxene, and clinopyroxene. (C) Representative plagioclase and clinopyroxene clot in alc. (D) Solitary clinopyroxene.

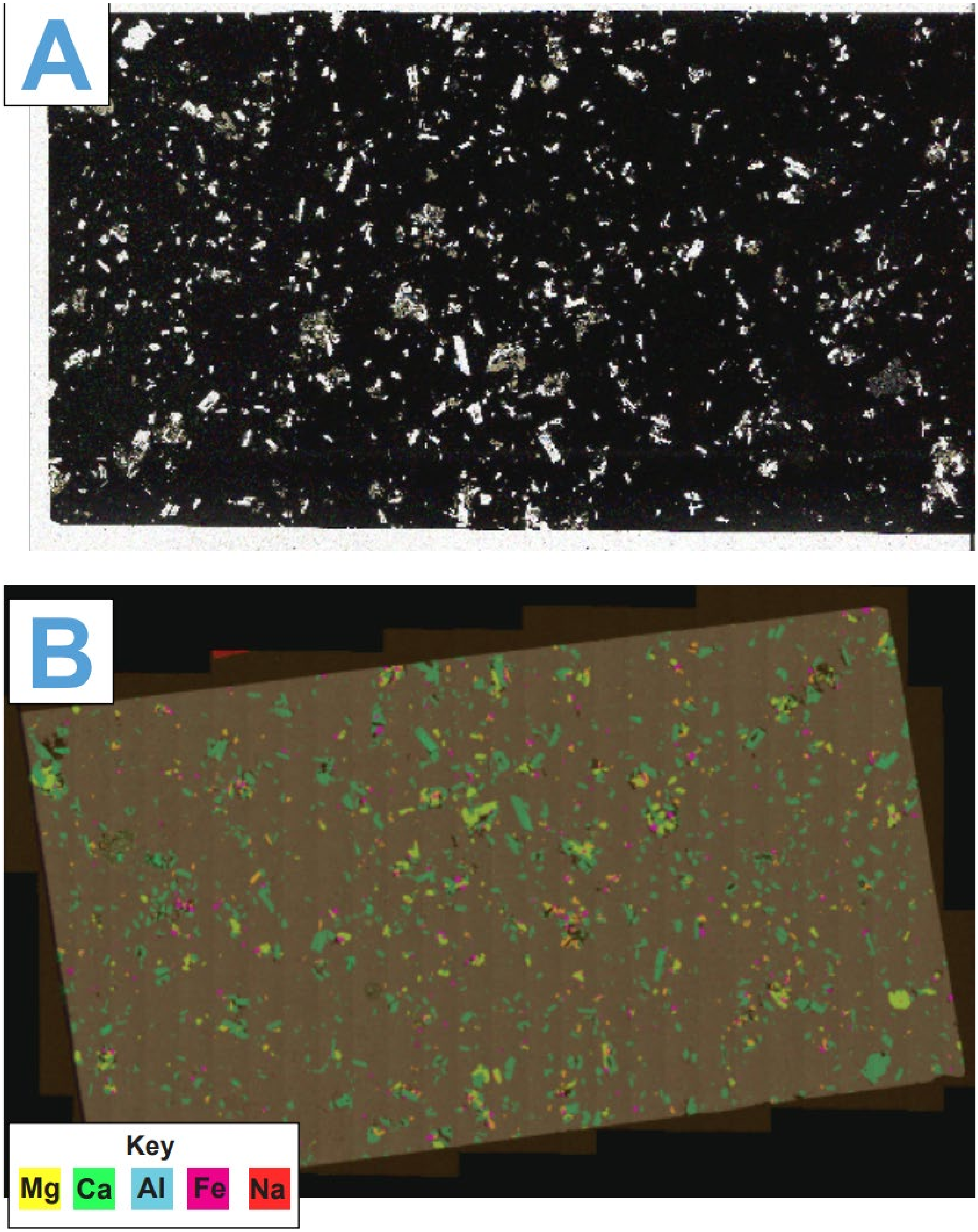

Figure 10. (A) Plain light scan of 030B (alc) thick section. (B) EDS Map of 030B (alc thick section).

4.1.3. Enclaves in the Andesite of Linton Creek (alc), Middle Sister

Two populations of enclaves were observed: one with olivine and another with pyroxene; some pyroxene-bearing enclaves are completely phaneritic. The large enclaves observed were up to 11 cm across, but most enclaves averaged 5 cm in length, and several were as small as 1-2 cm in length (Fig. 11). Southwest of the main outcrop there is an additional outcrop that is relatively smaller, but specific size could not be determined due to steep topography. The enclaves could also be lithic fragments, and there is likely a greater variety of enclaves and lithic fragments in alc (e.g., Fig. 11A), but they could not be sampled and therefore are not described in this study.

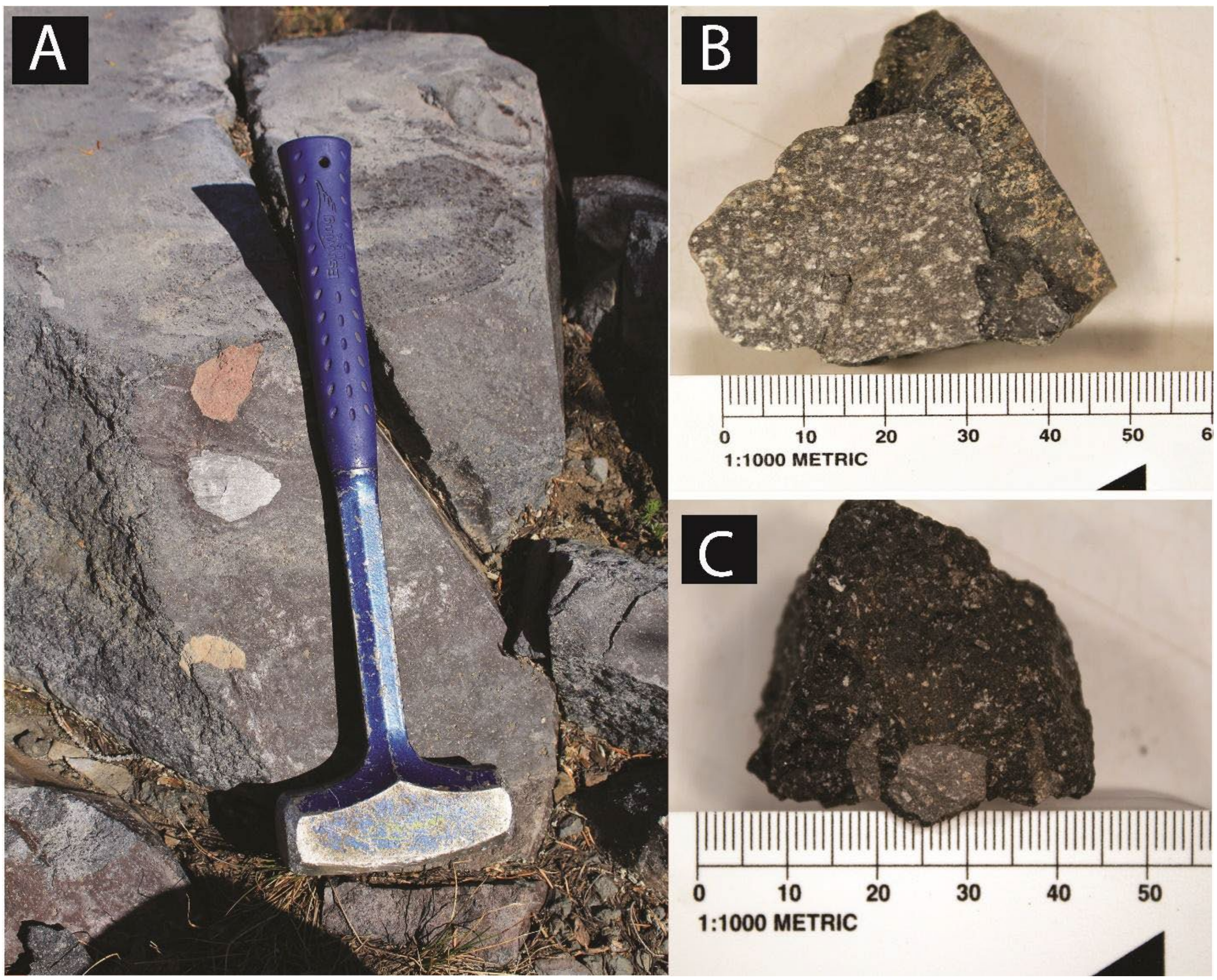

Figure 11. (A) Enclaves in outcrop (B) Olivine bearing enclave in hand sample. Approximately 30 mm in diameter (C) Orthopyroxene bearing enclave in hand sample. Approximately 10 mm in diameter.

4.1.3.1 Olivine Bearing (Type I)

Enclave type one consists of olivine-bearing enclaves with a holocrystalline matrix and 5% phenocrysts (Fig. 12). Phenocrysts consist of ~3% plagioclase crystals that are 0.25-1 mm in diameter, subhedral to anhedral, tabular to elongate, and randomly oriented. Plagioclase crystals are unsieved, polysythetically twinned, and some are oscillatory zoned. Plagioclase is found in plagioclase and oxides clots, as single phenocrysts, or plagioclase, olivine, and oxides clots. The remaining ~2% of phenocrysts constitute olivine, which are 0.25-1.25 mm in diameter, subhedral with a rhombohedral habit, randomly oriented, unzoned, untwinned, and unsieved, and are most commonly found in olivine and plagioclase clots. Out of the visible groundmass crystals, approximately ~95% are euhedral, elongate, randomly oriented plagioclase, ~3% are subhedral, equant oxides, and the remaining ~2 are euhedral, rhombohedral olivine. There is no zoning identified in groundmass crystals, but polysynthetic twining is present in groundmass plagioclase.

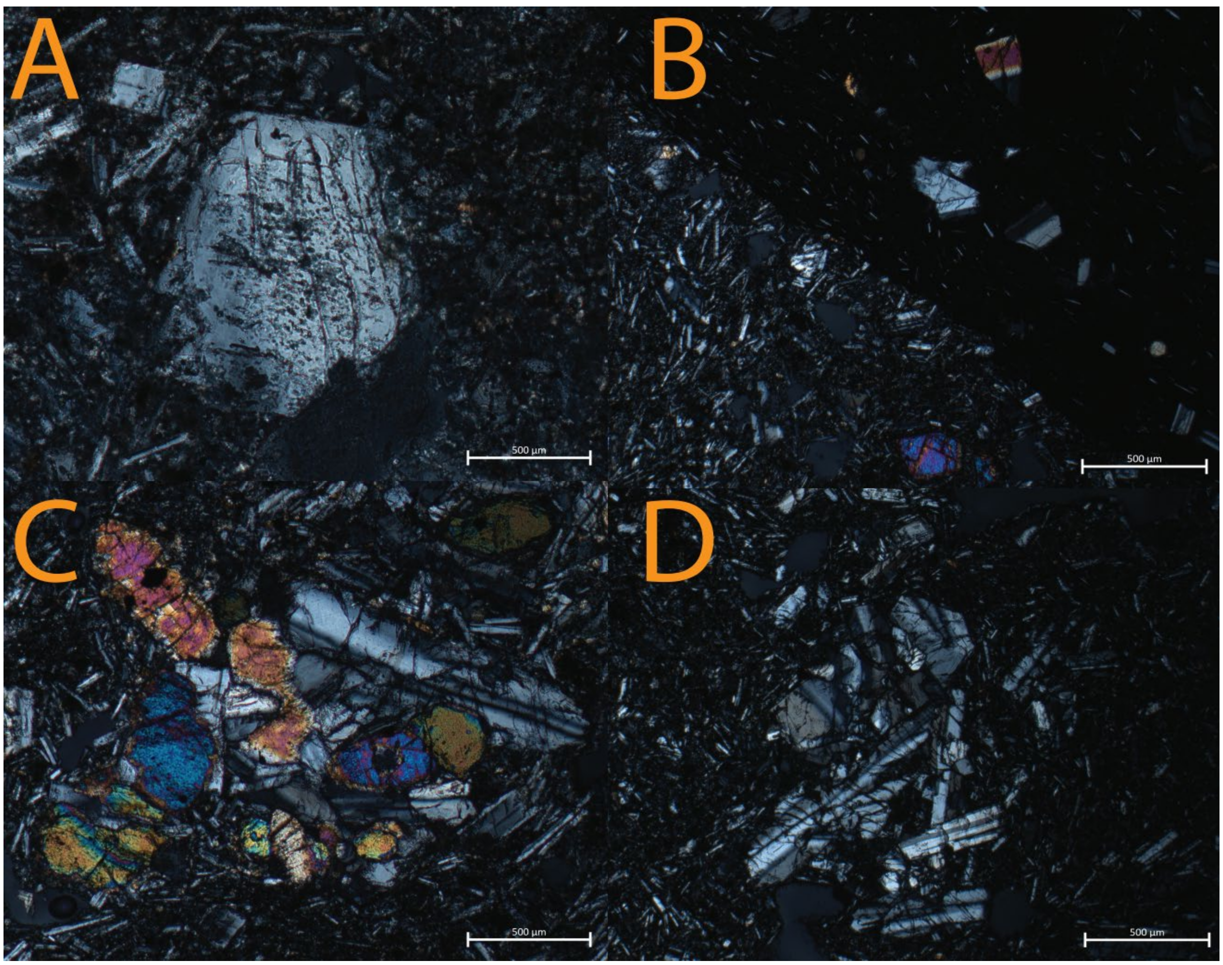

Figure 12. Petrographic images of olivine enclave in alc. (A) Displays large, fractured plagioclase. (B) Displays boundary between alc ground mass and enclave groundmass. (C) Displays representative olivine and plagioclase clot within the enclave. (D) Displays representative plagioclase clot within the enclave.

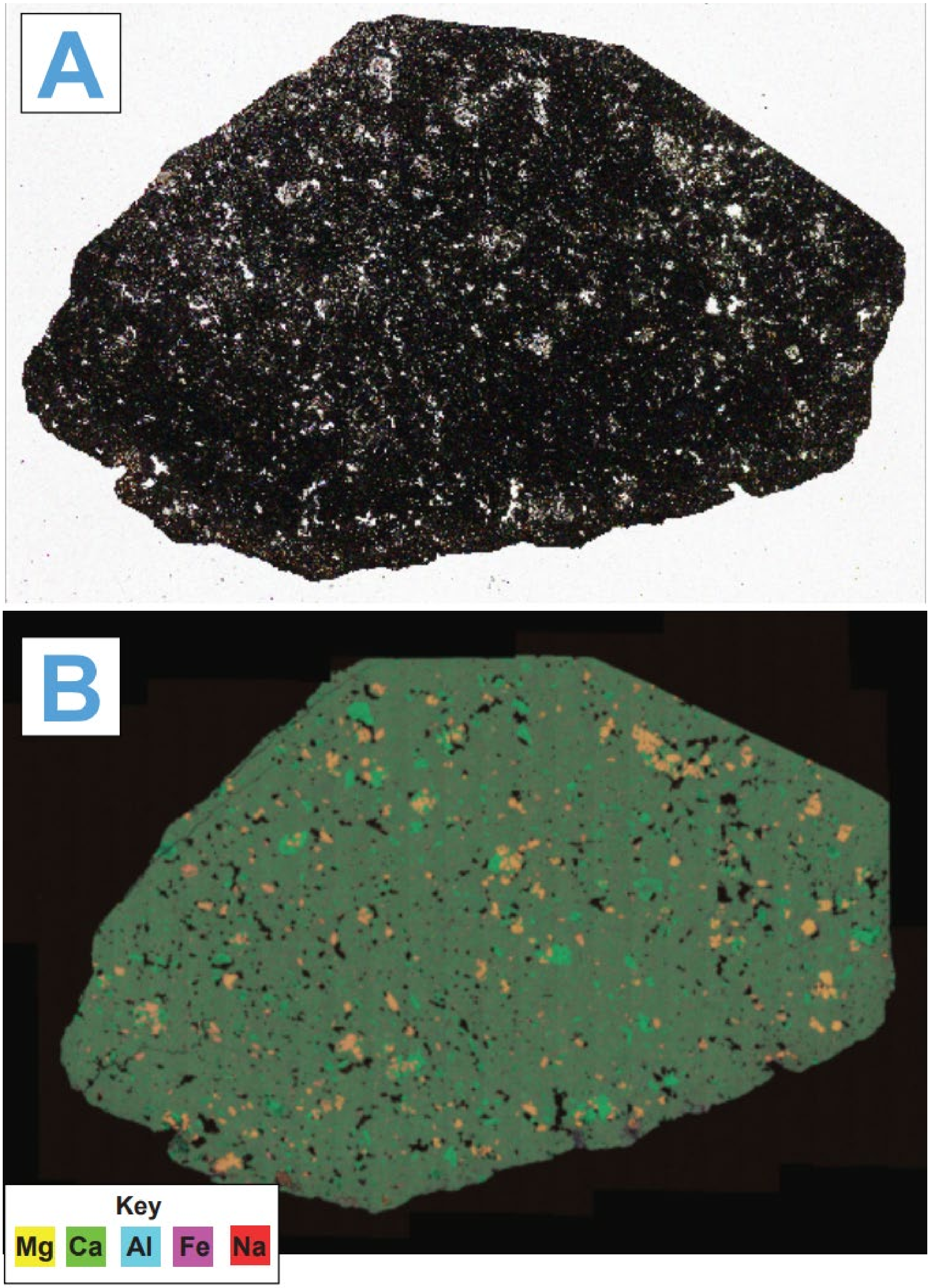

Figure 13. (A) Plain light scan of 030BE (olivine enclave) thick section. (B) EDS Map of 030BE (olivine enclave) thick section.

4.1.3.2 Orthopyroxene Bearing (Type II)

Enclave type two consists of orthopyroxene-bearing enclaves, some of which are completely crystalline, that contain plagioclase, orthopyroxene, and oxides (Fig. 14). Only a single phaneritic enclave was successfully sampled in thin section. This enclave consists of ~90% plagioclase crystals that are <0.25 mm in diameter, subhedral, tabular to elongate, and oriented in two directions. The plagioclase crystals are also unzoned, polysynthetic twinned, and unsieved. Orthopyroxene constitutes approximately ~9% of crystals which are <0.25 mm in diameter, subhedral, and equant to rounded. Orthopyroxene crystals show no zoning, no twining, and no sieving. The remaining ~1% of crystals consist of oxides crystals that are <0.25 mm in diameter, subhedral, equant, and most commonly attached to plagioclase.

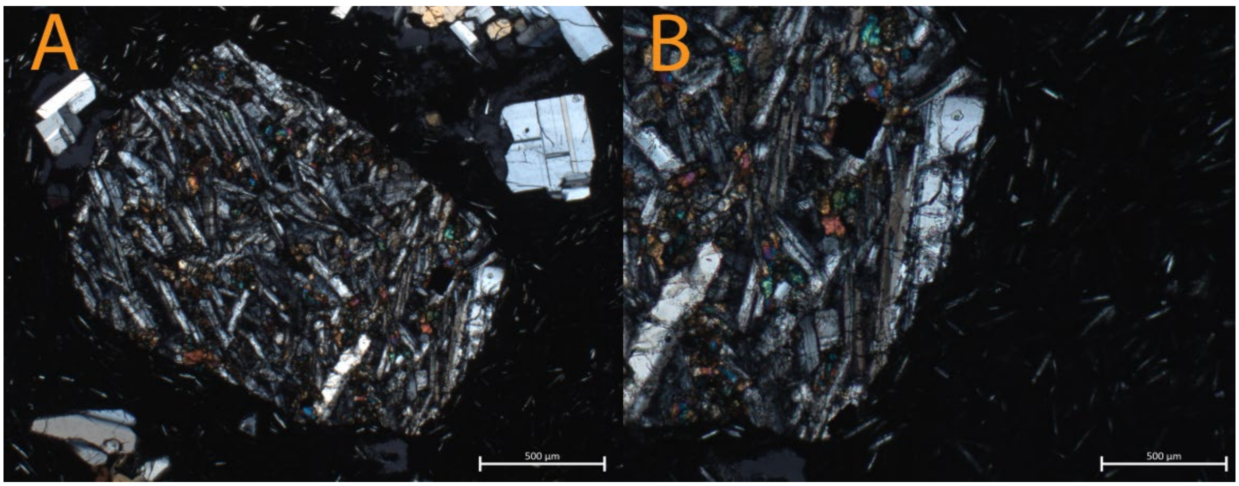

Figure 14. Petrographic image displaying orthopyroxene enclave in alc. (A) Displays the entire enclave. (B) Displays differences in groundmass between the host and enclave.

4.2. Whole Rock Geochemistry

4.2.1 alg

Whole rock analysis of alg yielded an andesitic composition on the total alkali-silica (TAS) diagram (Fig. 15) (Le Maitre, 1984). Concentrations of major elements across alg sample (total samples, n = 17; new samples from this study n = 1; previously published samples from Hildreth et al., 2012, n = 16) include 61-64 wt% SiO_2, 1.05-1.20 wt% TiO_2, 16.23-16.51 wt% Al_2O_3, 5.64-6.44 wt% FeO , 0.11-0.12 wt% MnO, 1.75- 2.27 wt% MgO, 4.30-4.99 wt% CaO**,** 4.74-5.04 wt% Na_2O, and 1.73-1.97 wt% K_2O. The Mg# (molar Mg/[Mg+Fe*0.85] *100) of the samples are 39-43. Whole rock compositions are shown in Figures 15-19 and are reported in Table A1.

4.2.2 alc

Whole rock analysis of alc yielded an andesitic composition on the TAS (Fig. 15). Major elements concentrations across alc samples (total samples, n = 15; new samples from this study n = 3; previously published samples from Hildreth et al., 2012, n = 12) are 61-63 wt% SiO_2, 1.15-1.27 wt% TiO_2 , 16.21-16.46 wt% Al_2O_3, 5.86-6.46 wt% FeO , 0.12-0.14 wt% MnO, 1.88-2.04 wt% MgO, 4.52-4.72 wt% CaO**,** 4.91-5.14 wt% Na_2O, and 1.69-1.95 wt% K_2O. The Mg# of the samples are 39-40. Whole rock compositions are shown in Figures 15-19 and are reported in Table A6.

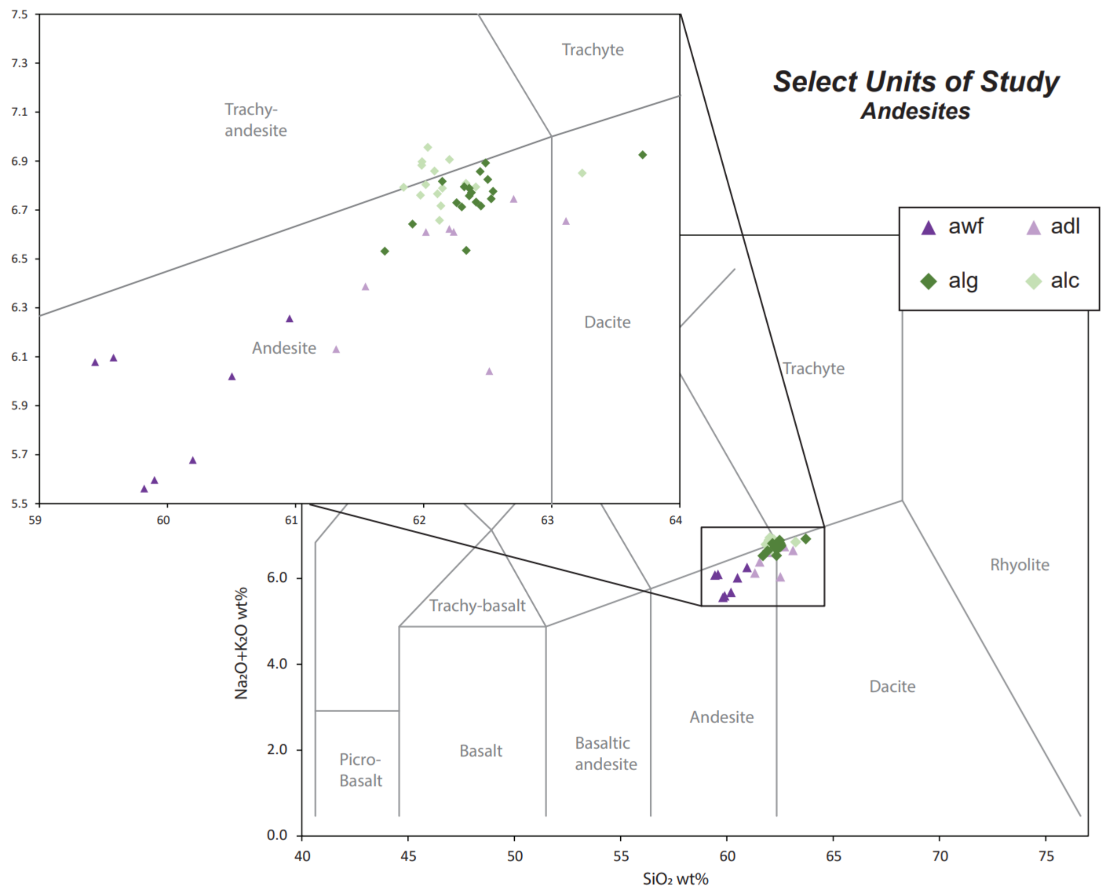

Figure 15. TAS diagram showing lava composition of alc and adl (Middle Sister), and alg and awf (South Sister). Units alg and alc (west flanks) are shown in green diamonds. Units awf and adl (east flanks) are shown in purple triangles. Units awf and adl are andesites and are shown for comparison as representative andesites from the eastern flanks of Middle Sister and South Sister that erupted ca. 24 ka (Hildreth et al., 2012). New whole rock data for units adl and awf were obtained using the same methods and are reported in Peale (2023).

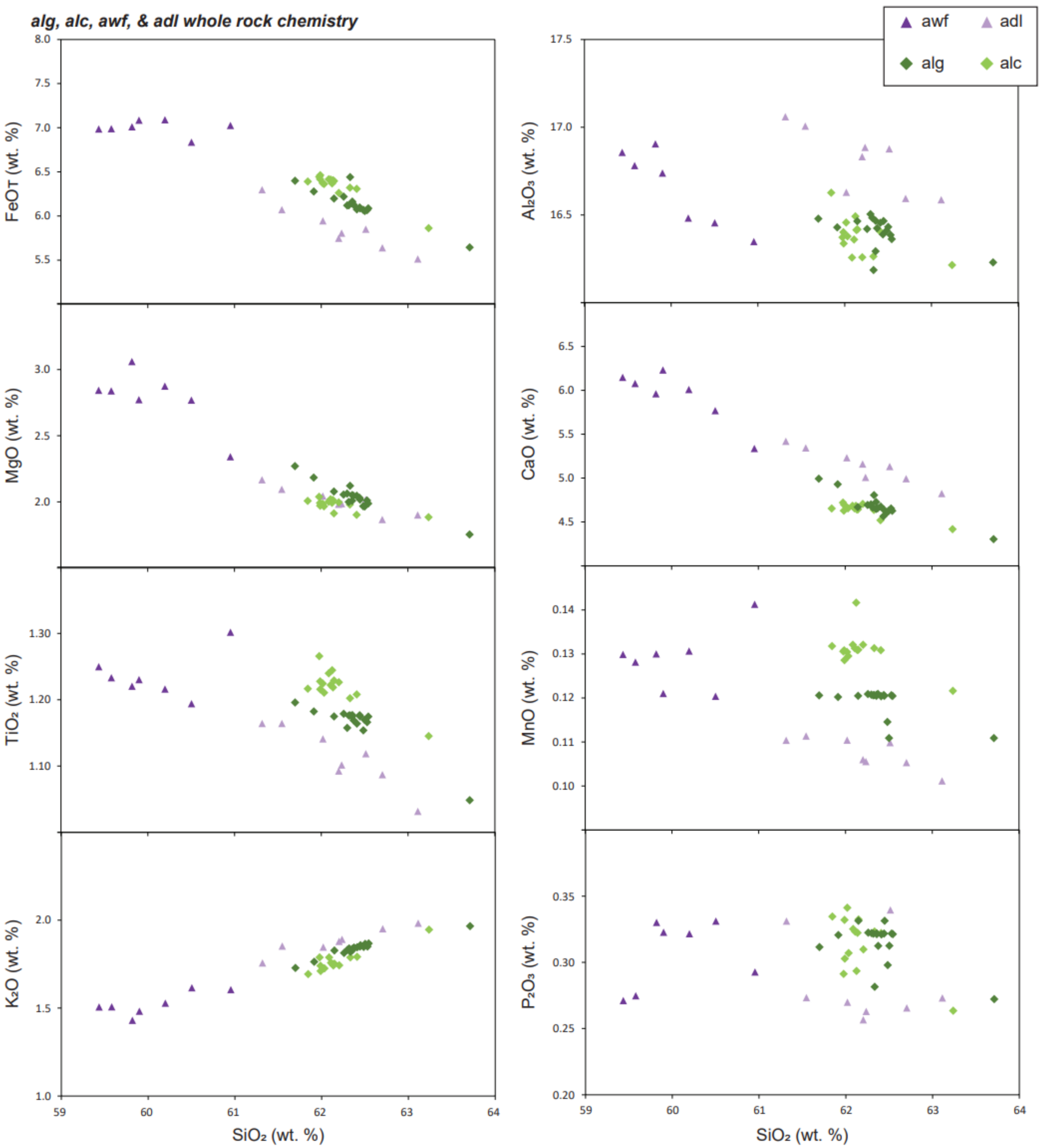

Figure 16. Bulk chemistry plots displaying SiO_2 on the x-axis and major element oxides on the y-axis. Units alg and alc are shown in green diamonds. Units awf and adl are shown in purple triangles.

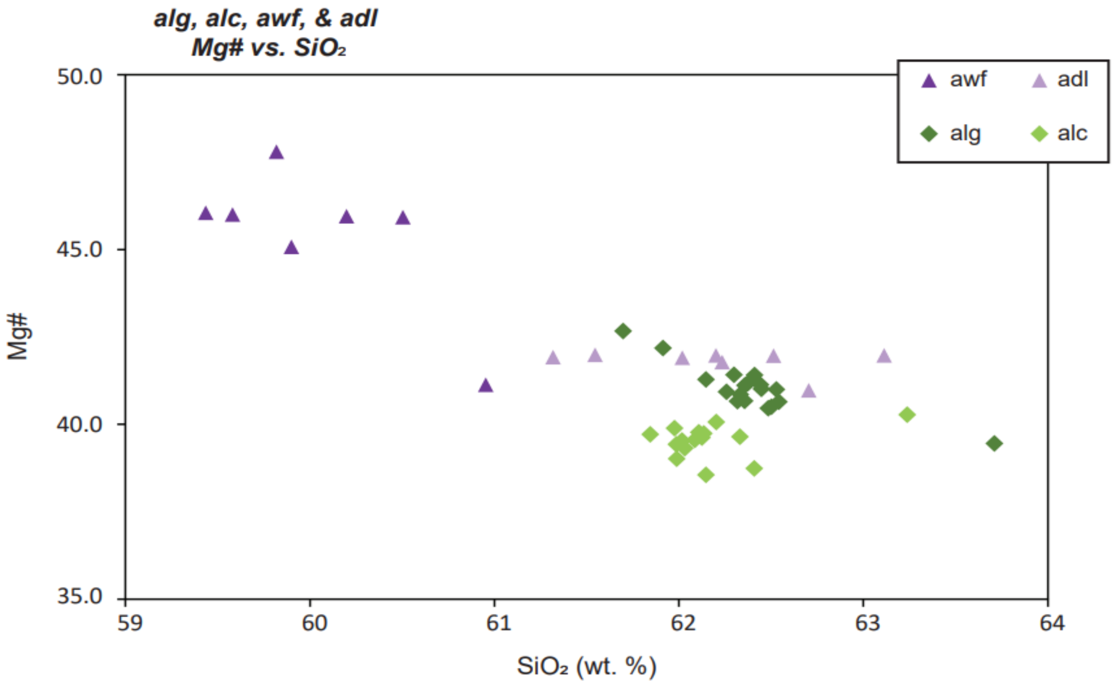

Figure 17. Plot displaying SiO_2 on the x-axis and whole rock Mg# on the y-axis. Units alg and alc are shown in green diamonds. Units awf and adl are shown in purple triangles.

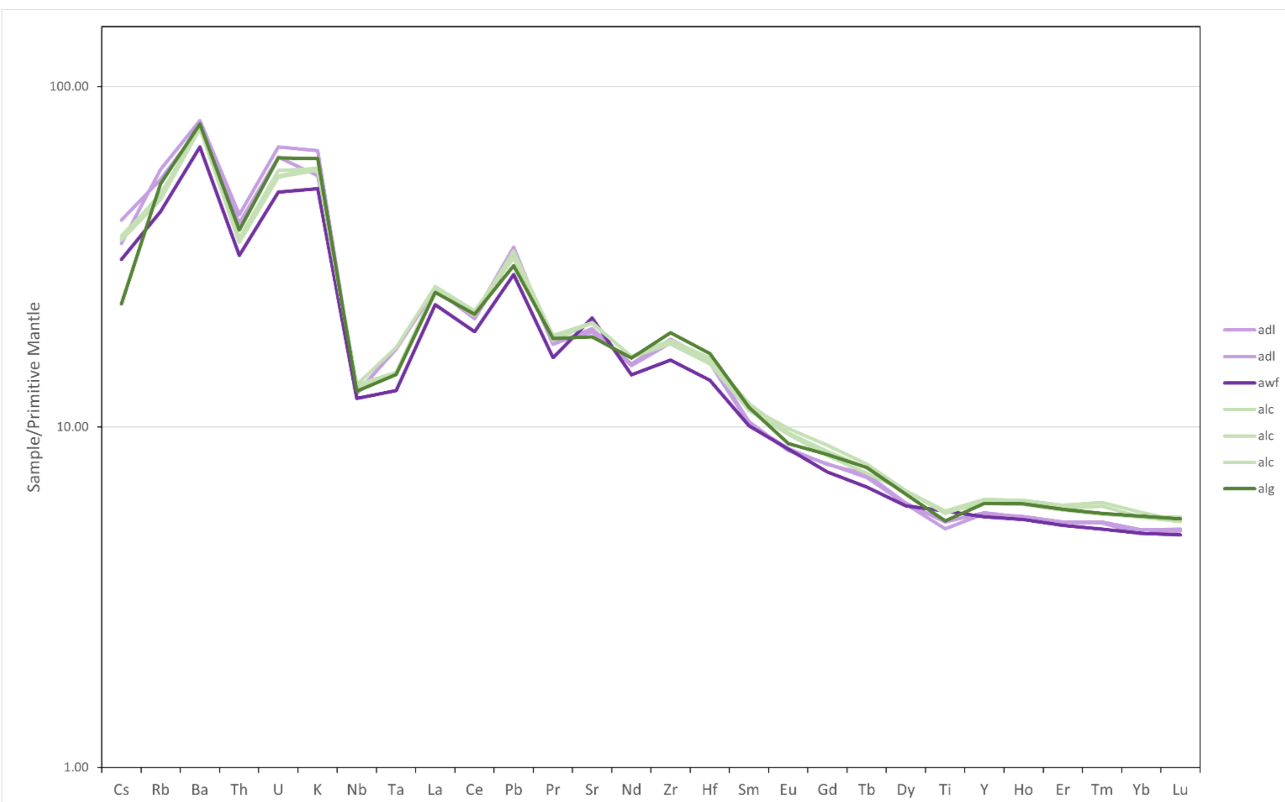

Figure 18. Spider diagram displaying trace elements on the x-axis and sample/primitive mantle values on the y-axis. Units alg and alc are shown in green. Units awf and adl are shown in purple.

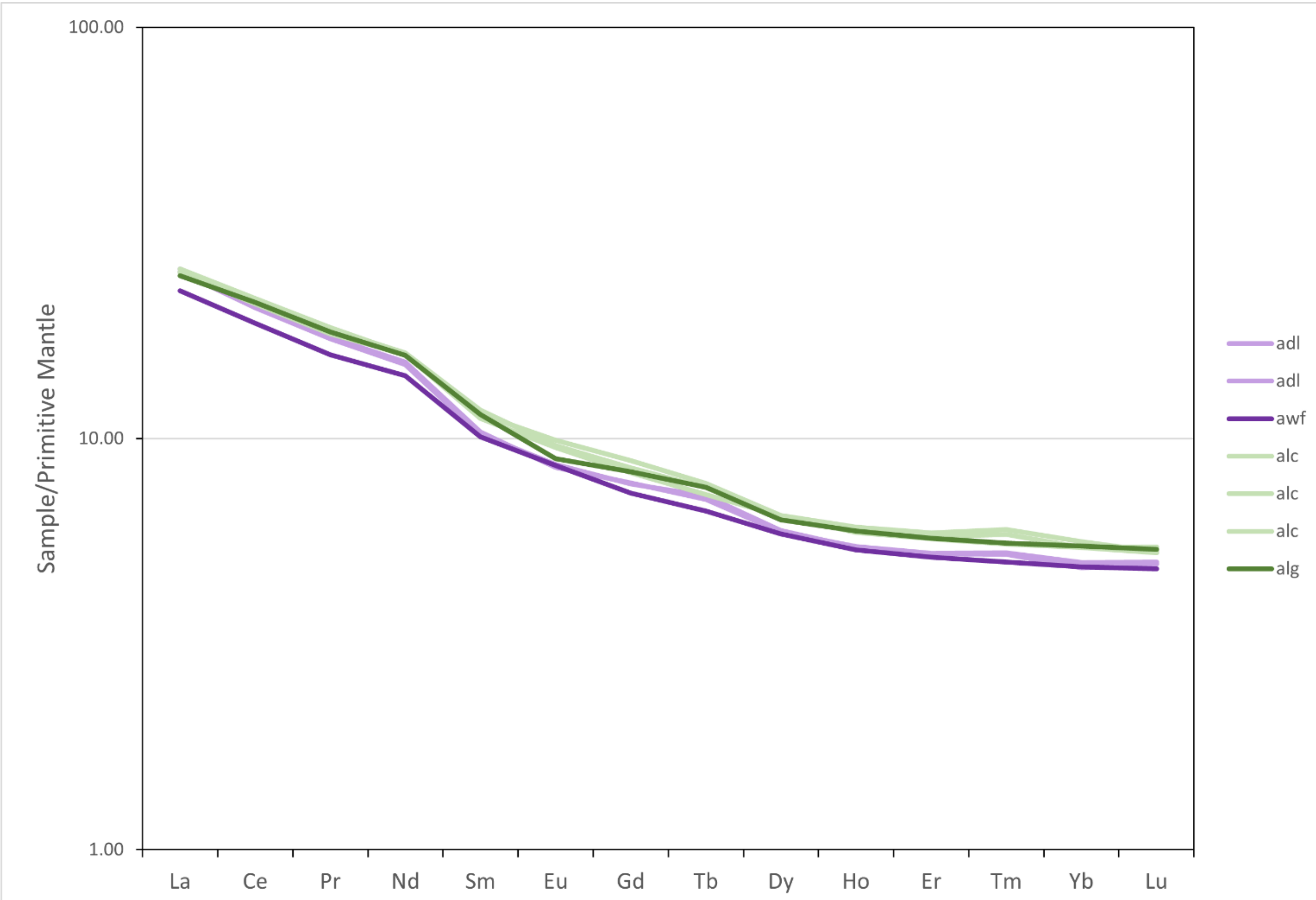

Figure 19. Plot displaying REE elements on the x-axis and sample/primitive values on the y-axis. Units alc and alg are represented in green. Units awf and adl are represented in purple.

4.3. Mineral Populations

4.3.1. Andesite Mineral Populations

Several mineral populations and crystal clusters were identified in alg and alc host. These populations reflect the most common textural and compositional groups identified within each mineral. Three plagioclase populations, two clinopyroxene populations, four orthopyroxene populations, and one olivine population were identified and characterized in alg and alc, and they are summarized in Figure 20. Mineral compositions are reported in Tables A3-A6 and shown in Figures 20-35. The most abundant crystal clusters identified are reported in Figure 21.

Plagioclase

Population	Texture	Description	An	found in clots with	alg	alc
1a		Patchy normal zoning with relict high An core. ~40% alg ~30% alc	Cores: 58-73 Rims: 51-54	plg (1a, 3), cpx (1a, 1b, 2b), opx (1b, 3, 4), olv (1)	X	X
1b		Sieved patchy normal zoning with relict high An core. ~20% alg ~40% alc	Cores: 64-73 Rims: 53-57	Solo, cpx (1b, 2b)	X	X
2		Patchy reverse zoning with resorbed low An core and low An rim. ~10% alg ~30% alc	Cores: 46-52 Mantles:50-54 Rims: 37	Solo, cpx (1a,1c, 2a), opx (1a, 2a)	X	X
3		Fine oscilations with similar An content reverse and normal zoned. ~20% alg	Cores: 47-53 Rims: 50-53	plg (1a, 3), opx (2b, 4), olv (1)	X	

Clinopyroxene

Population	Texture	Description	Mg#	found in clots with	alg	alc
1a		Slight normal zoning from core to rim. ~40% alc	Cores: 71-73 Rims: 68-72	plg (2), cpx (2a), opx (2a)		X
1b		Slight normal zoning from core to outer mantle. Fine reaction rim present. ~45% alg	Cores: 71-75 Outer Mantles: 69-72 Reaction Rims: ~56	plg (1a, 1b, 3), cpx (2b), opx (1b, 2c, 3, 4), olv (1)	X	
1c		Slight normal zoning from core to rim and heavily embayed ~5% alg	Cores: 72 Rims: 72	plg (2)	X	
2a		Slight reverse zoning from core to rim. ~40% alc	Cores: 71-72 Rims: 72-73	plg (2), cpx (1a), opx (2a)		X
2b		Slight reverse zoning from core to outer mantle with fine reaction rim. ~45% alg ~20% alc	Cores: 69-73 Outer mantles: 71-73 Reaction Rims: 56	plg (1a, 1b, 3), cpx (1b), opx (2b, 4), olv (1)	X	X
3		Reverse zoning with distinctly lower Mg values. ~5% alg	Cores: 67-68 Mantles:69-73 Reaction Rims: ~56	cpx (1b), opx (2c, 3)	X	

Orthopyroxene

Population	Texture	Description	Mg#	found in clots with	alg	alc
1a		Slight normal zoning from core to rim. ~40% alc	Cores: 71-72 Rims: 69-71	plg (2), cpx (1a, 2a)		X
1b		Slight normal zoning between core and outer mantle. Fine reaction rim present. ~10% alc ~20% alg	Cores: 72-74 Outer Mantles: 71-73 Reaction Rims: 60	plg (1a), cpx (1b, 2a, 2b), opx (2a, 3)	X	X
2a		Slight reverse zoning ~50% alc ~15% alg	Cores: 70-71 Rims: 70-71	plg (2), cpx (1a, 2a), opx (1b)		X
2b		Slight reverse zoning between core and outer mantle with fine reaction rim. ~40% alg	Cores: 68-70 Outer Mantles: 70-71 Reaction Rims: ~ 60	plg (3), cpx (1b, 2b)	X	
2c		Cloudy core with slight reverse zoning from core to outer mantle with fine reaction rim. ~5% alg	Cores: 73-74 Outer mantle: 72-73 Reaction Rims: ~60	cpx (1b, 2c), opx (3)	X	
3		Low core, moderate mantle, low outer mantle, reaction rim. ~5% alg	Cores: 70 Inner mantle:73 Outer mantle: 70-71 Reaction Rims: ~60	plg (1a), cpx (1b, 2b, 2c) opx (1b, 2c)	X	
4		Orthopyroxene reaction rim around olivine ~15% alg	Rims: 70-71	plg (1a, 3) , cpx (1b), olv (1)	X	

Olivine

Population	Texture	Description	Fo	found in clots with	alg	alc
1		Olivine reacting into orthopyroxene 100% alg	Cores: 65-67	plg (1a, 3), opx (4), olv (1)	X	

Figure 20. An illustrated summary table showing all mineral populations identified in alc and alg.

clot types		mineral populations	alg	alc
1		plg (1a), cpx (1a)		X
2		plg (1a), cpx (1b, 2b, 2c), opx (1b, 3)	X	
3		plg (2), cpx (1a, 2a)		X
4	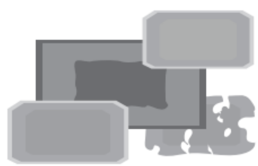	plg (2), cpx (1b, 2b, 1c)	X	
5	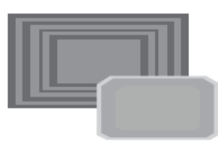	plg (3), opx (2b)	X	
6		plg (1a), cpx (1b), opx (4), olv (1)	X	

Figure 21. An illustrated summary table showing most abundant clots identified in alc and alg.

4.3.1.1. Plagioclase

Plagioclase population 1 is subdivided into populations 1a and 1b, both of which are found in alg and alc. These populations are compositionally similar but have distinct textural differences. Population 1a consists of tabular plagioclase with relict high anorthite cores (An_{58-73}) that display patchy to boxy zoning with low anorthite regions within the high anorthite core. Rims display uniform growth with a moderate anorthite content (An_{51-54}). Population 1b is similar compositionally with normal zoning from relict high anorthite patchy cores (An_{64-73}) to moderate anorthite rims (An_{53-57}). The main distinction in population 1b is that it is sieved throughout the core region of each crystal. Additionally, population 1b crystals tend to be much larger in size (~500 µm in diameter).

Plagioclase population 2 is characterized by reverse zoning with a low An core that has a resorbed boundary, a moderate An mantle, faint oscillations (<10 µm) throughout the core and the mantle, and a thin, low An rim. This population is found in both alg and alc and has core An_{46-52} and outer mantle An_{50-54}. It was challenging to successfully analyze the rims of this population because they are thin (often ≤10 µm), but a single successful analysis of an alg crystal yielded rim An_{37}.

Plagioclase population 3 is unique to alg. This population displays fine (~20 µm) oscillations throughout the entire crystal and includes both reverse and normally zoned crystals. This population has core An_{47-53} and rim An_{50-53}.

	Population	Texture	Description	An	found in clots with	alg	alc
Plagioclase	1a		Patchy normal zoning with relict high An core. ~40% alg ~30% alc	Cores: 58-73 Rims: 51-54	plg (1a, 3), cpx (1a, 1b, 2b), opx (1b, 3, 4), olv (1)	X	X
	1b		Sieved patchy normal zoning with relict high An core. ~20% alg ~40% alc	Cores: 64-73 Rims: 53-57	Solo, cpx (1b, 2b)	X	X
	2		Patchy reverse zoning with resorbed low An core and low An rim. ~10% alg ~30% alc	Cores: 46-52 Mantles:50-54 Rims: 37	Solo, cpx (1a,1c, 2a), opx (1a, 2a)	X	X
	3		Fine oscilations with similar An content reverse and normal zoned. ~20% alg	Cores: 47-53 Rims: 50-53	plg (1a, 3), opx (2b, 4), olv (1)	X	

Figure 22. An illustrated summary table showing plagioclase populations identified in alc and alg.

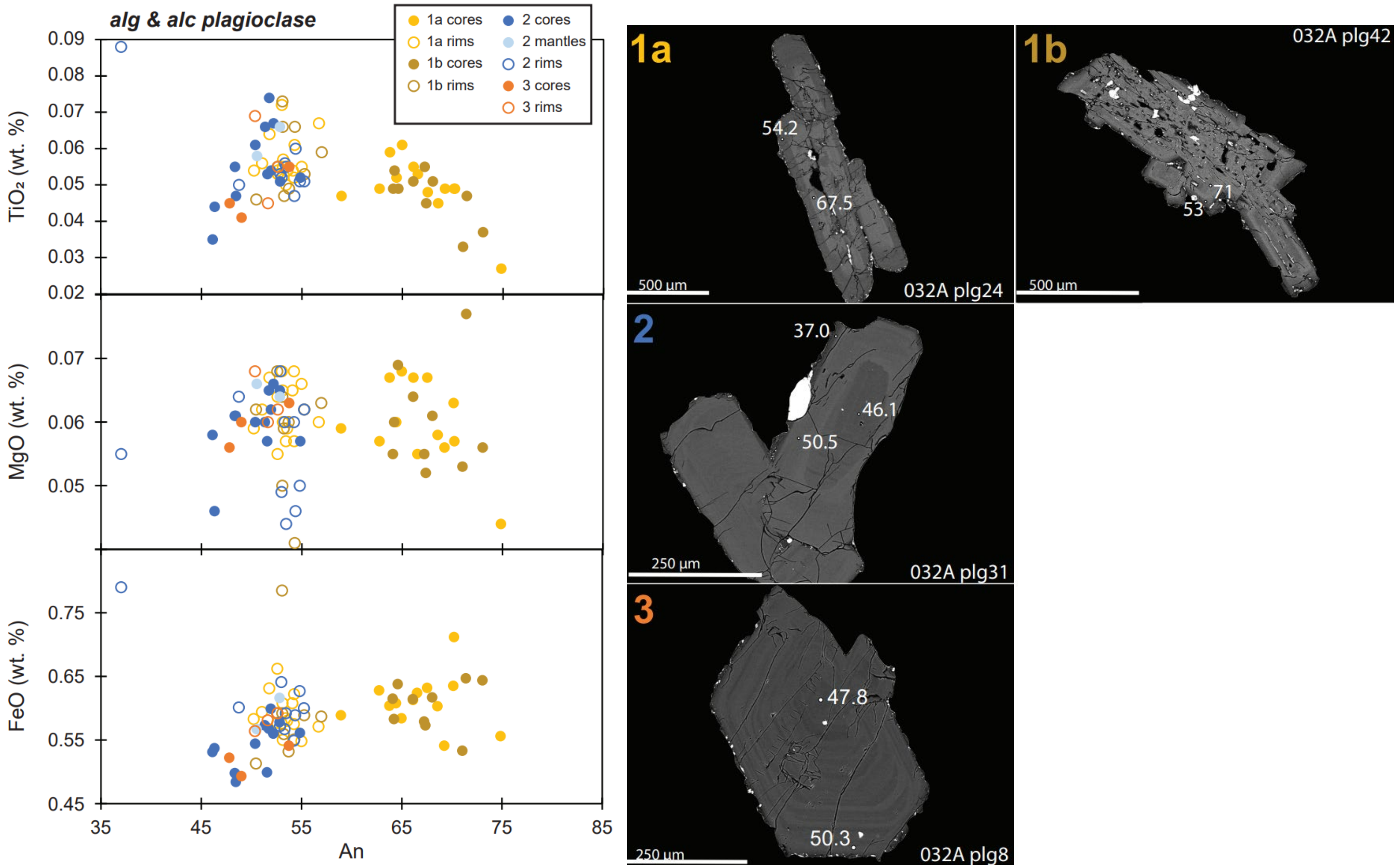

Figure 23. Plots displaying plagioclase data for alc and alg. An content is plotted on the x-axis and the y-axis shows minor oxide concentrations. Legend is shown in top right corner. BSE images on the left display corresponding populations for each population plotted on right side of figure.

4.3.1.2. Clinopyroxene

Clinopyroxene population 1 is subdivided into populations 1a, 1b, and 1c. These populations are compositionally similar but have distinct textural differences. Unit alc only contains population 1a, which is characterized by slight normal zoning. This population has core Mg#$_{71-73}$ and rim Mg#$_{68-72}$. Unit alg only contains populations 1b and 1c. Clinopyroxene population 1b is characterized by normal zoning and is distinct from 1a due to having a fine (≤10μm) reaction rim. This population has core Mg#$_{71-75}$ and outer mantle Mg#$_{69-72}$. The reaction rim was too narrow to be able to get reliable compositional data, but based on high brightness relative to the rest of the crystal in BSE imaging it is understood to have lower Mg#. Clinopyroxene population 1c is characterized by slight normal zoning and heavy embayment. This population has core Mg#$_{72}$ and rim Mg#$_{72}$. One crystal was identified in this population.

Clinopyroxene population 2 is subdivided into populations 2a and 2b. These populations are compositionally similar but have distinct textural differences. Population 2a is only identified alc and is characterized by reverse zoning. This population has core Mg#$_{71-72}$ and rim Mg#$_{72-73}$. Clinopyroxene population 2b is found in both alc and alg and is characterized by reverse zoning with a fine (≤10 μm) reaction rim. This population has core Mg#$_{69-72}$ and outer mantle Mg#$_{71-73}$. This reaction rim was only successfully analyzed in one alg crystal and yielded Mg#$_{56}$.

Clinopyroxene population 3 is characterized by a core, inner mantle, outer mantle and with a fine reaction rim (≤10 μm). This population is found in both alc and alg. This population has core Mg#$_{67-68}$ and mantle Mg#$_{69-73.}$ Based on BSE brightness, the reaction rim is understood to have a lower Mg#.

	Population	Texture	Description	Mg#	found in clots with	alg	alc
Clinopyroxene	1a		Slight normal zoning from core to rim. ~40% alc	Cores: 71-73 Rims: 68-72	plg (2), cpx (2a), opx (2a)		X
	1b		Slight normal zoning from core to outer mantle. Fine reaction rim present. ~45% alg	Cores: 71-75 Outer Mantles: 69-72 Reaction Rims: ~56	plg (1a, 1b, 3), cpx (2b), opx (1b, 2c, 3, 4), olv (1)	X	
	1c		Slight normal zoning from core to rim and heavily embayed ~5% alg	Cores: 72 Rims: 72	plg (2)	X	
	2a		Slight reverse zoning from core to rim. ~40% alc	Cores: 71-72 Rims: 72-73	plg (2), cpx (1a), opx (2a)		X
	2b		Slight reverse zoning from core to outer mantle with fine reaction rim. ~45% alg ~20% alc	Cores: 69-73 Outer mantles: 71-73 Reaction Rims: 56	plg (1a, 1b, 3), cpx (1b), opx (2b, 4), olv (1)	X	X
	3		Reverse zoning with distinctly lower Mg values. ~5% alg	Cores: 67-68 Mantles:69-73 Reaction Rims: ~56	cpx (1b), opx (2c, 3)	X	

Figure 24. An illustrated summary table showing clinopyroxene populations identified in alc and alg.

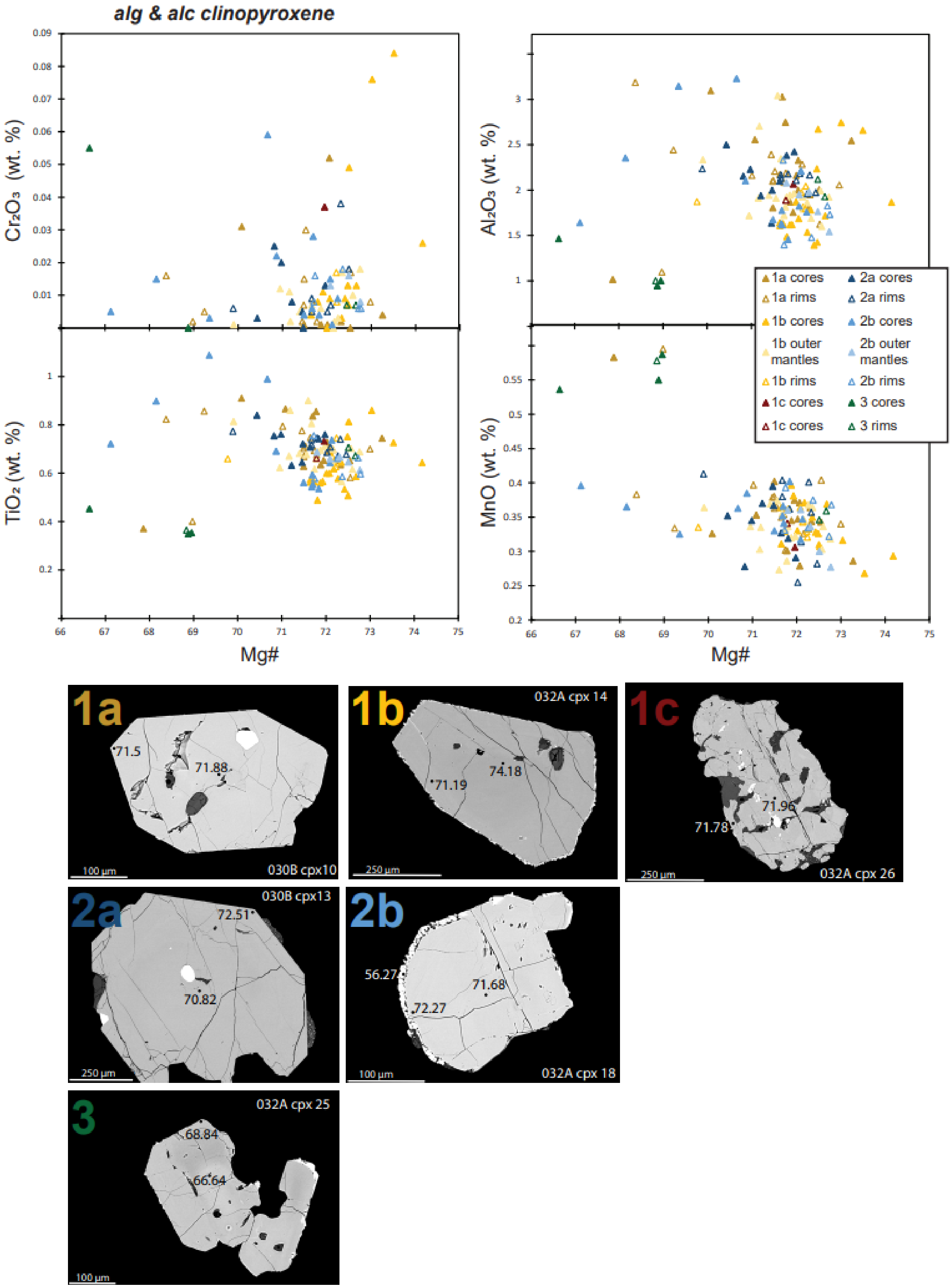

Figure 25. Plots displaying clinopyroxene data for alg and alc. Mg# is plotted on the x-axis and minor oxide compositions are plotted on the y-axis. Legend is displayed on right side of figure.

4.3.1.3. Orthopyroxene

Orthopyroxene population 1 is subdivided into populations 1a, 1b, and 1c. These populations are compositionally similar but have distinct textural differences. Population 1a is only found in unit alc and is characterized by normal zoning. This population has core Mg#$_{71\text{-}72}$ and rim Mg#$_{69\text{-}71}$. Population 1b is found in both alc and alg and is characterized by normal zoning with a fine (≤10 µm) reaction rim. This population has core Mg#$_{71\text{-}74}$, outer mantle Mg#$_{71\text{-}73}$, and rim Mg#$_{60}$. Population 1c is only found in alg and is characterized as a heavily embayed crystal with slight normal zoning. This population has core Mg#$_{72}$, and rim Mg#$_{72}$.

Orthopyroxene population 2 is subdivided into populations 2a, 2b, and 2c. These populations are compositionally similar but have distinct textural differences. Population 2a is only found in unit alc and is characterized by reverse zoning. This population has core Mg#$_{70\text{-}71}$ and rim Mg#$_{70\text{-}71}$. Orthopyroxene population 2b is only found in unit alg and is characterized by reverse zoning and a fine (≤10 µm) reaction rim. This population has core Mg#$_{68\text{-}70}$ and outer mantle Mg#$_{70\text{-}71}$. No rims were successfully analyzed, but based on relative BSE brightness they are understood to have lower Mg#. Orthopyroxene population 2c is also only found in unit alg and is characterized by reverse zoning with a fine (≤10 µm) reaction rim, but it is distinct due to having cloudy cores and higher core Mg#. This population has core Mg#$_{74}$ and outer mantle Mg#$_{74.5}$. No rims were successfully analyzed, but they are understood to have lower Mg# based on relative BSE brightness.

Orthopyroxene population 3 is characterized by similar Mg# in the cores and outer mantles, but with relatively higher Mg# inner mantles, and assumed (based on relative BSE brightness) lower Mg# fine (≤10 µm) reaction rims. This population has core Mg#$_{70}$, inner mantle Mg#$_{73}$, and outer mantle Mg#$_{70\text{-}71.}$ No rims were successfully analyzed.

Orthopyroxene population 4 is only found in unit alg. This population consists of a ring around an olivine crystal that is reacting into orthopyroxene with Mg#$_{70\text{-}71}$.

	Population	Texture	Description	Mg#	found in clots with	alg	alc
Orthopyroxene	1a		Slight normal zoning from core to rim. ~40% alc	Cores: 71-72 Rims: 69-71	plg (2), cpx (1a, 2a)		X
	1b		Slight normal zoning between core and outer mantle. Fine reaction rim present. ~10% alc ~20% alg	Cores: 72-74 Outer Mantles: 71-73 Reaction Rims: 60	plg (1a), cpx (1b, 2a, 2b), opx (2a, 3)	X	X
	2a		Slight reverse zoning ~50% alc ~15% alg	Cores: 70-71 Rims: 70-71	plg (2), cpx (1a, 2a), opx (1b)		X
	2b		Slight reverse zoning between core and outer mantle with fine reaction rim. ~40% alg	Cores: 68-70 Outer Mantles: 70-71 Reaction Rims: ~ 60	plg (3), cpx (1b, 2b)	X	
	2c		Cloudy core with slight reverse zoning from core to outer mantle with fine reaction rim. ~5% alg	Cores: 73-74 Outer mantle: 72-73 Reaction Rims: ~60	cpx (1b, 2c), opx (3)	X	
	3		Slight oscilarions between core inner mantle, and outer mantle. Reaction rim present. ~5% alg	Cores: 70 Inner mantle:73 Outer mantle: 70-71 Reaction Rims: ~60	plg (1a), cpx (1b, 2b, 2c) opx (1b, 2c)	X	
	4		Orthopyroxene reaction rim around olivine ~15% alg	Rims: 70-71	plg (1a, 3) , cpx (1b), olv (1)	X	

Figure 26. An illustrated summary table showing orthopyroxene populations identified in alc and alg.

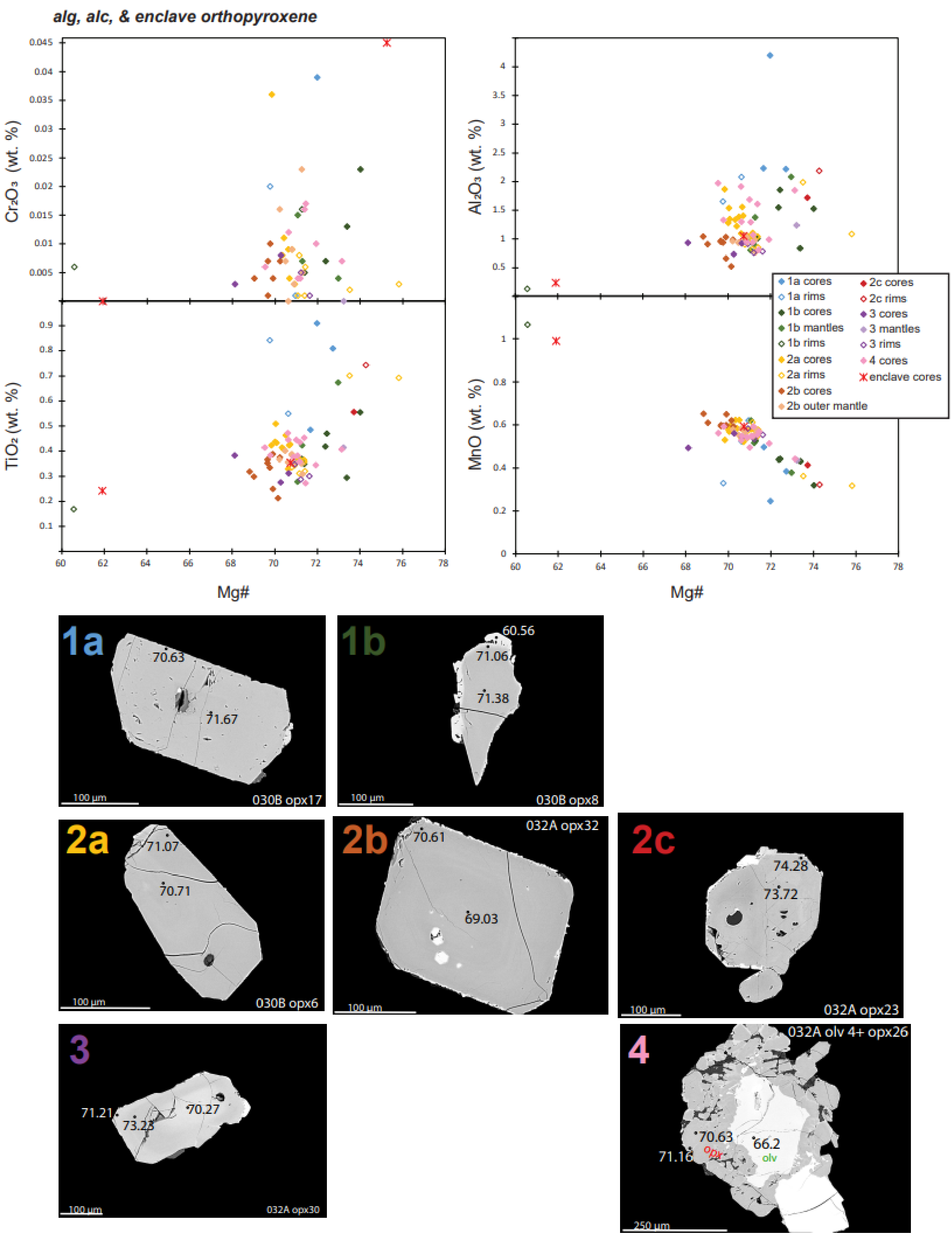

Figure 27. Plots displaying orthopyroxene data for the host and enclaves. Mg# is plotted on the x-axis and varying minor oxide compositions are plotted on the y-axis. Plot legend is shown on right side of plots.

4.3.1.4. Olivine

Olivine population 1 consists of only core analyses with $Fo_{65\text{-}67}$. This population is only identified in alg and consists of blobby olivine with a low Fo core that is reacting into orthopyroxene.

	Population	Texture	Description	Fo	found in clots with	alg	alc
Olivine	1		Olivine reacting into orthopyroxene 100% alg	Cores: 65-67	plg (1a, 3), opx (4), olv (1)	X	

Figure 28. An illustrated summary table showing olivine populations identified in alc and alg.

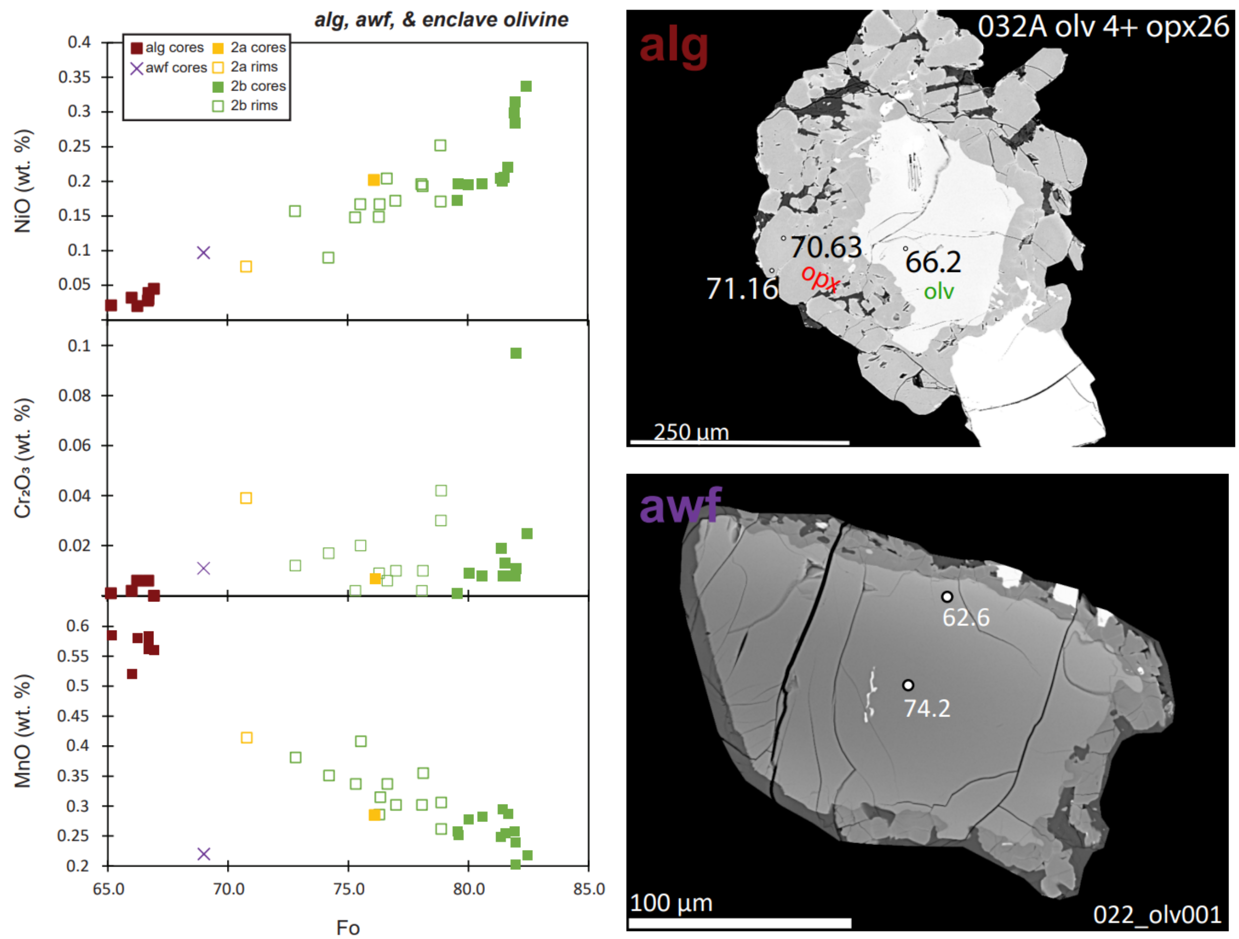

Figure 29. *Plot displaying olivine Fo vs. MnO, Cr_2O_3, NiO. Plots display enclave populations in yellow and green squares. Olivine data from alg are shown as red squares and from awf as purple Xs (Peale, 2023).*

4.3.2. Enclave Mineral Populations

Several mineral populations were identified in the enclaves found in alc. These populations reflect the most common textural and compositional groups within each mineral. Four plagioclase populations, one orthopyroxene population, and two olivine population were identified and characterized in the alc enclaves, and they are summarized in Figure 30. Mineral compositions are reported in Tables A3-A6 and shown in Figures 30-35. These populations are only found in the enclaves.

Mineral	Population	Texture	Description	An	found in clots with	1	2
Plagioclase	4		Coarse oscilatory zoning with alternating normal and reverse zoning ~60% enclave 1 (olv)	Cores: 68-79 Rims: 54-74	olv (2a,2b), plg (4, 5)	X	
	5		Sieved cores reverse and normal zoned. ~30% enclave 1 (olv)	Cores: 67-78 Rims: 59-65	plg (4,5)	X	
	6	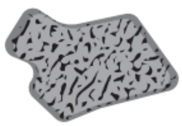	Extra large highly fractured and normally zoned. ~10% enclave 1(olv)	Rims: 62-66	Solo	X	
	7		Extra small and normally zoned. ~100% enclave 2 (opx)	Cores: 62-72	Completely crystaline		X
	Population	**Texture**	**Description**	**Mg#**	**found in clots with**	**1**	**2**
Orthopyroxene	5		Extra small assumed normal zoning. ~100% enclave 2 (opx)	Cores: 61-70	Completely Crystaline		X
	Population	**Texture**	**Description**	**Fo**	**found in clots with**	**1**	**2**
Olivine	2a		Normal zoning with moderate Fo content. ~90% enclave 1 (olv)	Cores: 80-82 Rims: 72-78	olv (2a,2b), plg (4)	X	
	2b		Normal zoning with low Fo content. ~10% enclave 1 (olv)	Cores: 76 Rims: 70	olv (2a,2b), plg (4)	X	

Figure 30. An illustrated summary table of all mineral populations identified within enclaves in alc.

4.3.2.1. Plagioclase

Plagioclase populations 4-6 are only found in the olivine-bearing enclaves (Type I). Plagioclase population 4 is characterized by coarse oscillatory zoning with alternating reverse and normal zones. This population has core An_{68-79} and rim An_{54-74}. Plagioclase population 5 is characterized by sieved crystals that are normal and reversely zoned. This population has core An_{67-78} and rim An_{59-65}. Plagioclase population 6 is characterized by large (>500 µm) highly fractured normally zone crystals. This population has unreliable core analysis and rim An_{62-66}.

Plagioclase population 7 is only found in the orthopyroxene-bearing enclaves (Type II). Plagioclase population 7 is characterized by extra small (<150 µm) This population has core An_{62-72}.

	Population	Texture	Description	An	found in clots with	1	2
Plagioclase	4		Coarse oscilatory zoning with alternating normal and reverse zoning ~60% enclave 1 (olv)	Cores: 68-79 Rims: 54-74	olv (2a,2b), plg (4, 5)	X	
	5		Sieved cores reverse and normal zoned. ~30% enclave 1 (olv)	Cores: 67-78 Rims: 59-65	plg (4,5)	X	
	6		Extra large highly fractured and normally zoned. ~10% enclave 1(olv)	Rims: 62-66	Solo	X	
	7	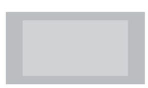	Extra small and normally zoned. ~100% enclave 2 (opx)	Cores: 62-72	Completely crystaline		X

Figure 31. An illustrated summary table showing mineral populations identified in enclaves in alc.

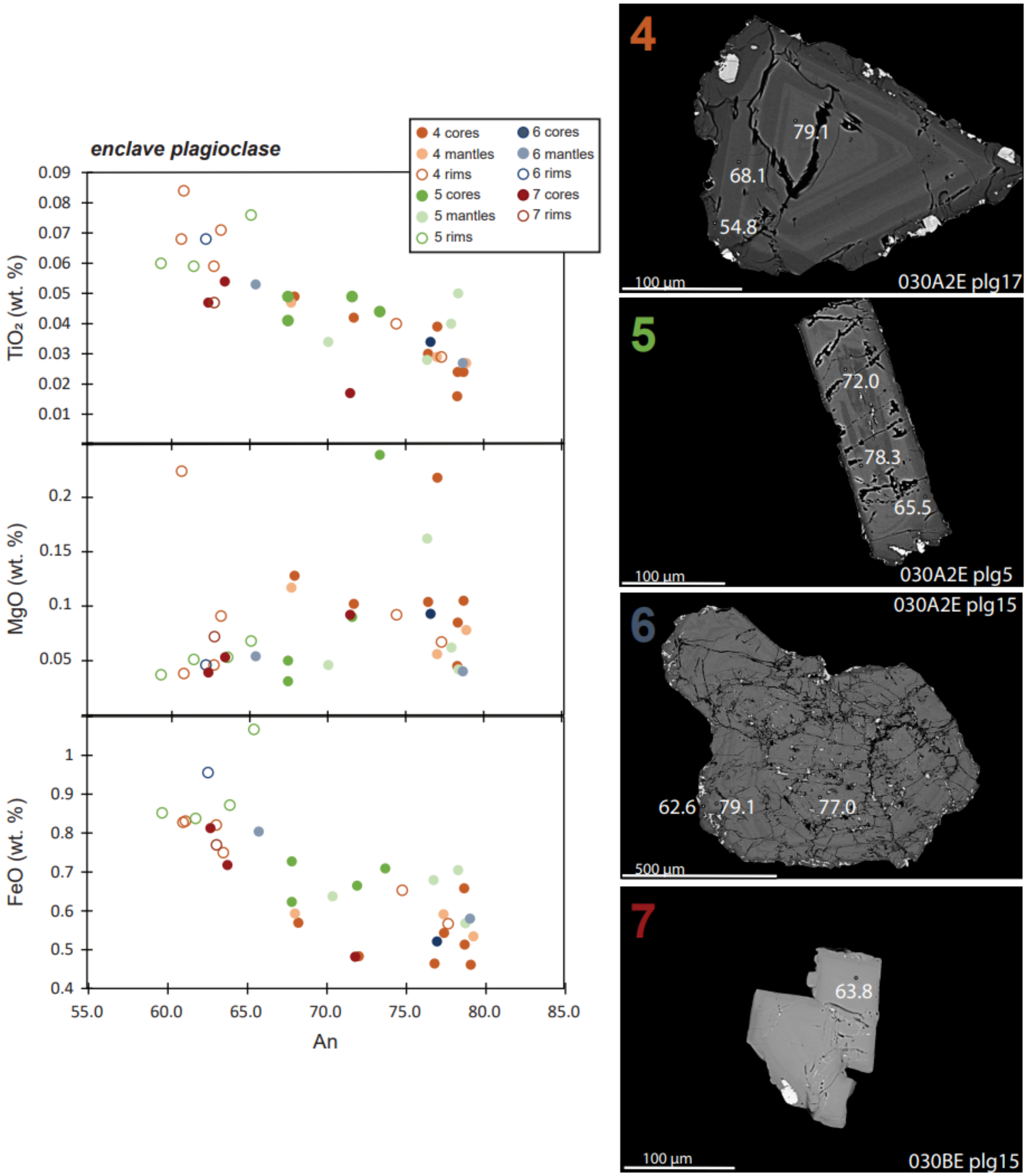

Figure 32. Plots displaying enclave plagioclase compositions. An is plotted on the x-axis and various minor element oxides are plotted on the y-axis. Legend is shown in upper right corner.

4.3.2.2. Orthopyroxene

Orthopyroxene population 5 is only found in the orthopyroxene-bearing enclaves (Type II). Orthopyroxene population 5 is characterized by small (<150 µm) crystals with low Mg# cores. This population has core $Mg\#_{62-72}$. Orthopyroxene population 5 is plotted with host orthopyroxene, see Figure 24.

	Population	Texture	Description	Mg#	found in clots with	1	2
Orthopyroxene	5		Extra small assumed normal zoning. ~100% enclave 2 (opx)	Cores: 61-70	Completely Crystaline		X

Figure 33. An illustrated summary table of orthopyroxene populations identified in enclaves in alc.

4.3.2.3. Olivine

Olivine population 2 is only found in the olivine-bearing enclaves (Type I) and is subdivided into populations 2a and 2b. Olivine population 2a is characterized by normal zoning with moderate Fo content. This population has core Fo_{80-82} and rim Fo_{72-78}. Olivine population 2b is characterized by low Fo content. This population has core Fo_{76} and rim Fo_{70}.

	Population	Texture	Description	Fo	found in clots with	1	2
Olivine	2a		Normal zoning with moderate Fo content. ~90% enclave 1 (olv)	Cores: 80-82 Rims: 72-78	olv (2a,2b), plg (4)	X	
	2b		Normal zoning with low Fo content. ~10% enclave 1 (olv)	Cores: 76 Rims: 70	olv (2a,2b), plg (4)	X	

Figure 34. An illustrated summary table of olivine populations present in enclaves in alc.

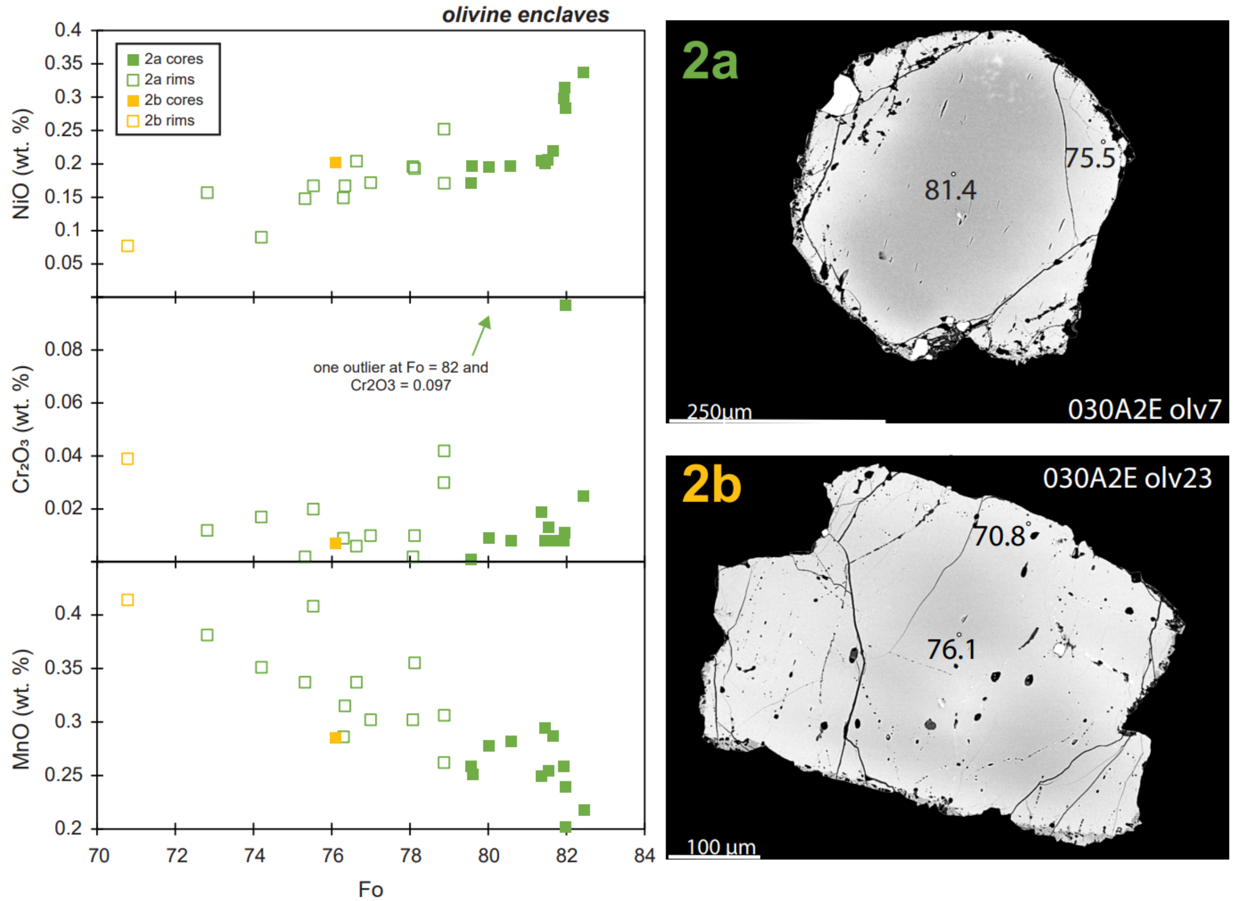

Figure 35. Plots displaying enclave olivine compositions. Fo content is plotted on the x-axis and various minor element concentrations are plotted on the y-axis.

5. Discussion

5.1 Mineral Populations

5.1.1 Plagioclase

Plagioclase populations 1a and 1b are present in both alc and alg. The cores of this population plot within the same compositional range for both units (Fig. 23). This strong correlation of cores indicates that this population likely share the same parental source.

Plagioclase population 2 is also identified in both alc and alg. This population is present in very similar crystal clots in both units (Fig. 21). Compositionally, this population contains a slightly lower anorthite content than population 1 (Fig. 23). Due to this slight difference in anorthite content it is likely that plagioclase population 2 likely originates from a more evolved, shallower source, which could be the same source for both units.

Plagioclase population 3 is unique to alg suggesting alg may have a slightly different history that could be associated with differentiation or mixing.

Plagioclase rims exhibit the final stage of growth before eruption. All plagioclase populations rims cluster in the same region in An vs. MgO, FeO, and TiO_2 suggesting that magmas experienced a final homogenization event before eruption.

5.1.2 Clinopyroxene

Clinopyroxene population 1a is present in alc and populations 1b and 1c are present in alg. These populations consistently plot together and are interpreted to originate from the same parent source (Fig. 25). Unit alg populations 1b and 1c experienced more time to react and grow reaction rims than alc populations. Other than reaction features, populations 1a, 1b, and 1c are interpreted to be the same, suggesting they could have originated from the same parent source.

Clinopyroxene populations 2a and 2b share a similar reaction discrepancy as population 1. Population 2a is found in alc with no reaction features. However, 2b found in alg contains a fine reaction rim. Cores and outer mantles from both populations consistently plot together suggesting they likely originated from the same parent source (Fig. 25). Unit alg populations experienced a greater time to react and grow reaction features.

Clinopyroxene population 3 is present in both alc and alg. This population consists of a possible second grouping of clinopyroxene outliers. Population 3 exhibits much more complex zoning than other populations but does not exhibit a clear source as its outer mantles consistently plot with other clinopyroxene. It is unclear where this population originated from with the given data.

All clinopyroxene populations plot extremely similarly, which makes it difficult to differentiate potential origins between populations. Further trace element analysis is required to discern between populations and determine potential origins and sourcing populations.

5.1.3 Orthopyroxene

Orthopyroxene populations 1a and 1b share a similar reaction discrepancy as clinopyroxene populations. Specifically, population 1a is found in alc with no reaction features. However, 1b found in alg contains a fine reaction rim. Cores and outer mantles from both populations consistently plot together suggesting they originated from the same parent source (Fig. 27). Unit alg populations experienced a greater time to react and grow reaction features.

Orthopyroxene population 2a is present in alc, populations 2b is present in alg. These populations consistently plot together and are interpreted to originate from the same parent source (Fig. 27). Population 2b, which is present in alg, experienced more time to react and grow a reaction rim than the 2a alc populations. Other than reaction features, populations 2a and 2b are interpreted to be the same and population.

Orthopyroxene populations 2c and 3 only present in alg consistently plot with other orthopyroxene populations (Fig. 27). Origins of these populations are difficult to determine due to populations largely clustering in the same area.

Orthopyroxene population 4 consists of a reaction rim around olivine only present in alg.

Further trace element analysis is needed to determine more specific trends, origins, and sourcing within orthopyroxene populations for units alc and alg.

5.1.4 Olivine

Olivine population 1 is only present in alg with a heavily reacted orthopyroxene rim. The source for this population remains unclear. Additional work is needed to determine sourcing and origins.

5.1.5 Enclaves or Lithic Fragments

Two types of enclaves were identified in alc. These enclaves were the only enclave samples successfully sampled during slide making, but field observations reveal a wider variety of enclaves (e.g., Fig. 11), therefore further work is needed. However, preliminary work in this study suggests that enclaves contain their own subset of mineral populations that are not identified in the host, alc (Fig. 30). Since data here do not show shared crystal cargos nor physical evidence for mixing (e.g., banding, mingling features), it is likely that alc did not undergo a liquid mixing event, rendering these enclaves as lithic fragments instead. These lithic fragments were likely incorporated into the magma during the final stages before eruption.

5.2 Magmatic System Implications

5.2.1 South Sister (alg)

The South Sister unit alg contains a slightly more complicated crystal cargo to unit alc. Unit alg contains more mineral populations across every mineral phase (Fig. 23), more complex clots (Fig. 24), and reaction rims present throughout several mineral phases. Findings from this study reflect a strong possibility that alg likely tapped into an alternative source that is not represented in alc. Crystals in alg reflect more time to react to a mobilizing liquid based on the presence of reaction rims throughout this unit.

5.2.2 Middle Sister (alc)

The Middle Sister unit alc tells a slightly less complicated story through its crystals. This unit contains the same dominant populations as alg. However, alc contains what is believed to be enclaves or lithic fragments. These enclaves or lithic fragments do not appear to alter this unit's chemistry. At some point before eruption this unit interacted with or possibly mixed with another mush or magma body picking up these enclaves or lithic fragments.

5.2.3 System Interconnectivity

Dominant plagioclase and pyroxene populations appear to be the same in alc and alg. Specifically, data shown here suggest that the west flank units of alc and alg share the same parent source and pre-eruptive homogenization. Furthermore, plagioclase data suggests shared sourcing at depth with population 1 and shared shallower sourcing with population 2. Unit alg exhibits a slightly different differentiation process seen through several mineral populations and reaction rims not present in alc. Though there are slight differences, these two units most likely share the same parent source. However, interpretations for this study are largely based on plagioclase data, due to the unclear nature of pyroxene data. Further trace element analysis is needed for more complete understanding.

6. Conclusion

This project compared two temporally related andesites on the west flank Middle Sister and South Sister in the Three Sisters Wilderness Area in central Oregon. Major and minor chemical analysis of dominant mineral phases, along with careful examination of mineral textures and clots, suggests that the two andesite from Middle Sister and South Sister shared both a deeper and shallower a reservoir system on the west flanks of these volcanoes ca. 27 ka. Evidence for this interconnectivity is best seen in plagioclase data. To further constrain the roots of this system, pyroxene trace element analysis is needed. Additional comparison between different compositional units can further discern potential plumbing system connections within the crust. This would also begin to shed light on major magmatic processes at play and the extent of interconnectivity between the two peaks.

References

Calvert, A. T., Fierstein, J. & Hildreth, W. (2018). Eruptive history of Middle Sister, Oregon Cascades, USA–Product of a late Pleistocene eruptive episode. *Geosphere* **14**, 2118–2139.

Carlson, R. W. & Hart, W. K. (1987). Crustal genesis on the Oregon Plateau. *Journal of Geophysical Research* **92**, 6191.

Cashman, K. V., Sparks, R. S. J. & Blundy, J. D. (2017). Vertically extensive and unstable magmatic systems: A unified view of igneous processes. *Science* **355**, eaag3055.

Conrey, R. M., Bailey, D. G., Singer, J. W., Wagoner, L., Parfitt, B., Hay, J. & Keh, O. (2019). Combined use of multiple internal and external standards in LA-ICPMS analysis of geologic samples using lithium borate fused glass. AGU Fall Meeting.

Eaton, G. P. (1982). The Basin and Range Province: Origin and Tectonic Significance. *Annual Review of Earth and Planetary Sciences* **10**, 409–440.

Fierstein, J., Hildreth, W. & Calvert, A. T. (2011). Eruptive history of South Sister, Oregon Cascades. *Journal of Volcanology and Geothermal Research* **207**, 145–179.

Fitton, J. G., James, D. & Leeman, W. P. (1991). Basic magmatism associated with Late Cenozoic extension in the western United States: Compositional variations in space and time. *Journal of Geophysical Research: Solid Earth* **96**, 13693–13711.

Ford, M. T., Grunder, A. L. & Duncan, R. A. (2013). Bimodal volcanism of the High Lava Plains and Northwestern Basin and Range of Oregon: Distribution and tectonic implications of age-progressive rhyolites: Age-Progressive Rhyolites of Oregon. *Geochemistry, Geophysics, Geosystems* **14**, 2836–2857.

Hildreth, W., Fierstein, J. & Calvert, A. T. (2012). Geologic Map of Three Sisters Volcanic Cluster, Cascade Range, Oregon. Scientific Investigations Map. USGS.

Jordan, B. T., Grunder, A. L., Duncan, R. A. & Deino, A. L. (2004). Geochronology of age-progressive volcanism of the Oregon High Lava Plains: Implications for the plume interpretation of Yellowstone. *Journal of Geophysical Research: Solid Earth* **109**, B10202.

Kent, A. J. R. (2014). Preferential eruption of andesitic magmas: Implications for volcanic magma fluxes at convergent margins. *Geological Society, London, Special Publications* **385**, 257–280.

Le Maitre, R. W. (1984). A proposal by the IUGS Subcommission on the Systematics of Igneous Rocks for a chemical classification of volcanic rocks based on the total alkali silica (TAS) diagram. *Australian Journal of Earth Sciences* **31**, 243–255.

Leeman, W. P. (2020). Old/New Subduction Zone Paradigms as Seen From the Cascades. *Frontiers in Earth Science* **8**, 535879.

MacLeod, N. S., Sherrod, D. R. & Jensen, R. A. (1995). Geologic Map of Newberry Volcano, Deschutes, Klamath, and Lake Counties, Oregon. US Geological Survey.

Peale, J. S. (2023). Using two coeval andesites from Middle Sister and South Sisters, Oregon, as clues to understanding connectivity at adjacent, coincident stratovolcanoes. B.S. Thesis, *Western Washington University*.

Shoemaker, K. A. & Hart, W. K. (2002). Temporal Controls on Basalt Genesis and Evolution on the Owyhee Plateau, Idaho and Oregon. In: Bonnichsen, B., White, C. M. & McCurry, M. (eds) Tectonic and Magmatic Evolution of the Snake River Plain Volcanic Province, 313–328.

Walker, G. W. & MacLeod, N. S. (1991). Geologic Map of Oregon. Geologic map of Oregon. *US Geological Survey*.

Weaver, C. S. & Baker, G. E. (1988). Geometry of the Juan de Fuca plate beneath Washington and northern Oregon from seismicity. *Bulletin of the Seismological Society of America* **78**, 264–275.

Wilson, D. S. (1993). Confidence intervals for motion and deformation of the Juan de Fuca plate. *Journal of Geophysical Research: Solid Earth* **98**, 16053–16071.

Appendix

I. Table A1. Whole Rock Data

Sample	TSO-30c	TSO-029B	TSO-075.1b	TSO-032B
Unit	alc	alc	alc	alg
		XRF		
SiO2	61.99	62.03	62.20	62.48
TiO2	1.22	1.21	1.23	1.15
Al2O3	16.34	16.38	16.26	16.41
FeO	6.46	6.36	6.26	6.07
MnO	0.13	0.13	0.13	0.11
MgO	1.97	1.97	2.00	1.97
CaO	4.70	4.66	4.71	4.61
Na2O	5.19	5.23	5.16	5.04
K2O	1.71	1.73	1.74	1.85
P2O5	0.30	0.31	0.31	0.30
LOI (%)	-0.1	-0.17	0.06	-0.17
total	99.33	99.38	99.21	98.96
F >=	0.09	0.11	n.d.	0.10
Cl >=	0.04	0.05	0.03	0.01
SO3 >=	0.03	0.03	n.d.	0.01
Br >=	1.21	1.31	3.34	0.51
As >=	0.00	0.00	3.45	2.02
Ni_XRF	0.51	0.09	3.37	3.54
Cr_XRF	3.10	2.10	7.28	5.40
V_XRF	117.30	115.31	121.58	114.31
Sc_XRF	17.03	16.63	18.35	16.14
Cu_XRF	11.92	13.64	11.63	18.67
Zn_XRF	82.27	82.74	83.64	74.37
Ga_XRF	19.49	20.40	18.91	17.78
Ba_XRF	524.53	535.45	539.18	543.31
Rb_XRF	29.24	30.56	30.53	33.31
Cs_XRF	2.42	2.12	4.44	0.00
Sr_XRF	429.34	424.49	428.93	392.52
Y_XRF	26.97	28.89	27.97	27.47
Zr_XRF	196.30	199.51	197.51	211.51
Hf_XRF	4.26	4.60	5.34	5.30
Nb_XRF	9.79	10.25	9.56	9.68
Ta_XRF	0.62	1.18	0.62	0.66
Mo_XRF	1.97	4.00	1.45	1.97
La_XRF	14.35	18.46	18.44	16.79
Ce_XRF	39.20	39.49	41.44	36.93
Nd_XRF	24.24	22.93	24.54	20.71
Sm_XRF	5.66	5.30	4.53	4.82
Dy_XRF	4.45	4.92	4.78	4.86
Yb_XRF	2.34	2.62	1.80	2.76
Th_XRF	3.05	2.32	2.27	2.84
U_XRF	2.81	1.61	2.21	1.04
Tl_XRF	0.00	0.10	n.d.	0.00
Pb_XRF	4.40	7.04	5.40	7.70
Sn_XRF	0.91	1.11	2.62	0.00
Bi_XRF	1.41	0.00	0.04	0.00
Sb_XRF	0.00	1.49	1.86	0.00

Sample	TSO-30c	TSO-029B	TSO-075.1b	TSO-032B
Unit	alc	alc	alc	alg
		ICPMS		
Ag	0.05	0.04	0.04	0.05
As	1.13	2.33	1.25	0.87
Ba	526.57	535.77	525.02	542.04
Bi	0.08	0.07	0.10	0.03
Cd	0.07	0.05	0.07	0.05
Cr	1.27	0.70	6.02	4.94
Cs	1.13	1.17	1.15	0.73
Cu	8.04	10.73	11.43	15.03
Ga	19.92	20.07	20.04	19.62
Ge	1.25	1.32	1.49	1.26
Hf	4.74	4.92	4.83	5.08
Mo	1.83	1.70	1.64	1.66
Nb	9.33	9.48	9.49	9.08
Ni	2.88	2.41	3.40	4.60
Pb	6.09	6.05	5.81	5.51
Rb	29.58	30.30	30.74	32.87
Sb	0.39	0.46	5.13	0.44
Sc	16.91	16.81	16.81	15.89
Sn	1.47	1.53	1.56	1.55
Sr	427.61	424.49	426.94	388.68
Ta	0.59	0.59	0.70	0.58
Th	2.96	3.05	3.02	3.22
Tl	0.14	0.14	0.12	0.19
U	1.14	1.19	1.15	1.30
V	119.94	117.39	115.34	114.10
Y	27.13	27.72	27.90	27.11
Zn	84.25	83.84	83.64	74.06
Zr	196.56	201.49	199.34	212.11
La	17.36	17.49	17.77	17.08
Ce	37.70	38.45	38.91	38.06
Pr	4.95	5.10	5.13	5.02
Nd	21.72	21.84	21.76	21.58
Sm	4.97	5.21	5.09	5.08
Eu	1.60	1.62	1.66	1.50
Gd	4.92	5.05	5.26	4.95
Tb	0.79	0.82	0.84	0.82
Dy	4.78	4.78	4.79	4.67
Ho	0.97	0.99	1.00	0.98
Er	2.74	2.77	2.83	2.75
Tm	0.41	0.43	0.44	0.41
Yb	2.68	2.68	2.77	2.70
Lu	0.39	0.40	0.39	0.40

II. Table A2. Petrographic Summary

groundmass	plagioclase (plg)	olivine (olv)	clinopyroxene (cpx)	orthopyroxene (opx)	oxides (ox)	clots
alg (west flank of South Sister); sample TSO-032A (~15% phenocrysts)						
Holocrystalline; out of visible crystals: ~90% plg, euhedral, narrow elongate crystals, locally oriented; ~9% oxides, subhedral, equant, rounded; ~1% pyroxenes, anhedral, rounded; no twinning or zoning identified in any groundmass crystals	~9%, 0.25-2.5 mm in diameter, predominantly tabular but some are bladed, randomly oriented, individual crystals are euhedral but in clots they are subhedral to euhedral, osc zoning is found in individual crystals and clots, poly twins in individual crystals and in clots, unsieved to coarse sieving present in individual crystals and clots, plg is more commonly be found in plg+plg or plg+cpx+opx+ox clots, some single phenos		~3%, 0.25-1 mm in diameter, euhedral to subhedral, equant to blocky, randomly oriented, unzoned, commonly poly twinned, unsieved, mostly in cpx+opx+plg clots, some found as single phenos	~1%, 0.25-0.75 mm in diameter, blocky to equant, euhedral to anhedral, no zoning, no twining, unsieved to very coarsely sieved, most commonly present in opx+cpx+plg clots, few single phenos	~2%, 0.25-0.75 mm in diameter, equant, subhedral, most commonly present in plg+cpx+opx+ox, some present as single phenos, some found as inclusions in pxn	two types total: (1) plg+cpx+opx+ox ≤4.5 mm, and (2) most common plg+ox ≤2.5 mm (3) cpx+plg+ox ≤ 1mm (4) opx+plg+ox ≤ 1.25mm (5) opx+cpx+ox ≤ 1mm
alc (west flank of Middle Sister); samples TSO-030A1, A2, A3, B (~15% phenocrysts)						
~70% cryptocrystalline and ~30% holocrystalline; out of visible crystals: ~95% plg, euhedral, narrow, and elongate crystals, locally oriented; ~4% oxides, subhedral, equant, and rounded crystals; ~1% mafic minerals, anhedral and rounded; no twinning or zoning identified in any groundmass crystals	~9%, 0.25-4 mm in diameter, euhedral, tabular to equant to elongate, randomly oriented, poly twinned and osc zoning found in individual crystals and in clot crystals, Most crystals unsieved, some individual coarsely sieved crystals, most commonly found as single phenos or plg+plg+ox clots, also found in plg+cpx+opx+ox clots		~2.5%, 0.25-1 mm in diameter, euhedral, equant to blocky, randomly oriented, some zoned, no twinning, unsieved, most commonly found in clots plg+cpx, also found in cpx+opx+plg+ox clots, some single-phenos present	~1% 0.25-0.5mm, euhedral to subhedral, blocky, unzoned, unsieved, no twining, most commonly in clots with cpx+ox, also found in clots with plg+cpx+ox, sparse single pheno	~2.5%, 0.25-0.5 mm in diameter, subhedral, equant to blocky, most commonly present as single phenos but also commonly found in clots plg+opx+ox clots, plg+opx, cpx+opx+ox	three types total: (1) plg+cpx+opx+ox ≤1 mm in diameter, (2) plg+ox ≤0.5 mm, (3) cpx+opx+ox ≤0.25 in diameter (4) cpx+plg+ox ≤1 mm diameter,(5) opx+plg+ox ≤1mm diameter
alc - olivine bearing enclave (Type I); sample TSO-030A2 (~5% phenocrysts)						
	~3%, 0.25-1 mm in diameter, sub-anhedral, tabular to elongate, randomly oriented, poly twinned, some osc zoned, unsieved, most commonly found in plg+plg+ox clots or single phenos, also in plg+olv+ox clots	~2%, 0.25-1.25 mm in diameter, subhedral, rhombohedral, randomly oriented, unzoned, no twining, unsieved, most commonly found as single phenos, also found in olv+plg clots, some in phenos and clots reacting into opx			~1%, ≤0.25 mm in diameter, subhedral, equant to rounded, most commonly found as single phenos, also found in clots with plg+olv+ox, also found in plg+plg+ox clots	two types total: (1) plg+plg+ox ≤3 mm, (2) plg+olv+ox ≤3.25 mm

III. EMPA Data Tables

i. Table A3. Plagioclase EMPA Data

Unit	Population	Location	SiO2	TiO2	Al2O3	FeO	MgO	CaO	Na2O	K2O	Total	An	Ab	Or
alg														
032A_plg010	1a	core	51.94	0.053	30.90	0.62	0.06	13.55	3.70	0.11	100.92	66.5	32.8	0.6
032A_plg008	3	core	55.89	0.045	27.58	0.52	0.06	9.54	5.62	0.22	99.46	47.8	50.9	1.3
032A_plg007	3	core	55.01	0.055	28.34	0.54	0.06	10.62	4.93	0.19	99.75	53.7	45.1	1.1
032A_plg003	2	core	57.23	0.055	27.60	0.50	0.06	9.57	5.50	0.23	100.74	48.3	50.3	1.4
032A_plg011	1a	core	52.44	0.049	30.35	0.63	0.06	12.73	4.10	0.13	100.48	62.7	36.5	0.8
032A_plg012	1a	core	52.29	0.045	31.27	0.60	0.06	13.62	3.39	0.10	101.37	68.5	30.8	0.6
032A_plg014	1a	core	51.45	0.049	31.32	0.54	0.06	13.87	3.34	0.10	100.72	69.2	30.2	0.6
032A_plg015	1a	core	53.36	0.047	29.74	0.59	0.06	11.78	4.45	0.14	100.16	58.9	40.2	0.8
032A_plg016	1b	core	50.21	0.033	31.87	0.53	0.05	14.45	3.19	0.10	100.44	71.0	28.4	0.6
032A_plg018	1a	core	51.47	0.049	31.38	0.64	0.06	14.00	3.23	0.10	100.92	70.1	29.3	0.6
032A_plg019	1a	core	52.67	0.059	30.32	0.60	0.07	12.73	3.92	0.12	100.48	63.8	35.5	0.7
032A_plg020	1a	core	50.86	0.049	31.29	0.71	0.06	14.06	3.24	0.08	100.35	70.2	29.3	0.5
032A_plg022	2	core	56.28	0.047	27.86	0.48	0.06	9.62	5.50	0.24	100.09	48.4	50.1	1.4
032A_plg023	1b	core	51.94	0.051	31.24	0.62	0.06	13.66	3.49	0.09	101.16	68.0	31.4	0.6
032A_plg024	1a	core	51.10	0.048	31.05	0.63	0.07	13.71	3.58	0.10	100.28	67.5	31.9	0.6
032A_plg028	1b	core	52.33	0.051	30.73	0.61	0.06	13.34	3.71	0.12	100.95	66.1	33.2	0.7
032A_plg031	2	core	56.91	0.035	27.38	0.53	0.06	9.24	5.81	0.24	100.19	46.1	52.5	1.4
032A_plg032	3	core	56.18	0.041	27.83	0.49	0.06	9.95	5.58	0.21	100.34	49.0	49.8	1.3
032A_plg033	1a	core	52.11	0.061	30.39	0.58	0.07	12.95	3.77	0.14	100.08	65.0	34.2	0.8
032A_plg034	1a	core	52.41	0.055	30.93	0.61	0.07	13.16	3.65	0.12	100.99	66.1	33.2	0.7
032A_plg038	1a	core	49.77	0.027	32.22	0.56	0.04	15.11	2.76	0.07	100.56	74.8	24.7	0.4
032A_plg039	2	core	56.71	0.044	27.49	0.54	0.05	9.24	5.75	0.25	100.06	46.3	52.2	1.5
032A_plg045	1b	core	52.32	0.054	30.70	0.58	0.06	12.84	3.88	0.11	100.55	64.2	35.1	0.7
032A_plg042	1b	core	51.26	0.047	31.92	0.65	0.08	14.61	3.18	0.09	101.82	71.4	28.1	0.5
032A_plg041	1b	core	51.99	0.055	31.17	0.58	0.06	13.52	3.57	0.11	101.06	67.2	32.1	0.7
032A_plg031	2	mantle	56.48	0.058	28.05	0.57	0.07	10.10	5.34	0.19	100.86	50.5	48.3	1.1
032A_plg022	2	mantle	54.86	0.066	28.47	0.62	0.06	10.51	5.04	0.23	99.85	52.8	45.8	1.4
032A_plg003	2	rim	55.23	0.053	28.52	0.57	0.07	10.50	5.04	0.21	100.18	52.9	45.9	1.3
032A_plg007	3	rim	54.97	0.055	28.54	0.59	0.06	10.68	5.17	0.21	100.28	52.6	46.1	1.2
032A_plg008	3	rim	55.31	0.069	28.08	0.56	0.07	10.04	5.33	0.21	99.67	50.3	48.4	1.3
032A_plg010	1a	rim	55.67	0.054	28.79	0.58	0.06	10.74	5.02	0.20	101.11	53.5	45.3	1.2
032A_plg011	1a	rim	55.59	0.057	28.45	0.55	0.06	10.68	5.07	0.20	100.66	53.1	45.7	1.2
032A_plg012	1a	rim	55.78	0.064	28.26	0.63	0.07	10.27	5.14	0.22	100.43	51.8	46.9	1.3
032A_plg014	1a	rim	54.71	0.053	28.46	0.58	0.06	10.51	5.12	0.18	99.67	52.6	46.3	1.1
032A_plg015	1a	rim	55.85	0.055	28.72	0.61	0.07	10.62	5.06	0.19	101.17	53.1	45.8	1.1
032A_plg016	1b	rim	55.65	0.046	28.11	0.51	0.06	10.10	5.35	0.20	100.02	50.5	48.4	1.2
032A_plg018	1a	rim	54.81	0.056	28.29	0.59	0.06	10.24	5.27	0.24	99.56	51.0	47.6	1.4
032A_plg019	1a	rim	55.73	0.054	28.30	0.58	0.06	9.99	5.32	0.23	100.27	50.2	48.4	1.4
032A_plg020	1a	rim	55.51	0.054	28.48	0.66	0.06	10.64	5.15	0.23	100.78	52.6	46.1	1.3
032A_plg023	1b	rim	54.39	0.053	28.80	0.59	0.06	11.00	4.80	0.18	99.87	55.3	43.7	1.1
032A_plg024	1a	rim	54.46	0.052	28.48	0.58	0.07	10.85	4.95	0.17	99.61	54.2	44.8	1.0
032A_plg028	1b	rim	54.89	0.049	28.64	0.53	0.06	10.61	4.93	0.20	99.90	53.7	45.1	1.2
032A_plg031	2	rim	59.00	0.088	25.84	0.79	0.06	7.44	6.69	0.47	100.37	37.0	60.2	2.8

032A_plg032	3	rim	55.84	0.045	28.70	0.58	0.06	10.47	5.28	0.21	101.18	51.6	47.1	1.3
032A_plg033	1a	rim	54.47	0.055	29.10	0.55	0.07	10.90	4.82	0.18	100.13	55.0	44.0	1.1
032A_plg034	1a	rim	55.72	0.072	28.37	0.58	0.07	10.57	5.05	0.19	100.62	53.0	45.9	1.1
032A_plg038	1a	rim	56.01	0.05	28.51	0.58	0.06	10.69	5.00	0.23	101.12	53.4	45.2	1.4
032A_plg039	1b	rim	55.84	0.05	27.77	0.60	0.06	9.78	5.52	0.25	99.87	48.7	49.8	1.5
032A_plg042	1b	rim	55.17	0.073	28.31	0.79	0.06	10.57	5.03	0.21	100.22	53.1	45.7	1.3
032A_plg041	1b	rim	56.77	0.055	28.29	0.59	0.07	10.51	5.12	0.19	101.59	52.6	46.3	1.1
032A_plg045	1a	rim	54.94	0.054	28.84	0.61	0.07	10.90	4.98	0.20	100.58	54.1	44.8	1.2
Unit	**Population**	**Location**	**SiO2**	**TiO2**	**Al2O3**	**FeO**	**MgO**	**CaO**	**Na2O**	**K2O**	**Total**	**An**	**Ab**	**Or**
alc														
030B_plg001	2	core	55.06	0.066	28.43	0.57	0.06	10.17	5.23	0.15	99.73	51.3	47.8	0.9
030B_plg002	2	core	55.97	0.058	28.69	0.58	0.06	10.64	5.14	0.17	101.30	52.8	46.2	1.0
030B_plg008	2	core	55.99	0.053	28.40	0.50	0.06	10.21	5.18	0.19	100.58	51.6	47.3	1.1
030B_plg011	1b	core	50.20	0.037	31.91	0.64	0.06	14.58	2.93	0.07	100.42	73.0	26.6	0.4
030B_plg012	1b	core	52.12	0.049	30.93	0.62	0.06	12.93	3.91	0.14	100.74	64.1	35.1	0.8
030B_plg020	1a	core	52.43	0.052	30.58	0.61	0.06	12.77	3.81	0.14	100.45	64.4	34.8	0.8
030B_plg021	1a	core	50.50	0.048	32.02	0.63	0.05	14.67	2.99	0.07	100.97	72.8	26.8	0.4
030B_plg018	1a	core	57.19	0.058	27.28	0.56	0.06	9.00	5.77	0.23	100.13	45.7	53.0	1.4
030B_plg024	1a	core	53.80	0.061	29.08	0.58	0.06	11.20	4.54	0.16	99.49	57.1	41.9	0.9
030B_plg027	2	core	54.27	0.052	29.03	0.56	0.06	11.17	4.98	0.16	100.28	54.8	44.2	0.9
030B_plg028	2	core	54.85	0.051	28.67	0.58	0.07	10.57	5.10	0.18	100.06	52.8	46.1	1.1
030B_plg029	2	core	54.98	0.067	28.50	0.56	0.07	10.49	5.20	0.18	100.04	52.2	46.8	1.0
030B_plg030	2	core	54.78	0.074	28.28	0.57	0.07	10.35	5.21	0.19	99.51	51.7	47.1	1.1
030B_plg026	1b	core	51.68	0.045	31.26	0.57	0.05	13.52	3.55	0.10	100.79	67.4	32.0	0.6
030B_plg033	2	core	55.59	0.061	28.28	0.54	0.06	10.16	5.41	0.18	100.29	50.4	48.6	1.1
030B_plg035	2	core	55.79	0.048	28.03	0.55	0.07	9.93	5.32	0.19	99.93	50.2	48.7	1.2
030B_plg035.5	2	mantle	52.36	0.062	30.89	0.50	0.05	13.23	3.79	0.11	100.99	65.4	33.9	0.6
030B_plg036	2	core	55.46	0.054	28.40	0.60	0.06	10.28	5.12	0.20	100.18	51.9	46.8	1.2
030B_plg039	1b	core	51.35	0.049	30.87	0.64	0.07	12.94	3.85	0.10	99.88	64.6	34.8	0.6
030B_plg018	1a	rim	56.44	0.063	28.37	0.53	0.06	10.72	5.05	0.19	101.42	53.4	45.5	1.1
030B_plg001	2	rim	54.71	0.047	28.82	0.55	0.06	10.92	4.96	0.20	100.27	54.2	44.6	1.2
030B_plg002	2	rim	54.83	0.069	28.91	0.59	0.06	10.52	5.04	0.17	100.19	53.0	46.0	1.0
030B_plg008	3	rim	54.84	0.06	29.09	0.59	0.05	10.85	4.87	0.25	100.59	54.4	44.2	1.5
030B_plg011	1a	rim	54.09	0.059	29.02	0.59	0.06	11.40	4.65	0.17	100.03	57.0	42.1	1.0
030B_plg012	1a	rim	54.84	0.066	28.93	0.55	0.04	10.80	4.87	0.24	100.33	54.3	44.3	1.4
030B_plg020	1a	rim	54.97	0.061	28.68	0.62	0.06	10.78	4.91	0.17	100.25	54.3	44.7	1.0
030B_plg021	1a	rim	54.04	0.067	29.17	0.57	0.06	11.43	4.73	0.15	100.22	56.7	42.4	0.9
030B_plg024	1a	core	54.45	0.051	28.81	0.61	0.05	10.62	4.96	0.23	99.78	53.4	45.2	1.4
030B_plg027	2	rim	55.15	0.056	28.79	0.57	0.06	10.64	5.01	0.21	100.48	53.3	45.4	1.3
030B_plg028	2	rim	54.87	0.051	28.97	0.60	0.06	10.89	4.74	0.21	100.39	55.2	43.5	1.3
030B_plg029	2	rim	55.18	0.059	28.70	0.54	0.06	10.82	5.05	0.20	100.60	53.6	45.2	1.2
030B_plg030	2	rim	54.82	0.052	28.43	0.64	0.05	10.63	5.06	0.23	99.91	53.0	45.6	1.4
030B_plg026	1b	rim	55.65	0.047	28.90	0.56	0.06	10.73	5.06	0.23	101.22	53.2	45.4	1.3
030B_plg033	2	rim	54.83	0.051	29.04	0.63	0.05	10.87	4.80	0.23	100.50	54.8	43.8	1.4
030B_plg035	2	rim	55.90	0.063	28.62	0.62	0.07	10.50	5.16	0.20	101.13	52.3	46.5	1.2
030B_plg035.5	2	rim	56.36	0.062	28.46	0.57	0.06	10.57	5.12	0.22	101.41	52.6	46.1	1.3
030B_plg036	2	rim	54.12	0.055	29.16	0.59	0.04	10.65	4.99	0.22	99.83	53.4	45.3	1.3
030B_plg039	1b	rim	55.27	0.066	28.45	0.59	0.05	10.54	5.00	0.23	100.18	53.1	45.6	1.4
Unit	**Population**	**Location**	**SiO2**	**TiO2**	**Al2O3**	**FeO**	**MgO**	**CaO**	**Na2O**	**K2O**	**Total**	**An**	**Ab**	**Or**
alc enclv 1 (olv)														

030A2e_plg003	4	core	51.29	0.02	30.41	0.57	0.13	13.05	3.27	0.12	98.88	68.3	31.0	0.8
030A2e_plg003	4	rim	50.28	0.05	32.58	0.65	0.09	14.95	2.72	0.09	101.41	74.8	24.7	0.5
030A2e_plg004	4	core	50.50	0.05	31.80	0.48	0.10	14.42	3.03	0.08	100.46	72.1	27.4	0.5
030A2e_plg004.5	4	core	49.14	0.05	32.96	0.51	0.09	15.81	2.31	0.08	100.90	78.7	20.8	0.5
030A2e_plg005	4	core	50.21	0.05	31.76	0.71	0.09	14.36	3.02	0.11	100.30	72.0	27.4	0.7
030A2e_plg010	5	core	50.88	0.04	31.42	0.67	0.03	13.53	3.42	0.18	100.18	67.9	31.0	1.1
030A2e_plg012	5	core	49.97	0.04	32.28	0.62	0.05	14.53	2.79	0.11	100.38	73.8	25.6	0.6
030A2e_plg021	4	core	48.93	0.02	32.90	0.54	0.22	15.59	2.46	0.08	100.76	77.4	22.1	0.5
030A2e_plg019	5	core	51.32	0.04	30.83	0.73	0.24	13.36	3.52	0.15	100.19	67.1	32.0	0.9
030A2e_plg017	4	core	48.78	0.05	33.46	0.46	0.11	15.92	2.29	0.05	101.09	79.1	20.6	0.3
030A2e_plg015	6	core	48.61	0.04	32.94	0.52	0.09	15.56	2.52	0.07	100.35	77.0	22.6	0.4
030A2e_plg025	4	core	48.96	0.04	33.40	0.66	0.05	16.05	2.36	0.06	101.54	78.7	20.9	0.4
030A2e_plg026	4	core	49.01	0.05	32.80	0.46	0.10	15.35	2.50	0.08	100.34	76.8	22.7	0.5
030A2e_plg028	4	core	49.74	0.02	32.61	0.54	0.10	15.05	2.74	0.07	100.89	74.9	24.6	0.4
030A2e_plg031	5	core	48.23	0.03	33.62	0.50	0.09	15.82	2.23	0.06	100.58	79.4	20.3	0.3
030A2e_plg027	6	core	47.48	0.02	31.06	0.66	0.02	13.37	2.67	0.13	95.42	72.9	26.3	0.8
030A2e_plg004	4	mantle	49.43	0.03	32.96	0.59	0.06	15.39	2.43	0.08	100.97	77.4	22.1	0.5
030A2e_plg005	4	mantle	48.71	0.03	32.85	0.68	0.06	15.83	2.37	0.07	100.60	78.3	21.2	0.4
030A2e_plg010	5	mantle	50.94	0.03	31.75	0.71	0.05	14.14	3.16	0.18	100.95	70.5	28.5	1.0
030A2e_plg012	5	mantle	48.69	0.04	33.12	0.64	0.04	15.64	2.27	0.09	100.51	78.8	20.7	0.5
030A2e_plg019	5	mantle	49.34	0.03	32.62	0.57	0.16	15.39	2.51	0.10	100.72	76.8	22.6	0.6
030A2e_plg017	4	mantle	51.44	0.03	31.71	0.59	0.12	13.86	3.51	0.13	101.39	68.1	31.2	0.7
030A2e_plg015	6	mantle	47.96	0.04	33.53	0.58	0.04	15.85	2.26	0.09	100.34	79.1	20.4	0.5
030A2e_plg025	4	mantle	48.46	0.03	33.28	0.53	0.08	15.91	2.25	0.07	100.61	79.3	20.3	0.4
030A2e_plg028	4	mantle	48.71	0.05	33.37	0.71	0.04	15.65	2.28	0.08	100.87	78.7	20.8	0.5
030A2e_plg031	5	mantle	51.16	0.05	31.48	0.70	0.08	13.92	3.19	0.15	100.71	70.1	29.0	0.9
030A2e_plg027	6	mantle	51.77	0.03	30.72	0.80	0.05	13.11	3.66	0.16	100.33	65.8	33.3	0.9
030A2e_plg004	4	rim	52.42	0.03	30.15	0.82	0.05	12.55	3.93	0.18	100.15	63.1	35.8	1.1
030A2e_plg004.5	4	rim	49.29	0.04	33.20	0.57	0.07	15.44	2.40	0.08	101.07	77.7	21.8	0.4
030A2e_plg005	4	rim	52.12	0.04	30.47	1.07	0.07	13.07	3.70	0.16	100.70	65.5	33.5	1.0
030A2e_plg010	5	rim	53.36	0.05	29.81	0.85	0.04	11.80	4.24	0.25	100.42	59.7	38.8	1.5
030A2e_plg012	5	rim	51.97	0.06	30.07	0.84	0.05	12.35	4.07	0.22	99.63	61.8	36.9	1.3
030A2e_plg021	4	rim	53.04	0.03	30.31	0.75	0.09	12.68	3.90	0.18	101.01	63.6	35.4	1.1
030A2e_plg019	5	rim	51.80	0.06	30.56	0.87	0.05	12.91	3.87	0.21	100.33	64.0	34.8	1.3
030A2e_plg017	4	rim	55.16	0.08	28.50	1.15	0.45	10.92	4.77	0.32	101.34	54.8	43.3	1.9
030A2e_plg015	6	rim	52.82	0.06	30.36	0.96	0.05	12.59	4.03	0.20	101.07	62.6	36.2	1.2
030A2e_plg025	4	rim	53.13	0.07	29.97	0.83	0.04	12.30	4.16	0.23	100.74	61.2	37.4	1.4
030A2e_plg026	4	rim	53.37	0.06	30.12	0.83	0.22	12.22	4.17	0.21	101.21	61.0	37.7	1.2
030A2e_plg028	4	rim	52.88	0.09	30.33	0.92	0.03	12.59	4.04	0.21	101.05	62.5	36.3	1.2

Unit	**Population**	**Location**	**SiO2**	**TiO2**	**Al2O3**	**FeO**	**MgO**	**CaO**	**Na2O**	**K2O**	**Total**	**An**	**Ab**	**Or**
alc enclv 2 (opx)														
030B_plg014	7	core	50.55	0.07	32.19	0.48	0.09	14.34	3.07	0.06	100.79	71.9	27.8	0.3
030B_plg015	7	core	52.59	0.08	30.44	0.72	0.05	12.87	3.94	0.14	100.80	63.8	35.3	0.8
030B_plg016	7	core	52.85	0.07	30.25	0.81	0.04	12.48	3.98	0.17	100.63	62.8	36.2	1.0
030B_plg014	7	core	51.57	0.06	30.40	0.77	0.07	12.69	3.99	0.16	99.69	63.1	35.9	0.9

EMPA standard analyses (wt%) of NMNH 115900

	Reported*	Analysed	+/-
SiO2	51.25	51.29	0.92
TiO2	0.05	0.04	0.01
Al2O3	30.91	30.74	0.33
ΣFeo	0.49	0.44	0.04
MgO	0.14	0.13	0.00
CaO	13.64	13.58	0.22
Na2O	3.45	3.37	0.24
K2O	0.18	0.12	0.01
Total	100.11	99.71	0.90
			2sd, n=15

*Stewart, D.B., Walker, G.W., Wright, T.L., Fahey, J.J. (1966) Physical Properties of calcic Labradorite from Lake County, Oregon; American Mineralogist 51, 177-197
*Jarosewich, E., Nelen, J. A., and Norberg, J. A. (1980) Reference Samples for Electron Microprobe Analysis. Geostandards Newsletter 4, p. 43-47

ii. Table A4. Clinopyroxene EMPA Data

Unit	Population	Location	SiO2	TiO2	Al2O3	Cr2O3	FeO	MnO	MgO	CaO	Na2O	K2O	Total	Mg#	Wo	En	Fs
alg																	
032A_cpx034	2b	core	52.83	0.59	1.78	0.00	10.87	0.37	15.46	18.14	0.01	0.33	100.37	71.69	37.4	44.4	18.1
032A_cpx035	2b	core	51.62	0.72	1.64	0.01	13.32	0.40	15.21	16.53	0.02	0.41	99.86	67.12	34.2	43.8	22.1
032A_cpx002	1b	core	52.21	0.60	1.69	0.01	10.59	0.36	15.33	18.75	0.00	0.30	99.84	72.08	38.6	43.9	17.6
032A_cpx003	1b	core	52.58	0.60	1.87	0.00	10.88	0.33	15.73	17.77	-0.01	0.32	100.14	72.02	36.7	45.2	18.1
032A_cpx003.5	1b	core	53.24	0.59	1.72	0.01	10.43	0.37	15.59	18.61	0.01	0.32	100.89	72.68	38.2	44.5	17.3
032A_cpx004	1b	core	53.12	0.62	1.82	-0.01	10.57	0.37	15.42	18.42	0.01	0.32	100.66	72.18	38.0	44.3	17.7
032A_cpx005	2b	core	52.66	0.55	1.62	0.03	10.85	0.34	15.43	18.28	0.01	0.31	100.07	71.70	37.7	44.3	18.0
032A_cpx006	1b	core	50.86	0.81	2.67	0.05	10.63	0.31	15.67	18.07	0.00	0.36	99.44	72.52	37.4	45.1	17.6
032A_cpx007	1b	core	52.29	0.86	2.74	0.08	10.10	0.32	15.37	18.62	0.01	0.31	100.68	73.04	38.7	44.4	16.9
032A_cpx008	1b	core	53.51	0.58	1.54	-0.01	11.00	0.33	16.13	17.68	-0.01	0.27	101.04	72.27	36.1	45.8	18.1
032A_cpx021	1b	core	51.85	0.53	1.39	0.01	10.62	0.33	15.60	18.63	0.02	0.31	99.30	72.42	38.1	44.4	17.4
032A_cpx014	1b	core	52.47	0.64	1.87	0.03	10.14	0.29	16.33	17.87	0.01	0.31	99.95	74.18	36.7	46.6	16.7
032A_cpx015	1b	core	51.98	0.68	2.22	0.02	9.51	0.26	16.14	18.17	-0.01	0.31	99.28	75.15	37.6	46.5	15.8
032A_cpx016	1b	core	52.75	0.56	1.67	0.00	10.91	0.33	15.36	18.49	-0.01	0.33	100.40	71.49	38.0	43.9	18.1
032A_cpx017	1b	core	52.86	0.57	1.63	-0.01	10.80	0.33	15.39	18.58	0.01	0.31	100.47	71.72	38.2	44.0	17.9
032A_cpx018	2b	core	51.91	0.54	1.63	0.01	11.05	0.35	15.65	18.17	0.00	0.34	99.65	71.68	37.2	44.6	18.2
032A_cpx033	1b	core	52.27	0.56	1.62	-0.01	10.76	0.40	15.40	18.48	0.01	0.31	99.80	71.87	38.0	44.1	17.9
032A_cpx029	2b	core	51.43	1.09	3.15	0.00	11.50	0.33	14.61	18.30	-0.02	0.33	100.73	69.35	38.2	42.5	19.3
032A_cpx030	1b	core	52.63	0.57	1.62	0.01	10.68	0.38	15.37	18.24	0.01	0.29	99.79	71.92	37.8	44.3	17.9
032A_cpx031	2b	core	51.03	0.99	3.23	0.06	11.51	0.36	15.51	17.35	0.00	0.35	100.38	70.67	36.0	44.8	19.2
032A_cpx032	2b	core	53.23	0.54	1.46	0.00	10.83	0.40	15.54	18.19	0.00	0.27	100.47	71.84	37.4	44.5	18.1
032A_cpx028	1b	core	52.36	0.57	1.64	0.00	10.83	0.36	15.34	18.44	0.03	0.33	99.91	71.65	38.0	44.0	18.0
032A_cpx027	1b	core	51.90	0.75	2.23	0.01	10.57	0.33	15.59	18.43	0.00	0.35	100.16	72.49	37.9	44.6	17.5
032A_cpx027.5	2b	core	52.79	0.66	1.76	0.01	10.71	0.33	15.66	18.27	-0.01	0.31	100.51	72.26	37.5	44.8	17.7
032A_cpx013	2b	core	51.34	0.90	2.36	0.02	12.52	0.37	15.01	16.84	-0.01	0.42	99.76	68.15	35.2	43.7	21.0
032A_cpx010	1b	core	51.58	0.75	2.37	0.04	9.48	0.26	16.05	18.42	-0.02	0.29	99.24	75.14	38.1	46.2	15.7
032A_cpx011	1b	core	52.98	0.49	1.49	0.01	10.85	0.36	15.52	18.19	0.01	0.33	100.23	71.81	37.5	44.5	18.1
032A_cpx012	1b	core	52.23	0.56	1.61	0.00	10.93	0.31	15.48	18.33	0.01	0.34	99.81	71.65	37.7	44.3	18.0
032A_cpx001	1b	core	51.96	0.73	2.66	0.08	9.87	0.27	15.40	18.64	-0.01	0.33	99.94	73.53	38.8	44.7	16.5
032A_cpx026	1c	core	51.98	0.73	2.07	0.04	10.66	0.31	15.33	18.28	0.02	0.36	99.76	71.96	37.9	44.3	17.8
032A_cpx024	1b	core	51.85	0.65	1.78	0.00	10.38	0.35	15.23	18.37	0.02	0.32	98.94	72.35	38.3	44.2	17.5
032A_cpx025	3b	core	52.70	0.45	1.47	0.06	21.68	0.54	24.04	1.88	0.00	0.03	102.84	66.64	3.6	63.7	32.7
032A_cpx023	1b	core	51.99	0.51	1.42	0.01	10.53	0.31	15.57	18.08	0.01	0.28	98.71	72.50	37.5	44.9	17.6
032A_cpx018	1b	outer mantle	52.32	0.66	1.86	0.00	10.67	0.37	15.58	18.29	0.02	0.33	100.09	72.27	37.6	44.6	17.7
032A_cpx034	2b	outer mantle	52.67	0.60	1.73	0.01	10.43	0.37	15.67	18.29	0.01	0.27	100.03	72.78	37.7	44.9	17.4
032A_cpx035	2b	outer mantle	52.32	0.59	1.48	0.02	10.88	0.38	15.97	17.83	0.01	0.31	99.78	72.37	36.5	45.5	18.0
032A_cpx002	1b	outer mantle	52.09	0.81	2.34	0.00	11.57	0.36	15.08	17.88	-0.01	0.34	100.47	69.90	37.1	43.5	19.3
032A_cpx003	1b	outer mantle	52.19	0.57	1.69	0.02	10.46	0.36	15.36	18.75	-0.01	0.29	99.68	72.36	38.6	44.0	17.4
032A_cpx003.5	1b	outer mantle	51.95	0.66	1.87	-0.01	11.61	0.34	15.01	17.87	0.05	0.41	99.76	69.77	37.2	43.5	19.4
032A_cpx004	1b	outer mantle	51.99	0.67	1.98	-0.02	10.53	0.34	15.30	18.22	-0.01	0.33	99.35	72.14	38.0	44.3	17.7
032A_cpx005	2b	outer mantle	52.04	0.66	1.83	0.01	10.34	0.32	15.46	18.37	0.02	0.34	99.39	72.73	38.1	44.6	17.3
032A_cpx006	1b	outer mantle	53.14	0.62	1.72	0.01	11.15	0.34	15.29	18.56	0.01	0.34	101.18	70.95	38.0	43.6	18.4
032A_cpx007	1b	outer mantle	51.64	0.70	1.94	0.01	10.71	0.32	15.34	18.23	-0.01	0.32	99.20	71.88	37.8	44.3	17.9
032A_cpx008	1b	outer mantle	51.85	0.69	1.92	-0.01	10.80	0.34	15.42	18.15	0.02	0.35	99.54	71.80	37.6	44.4	18.0
032A_cpx021	1b	outer mantle	52.97	0.75	2.05	0.01	10.47	0.32	15.34	18.31	0.00	0.36	100.57	72.24	38.1	44.4	17.6

032A_cpx014	1b	outer mantle	51.17	0.86	2.70	0.00	10.79	0.34	14.94	18.18	0.01	0.35	99.34	71.19	38.1	43.6	18.2
032A_cpx015	1b	outer mantle	52.36	0.67	1.91	0.01	11.01	0.30	15.24	18.40	0.00	0.33	100.22	71.16	38.0	43.8	18.2
032A_cpx016	1b	outer mantle	52.36	0.70	1.92	0.00	10.62	0.35	15.45	18.50	0.00	0.30	100.20	72.16	38.1	44.3	17.6
032A_cpx017	1b	outer mantle	52.50	0.62	1.60	0.01	10.57	0.34	15.71	18.08	0.02	0.31	99.75	72.60	37.3	45.1	17.6
032A_cpx018	2b	rim	52.55	0.42	0.50	-0.01	26.57	0.86	19.01	3.67	0.07	0.11	103.76	56.27	7.1	51.5	41.4
032A_cpx033	1b	outer mantle	52.39	0.68	1.91	-0.01	11.03	0.37	15.58	17.92	0.00	0.32	100.19	71.56	36.9	44.7	18.4
032A_cpx029	2b	outer mantle	52.39	0.61	1.54	0.01	10.50	0.28	15.76	18.00	0.02	0.28	99.39	72.77	37.2	45.3	17.4
032A_cpx030	1b	outer mantle	51.90	0.81	2.35	0.01	10.76	0.36	15.26	18.31	0.01	0.38	100.12	71.67	38.0	44.0	18.0
032A_cpx031	2b	outer mantle	52.08	0.65	1.76	0.02	10.37	0.30	15.35	18.22	0.02	0.33	99.09	72.51	38.0	44.6	17.4
032A_cpx032	2b	outer mantle	51.55	0.67	1.98	-0.01	10.82	0.34	15.79	18.01	0.01	0.35	99.51	72.31	37.0	45.2	17.8
032A_cpx028	1b	outer mantle	52.82	0.64	1.79	0.00	10.64	0.34	15.50	18.46	0.01	0.31	100.52	72.18	38.0	44.4	17.7
032A_cpx027	1b	outer mantle	52.04	0.70	1.99	-0.01	10.41	0.30	15.43	18.53	0.02	0.35	99.76	72.57	38.3	44.4	17.3
032A_cpx027.5	2b	outer mantle	51.35	0.90	3.04	-0.01	10.63	0.27	15.03	18.26	0.01	0.38	99.88	71.60	38.3	43.9	17.8
032A_cpx013	2b	outer mantle	52.54	0.58	1.40	0.02	11.18	0.39	15.92	17.56	0.01	0.26	99.86	71.74	36.0	45.5	18.5
032A_cpx010	1b	outer mantle	52.49	0.66	1.82	-0.02	10.76	0.29	15.36	18.46	-0.01	0.31	100.14	71.78	38.1	44.1	17.8
032A_cpx011	1b	outer mantle	52.74	0.62	1.72	0.00	10.71	0.33	15.28	18.41	0.02	0.32	100.14	71.74	38.1	44.0	17.9
032A_cpx012	1b	outer mantle	52.86	0.71	1.96	-0.01	10.72	0.32	15.45	18.53	0.01	0.32	100.87	71.97	38.1	44.2	17.7
032A_cpx001	1b	outer mantle	51.86	0.68	1.94	0.01	11.02	0.37	15.40	18.21	0.02	0.34	99.84	71.40	37.5	44.2	18.3
032A_cpx026	1c	rim	52.50	0.66	1.89	0.00	10.79	0.34	15.41	18.26	0.01	0.31	100.16	71.78	37.7	44.3	18.0
032A_cpx024	1b	outer mantle	52.55	0.69	1.92	0.02	10.21	0.32	15.33	18.54	0.00	0.34	99.91	72.76	38.5	44.3	17.1
032A_cpx025	3b	rim	54.24	0.37	1.00	-0.01	20.31	0.58	25.02	1.45	0.00	0.02	102.98	68.84	2.8	66.3	30.9
032A_cpx023	1b	outer mantle	51.64	0.63	1.80	0.02	10.56	0.33	15.40	17.85	0.00	0.33	98.55	72.22	37.4	44.8	17.8

Unit	**Population**	**Location**	**SiO2**	**TiO2**	**Al2O3**	**Cr2O3**	**FeO**	**MnO**	**MgO**	**CaO**	**Na2O**	**K2O**	**Total**	**Mg#**	**Wo**	**En**	**Fs**
alc																	
030B_cpx018	1a	core	52.57	0.70	2.33	0.05	10.71	0.28	15.51	18.25	0.00	0.35	100.75	72.07	37.7	44.6	17.7
030B_cpx012	1a	core	52.63	0.65	1.81	-0.01	10.71	0.36	15.70	18.18	-0.01	0.32	100.37	72.30	37.4	44.9	17.8
030B_cpx013	2a	core	52.22	0.76	2.15	0.03	11.54	0.28	15.71	17.14	0.02	0.39	100.24	70.82	35.5	45.3	19.1
030B_cpx014	2a	core	54.84	0.35	1.00	0.00	20.37	0.59	25.24	1.53	0.00	0.02	103.93	68.95	2.9	66.4	30.8
030B_cpx015	2b	core	51.58	0.69	2.10	0.02	11.22	0.39	15.29	17.94	-0.01	0.38	99.60	70.87	37.2	44.1	18.7
030B_cpx026	2a	core	51.87	0.76	2.42	0.01	10.73	0.29	15.47	17.70	-0.01	0.38	99.64	71.98	37.0	45.0	18.0
030B_cpx027	1a	core	52.04	0.65	2.00	0.00	10.56	0.34	15.65	17.85	0.01	0.36	99.46	72.54	37.1	45.2	17.7
030B_cpx028	1a	core	51.29	0.84	3.03	0.01	10.92	0.35	15.49	17.72	0.01	0.40	100.08	71.70	36.9	44.8	18.3
030B_cpx016	2a	core	52.43	0.71	2.10	0.00	10.87	0.33	15.42	17.99	0.00	0.40	100.24	71.65	37.3	44.5	18.2
030B_cpx017	2b	core	52.01	0.64	1.82	0.02	10.80	0.32	15.62	18.22	0.00	0.32	99.77	72.09	37.5	44.7	17.8
030B_cpx007	2a	core	53.44	0.63	1.94	0.01	11.07	0.37	15.43	17.84	0.00	0.35	101.08	71.22	37.0	44.5	18.6
030B_cpx004	3a	core	52.31	0.75	2.38	-0.01	10.71	0.32	15.31	18.20	0.02	0.38	100.38	71.80	37.8	44.3	17.9
030B_cpx005	1a	core	51.62	0.86	2.75	-0.01	10.66	0.30	15.21	18.28	-0.01	0.30	99.98	71.78	38.1	44.1	17.8
030B_cpx010	1a	core	52.82	0.64	1.87	0.00	10.85	0.35	15.57	18.30	0.01	0.34	100.74	71.88	37.6	44.5	18.0
030B_cpx006	2a	core	52.31	0.65	1.64	0.01	11.14	0.40	15.63	18.13	0.01	0.32	100.22	71.46	37.1	44.5	18.4
030B_cpx002	2a	core	52.08	0.84	2.50	0.00	11.29	0.35	15.11	17.85	-0.02	0.37	100.40	70.44	37.2	43.8	19.0
030B_cpx003	1a	core	51.86	0.69	2.00	-0.02	10.76	0.37	15.53	18.53	0.00	0.36	100.11	72.06	38.0	44.3	17.8
030B_cpx024	3a	core	54.38	0.35	0.95	0.00	20.39	0.55	25.14	1.57	0.01	0.02	103.35	68.87	3.0	66.3	30.8
030B_cpx023	2a	core	52.39	0.72	2.00	0.00	10.96	0.37	15.39	18.49	0.01	0.38	100.69	71.48	37.9	43.9	18.1
030B_cpx022	1a	core	51.39	0.91	3.10	0.03	11.10	0.33	14.59	18.28	0.00	0.40	100.13	70.08	38.5	42.7	18.8
030B_cpx021	1a	core	51.92	0.87	2.56	-0.01	11.10	0.35	15.31	17.86	0.00	0.34	100.31	71.08	37.1	44.3	18.6
030B_cpx025	1a	core	52.27	0.64	1.95	0.00	10.87	0.34	15.93	17.61	0.00	0.37	99.99	72.33	36.3	45.7	18.0
030B_cpx011	1a	core	52.78	0.65	1.75	-0.02	10.91	0.38	15.72	18.00	-0.01	0.32	100.51	71.95	37.0	44.9	18.1
030B_cpx008	1a	core	52.69	0.63	1.81	0.00	11.15	0.40	15.69	17.84	-0.01	0.35	100.55	71.49	36.6	44.8	18.5
030B_cpx008.5	1a	core	53.44	0.37	1.02	0.00	21.14	0.58	24.81	1.52	-0.01	0.03	102.90	67.86	2.9	65.3	31.8
030B_cpx009	1a	core	51.69	0.75	2.54	0.00	10.20	0.29	15.68	18.06	0.00	0.34	99.56	73.27	37.6	45.4	17.0

030B_cpx020	1a	core	52.53	0.73	2.16	0.00	10.73	0.35	15.52	17.99	0.02	0.36	100.38	72.02	37.3	44.8	18.0
030B_cpx019	2b	core	52.24	0.74	2.21	0.00	10.62	0.35	15.42	18.30	0.00	0.36	100.24	72.13	37.9	44.4	17.7
030B_cpx018	1a	rim	53.11	0.68	2.19	0.00	10.61	0.36	15.22	18.00	-0.01	0.37	100.53	71.79	37.7	44.3	18.0
030B_cpx012	1a	rim	52.24	0.75	2.17	-0.01	10.90	0.35	15.44	18.20	0.00	0.36	100.40	71.65	37.5	44.3	18.1
030B_cpx013	2a	core	52.69	0.71	2.12	0.02	10.40	0.35	15.42	18.28	0.03	0.34	100.33	72.51	38.0	44.6	17.5
030B_cpx014	2a	rim	52.95	0.71	2.18	0.01	10.58	0.31	15.37	18.42	0.02	0.35	100.90	72.10	38.1	44.3	17.6
030B_cpx015	2b	outer mantle	52.07	0.66	1.95	0.01	10.58	0.36	15.33	18.17	0.00	0.35	99.48	72.09	37.8	44.4	17.8
030B_cpx026	2a	rim	51.86	0.68	1.97	0.01	10.32	0.28	15.24	18.46	0.00	0.35	99.18	72.46	38.5	44.2	17.3
030B_cpx027	1a	rim	51.59	0.70	2.29	-0.01	10.55	0.33	15.32	18.12	-0.01	0.40	99.29	72.15	37.8	44.5	17.7
030B_cpx028	1a	rim	51.42	0.86	2.44	0.01	12.07	0.33	15.24	16.83	0.02	0.37	99.58	69.24	35.3	44.4	20.3
030B_cpx016	2a	rim	52.27	0.67	1.96	0.00	10.65	0.40	15.54	18.63	0.02	0.33	100.46	72.27	38.1	44.2	17.6
030B_cpx017	2b	outer mantle	52.86	0.69	2.08	0.00	10.90	0.36	15.59	18.03	0.00	0.35	100.86	71.80	37.1	44.7	18.1
030B_cpx007	2a	rim	52.42	0.74	2.17	0.04	10.47	0.36	15.38	18.14	0.01	0.33	100.04	72.33	37.8	44.6	17.6
030B_cpx004	3a	rim	53.35	0.69	2.11	0.01	10.52	0.26	15.26	18.45	-0.01	0.34	100.98	72.02	38.3	44.1	17.6
030B_cpx005	1a	rim	52.16	0.69	2.09	0.00	10.73	0.30	15.28	18.43	-0.01	0.35	100.04	71.74	38.2	44.0	17.8
030B_cpx006	2a	rim	51.90	0.74	2.13	0.01	10.76	0.38	15.27	18.16	0.00	0.35	99.68	71.67	37.7	44.2	18.1
030B_cpx010	1a	rim	52.72	0.67	2.11	0.02	10.93	0.36	15.39	18.29	0.02	0.35	100.85	71.50	37.7	44.1	18.2
030B_cpx002	2a	rim	51.97	0.72	2.17	0.01	10.76	0.40	15.27	18.22	-0.01	0.36	99.88	71.67	37.8	44.1	18.1
030B_cpx003	1a	rim	52.40	0.79	2.16	-0.02	11.20	0.40	15.40	17.96	-0.01	0.34	100.65	71.02	37.1	44.2	18.7
030B_cpx024	3a	rim	52.91	0.67	1.93	0.01	10.45	0.36	15.61	18.25	0.02	0.34	100.54	72.67	37.7	44.9	17.5
030B_cpx023	2a	rim	51.95	0.77	2.24	0.01	12.07	0.41	15.68	17.18	0.02	0.34	100.66	69.89	35.3	44.8	20.0
030B_cpx022	1a	rim	53.31	0.58	1.62	0.02	10.58	0.40	15.72	18.22	0.01	0.32	100.78	72.55	37.4	44.9	17.7
030B_cpx021	1a	rim	52.25	0.70	2.06	0.01	10.23	0.34	15.53	18.20	0.01	0.32	99.63	73.00	37.9	44.9	17.2
030B_cpx020	1a	rim	52.00	0.78	2.39	0.00	10.83	0.38	15.22	17.93	-0.01	0.41	99.95	71.45	37.5	44.2	18.3
030B_cpx019	2b	rim	51.89	0.76	2.33	0.01	10.80	0.33	15.35	18.15	0.01	0.40	100.01	71.72	37.7	44.3	18.0
030B_cpx025	1a	rim	52.35	0.71	2.21	0.03	10.78	0.37	15.22	17.99	0.01	0.38	100.03	71.53	37.6	44.2	18.2
030B_cpx011	1a	rim	51.95	0.82	3.19	0.02	11.92	0.38	14.46	17.04	0.07	0.82	100.67	68.37	36.4	43.0	20.5
030B_cpx008	1a	rim	52.27	0.70	2.10	0.01	10.94	0.38	15.39	18.14	-0.01	0.33	100.26	71.49	37.5	44.2	18.3
030B_cpx008.5	1a	rim	54.04	0.40	1.10	0.00	20.38	0.60	25.23	1.33	0.01	0.03	103.10	68.97	2.5	66.6	30.9
030B_cpx009	1a	rim	52.78	0.64	2.00	0.01	10.97	0.35	15.24	18.10	0.00	0.40	100.50	71.19	37.6	44.0	18.4

EMPA standard analyses (wt%) of NMNH 122142

	Reported*	Analysed	+/-
SiO2	50.73	50.78	0.71
TiO2	0.74	0.85	0.02
Al2O3	8.73	8.64	0.14
Cr2O3		0.16	0.03
ΣFeo	6.45	6.97	0.32
MnO	0.13	0.14	0.05
MgO	16.65	16.45	0.09
CaO	15.82	14.75	0.17
Na2O	1.27	1.28	0.07
K2O	0.00	0.01	0.02
Total	100.52	100.02	0.81
			2sd, n=14

*Jarosewich, E., Nelen, J. A., and Norberg, J. A. (1980) Reference Samples for Electron Microprobe Analysis. Geostandards Newsletter 4, p. 43-47

*Mason, B. (1966) Pyrope, augite and hornblende frouter mantle Kakanui, New Zealand. New Zealand Journal of Geology and Geophysics 9 (4), p. 474-480

*Mason, B. and Allen, R.O. (1973) Minor and trace elements in augite, hornblende and pyrope megacrysts frouter mantle Kakanui, New Zealand; New Zealand Journal of Geology and Geophysics, 16 (4), p. 935-947

iii. Table A5. Orthopyroxene EMPA Data

Unit	Population	Location	SiO2	TiO2	Al2O3	Cr2O3	FeO	MnO	MgO	CaO	Na2O	K2O	Total	Mg#	Wo	En	Fs
alg																	
032A_opx002	2b	core	52.83	0.35	0.95	0.00	19.26	0.60	24.65	1.42	0.03	-0.01	100.08	69.65	2.8	67.1	30.1
032A_opx001	2b	core	52.83	0.21	0.52	-0.01	19.00	0.62	24.87	1.40	0.03	0.01	99.50	70.15	2.7	67.6	29.7
032A_opx005	4	core	51.75	0.38	1.33	-0.01	18.95	0.59	24.35	1.68	0.05	0.01	99.11	69.78	3.3	66.8	29.9
032A_opx006	4	core	51.76	0.47	1.91	-0.01	18.47	0.53	24.69	1.82	0.02	-0.02	99.67	70.61	3.6	67.5	28.9
032A_opx018	2a	core	51.47	0.42	1.87	0.04	19.05	0.53	24.52	1.52	0.03	0.01	99.44	69.84	3.0	67.2	29.8
032A_opx009	1b	core	51.23	0.53	2.28	0.02	18.91	0.52	23.92	1.69	0.04	-0.01	99.15	69.43	3.4	66.5	30.1
032A_opx010	1b	core	52.97	0.42	1.55	0.01	17.60	0.44	25.73	1.46	0.03	-0.01	100.21	72.38	2.8	69.8	27.3
032A_opx011	4	core	51.41	0.45	1.69	-0.01	18.18	0.49	24.73	2.07	0.03	0.00	99.04	71.01	4.1	67.6	28.4
032A_opx012	4	core	52.26	0.41	1.85	0.01	17.05	0.44	25.85	1.54	0.02	0.00	99.42	73.14	3.0	70.4	26.5
032A_opx013	2b	core	53.21	0.34	0.94	0.01	19.12	0.60	24.64	1.36	0.02	0.01	100.24	69.76	2.7	67.2	30.1
032A_opx014	2b	core	52.33	0.32	1.04	-0.01	19.54	0.65	24.05	1.58	0.02	0.00	99.53	68.82	3.1	66.0	30.9
032A_opx015	2b	core	51.77	0.39	1.03	0.00	18.94	0.60	24.46	1.53	0.04	0.01	98.77	69.90	3.0	67.1	29.8
032A_opx016	2b	core	53.51	0.25	0.66	-0.01	19.02	0.65	24.69	1.43	0.02	0.00	100.23	69.90	2.8	67.2	30.0
032A_opx019	2b	core	52.54	0.38	0.99	0.01	18.93	0.59	24.89	1.34	0.02	0.01	99.69	70.23	2.6	67.7	29.6
032A_opx025	3	core	52.34	0.31	0.92	-0.01	18.75	0.54	25.11	1.44	0.04	-0.01	99.45	70.65	2.8	68.1	29.1
032A_opx023	2c	core	51.09	0.56	1.72	-0.02	10.22	0.41	16.03	17.13	0.32	0.01	97.49	73.72	35.9	46.8	17.4
032A_opx026	4	core	51.74	0.45	1.30	0.01	18.23	0.55	24.41	2.12	0.04	0.01	98.86	70.63	4.2	67.1	28.7
032A_opx027	4	core	53.10	0.45	1.61	0.02	18.19	0.55	25.32	1.45	0.04	0.00	100.73	71.38	2.8	68.7	28.4
032A_opx028	4	core	51.16	0.38	1.29	0.00	18.58	0.55	25.28	1.51	0.01	-0.01	98.77	71.07	2.9	68.4	28.7
032A_opx029	1b	core	54.15	0.30	0.84	0.01	17.04	0.43	26.26	1.48	0.03	0.01	100.55	73.39	2.9	70.8	26.3
032A_opx030	3	core	52.47	0.38	0.93	0.00	20.01	0.49	23.85	1.61	0.01	0.01	99.77	68.12	3.2	65.4	31.4
032A_opx031	3	core	53.51	0.28	0.73	0.01	18.83	0.56	24.86	1.56	0.03	0.00	100.35	70.27	3.0	67.5	29.4
032A_opx032	2b	core	53.02	0.30	0.91	0.00	19.49	0.61	24.26	1.51	0.03	0.01	100.13	69.03	3.0	66.3	30.7
032A_opx033	1b	core	51.88	0.47	1.86	-0.01	17.34	0.44	25.37	1.96	0.04	-0.01	99.35	72.45	3.8	69.2	27.0
032A_opx034	1b	core	51.20	0.56	1.53	0.02	9.57	0.32	15.27	18.51	0.28	0.00	97.25	74.02	39.0	44.8	16.2
032A_opx035	2b	core	53.32	0.37	0.96	0.01	19.06	0.59	24.47	1.43	0.03	-0.01	100.23	69.65	2.8	67.1	30.1
032A_opx018	2a	rim	52.80	0.34	0.90	0.01	18.39	0.54	24.88	1.45	0.02	0.01	99.33	70.79	2.9	68.2	29.0
032A_opx030	3	outer mantle	52.83	0.38	1.28	0.02	16.87	0.45	26.27	1.49	0.04	0.01	99.63	73.66	2.9	71.0	26.1
032A_opx031	3	inner mantle	52.95	0.41	1.24	0.00	17.25	0.44	26.28	1.47	0.03	0.02	100.08	73.23	2.8	70.7	26.5
032A_opx002	2b	outer mantle	52.84	0.39	1.00	0.00	18.50	0.57	25.02	1.47	0.04	-0.01	99.82	70.80	2.9	68.1	29.0
032A_opx001	2b	outer mantle	52.65	0.31	0.77	0.01	18.23	0.58	25.23	1.47	0.03	-0.01	99.27	71.29	2.9	68.6	28.5
032A_opx005	4	core	52.83	0.41	1.97	0.01	19.09	0.56	24.33	1.50	0.03	0.00	100.73	69.53	3.0	66.9	30.2
032A_opx009	1b	rim	52.67	0.37	0.91	-0.01	18.77	0.55	24.86	1.43	0.03	0.00	99.58	70.38	2.8	67.8	29.4
032A_opx010	1b	outer mantle	53.05	0.36	0.90	-0.01	18.16	0.52	25.10	1.53	0.02	0.01	99.65	71.22	3.0	68.5	28.5
032A_opx011	4	core	52.18	0.38	0.94	0.00	18.50	0.54	25.06	1.45	0.03	-0.01	99.08	70.87	2.8	68.3	28.9
032A_opx012	4	core	52.90	0.35	0.99	0.01	17.80	0.51	25.44	1.44	0.03	0.02	99.47	71.93	2.8	69.3	27.9
032A_opx013	2b	rim	52.80	0.36	0.89	0.02	17.98	0.58	25.22	1.48	0.03	0.00	99.35	71.54	2.9	68.8	28.3
032A_opx014	2b	outer mantle	52.55	0.37	0.96	0.02	18.81	0.58	24.72	1.45	0.03	0.01	99.48	70.21	2.8	67.6	29.6
032A_opx015	2b	outer mantle	52.54	0.36	1.03	0.00	18.40	0.54	24.98	1.43	0.02	-0.01	99.29	70.88	2.8	68.3	28.9
032A_opx016	2b	outer mantle	52.66	0.35	0.98	0.02	18.16	0.56	25.09	1.57	0.03	0.01	99.41	71.25	3.1	68.4	28.5
032A_opx019	2b	outer mantle	52.24	0.39	1.06	0.01	18.24	0.58	24.65	1.74	0.03	0.01	98.93	70.79	3.4	67.7	28.9
032A_opx020	2b	outer mantle	50.26	0.73	2.05	0.00	9.75	0.33	15.35	18.19	0.32	-0.02	96.99	73.80	38.4	45.1	16.6
032A_opx021	2b	outer mantle	51.91	0.41	1.14	-0.01	18.40	0.54	24.84	1.54	0.04	0.02	98.84	70.81	3.0	68.1	28.9
032A_opx022	2b	outer mantle	52.60	0.36	0.90	0.01	18.13	0.50	25.16	1.50	0.05	0.00	99.22	71.34	2.9	68.7	28.4
032A_opx025	3	outer mantle	53.05	0.30	0.78	0.00	17.99	0.55	25.34	1.49	0.02	0.00	99.53	71.62	2.9	68.9	28.2

032A_opx023	2c	rim	50.93	0.74	2.19	-0.01	9.36	0.32	15.14	18.44	0.38	0.02	97.52	74.28	39.2	44.8	16.0
032A_opx026	4	core	52.52	0.36	0.94	-0.01	18.30	0.55	25.15	1.50	0.03	0.01	99.35	71.16	2.9	68.5	28.6
032A_opx027	4	core	52.20	0.27	0.81	0.02	18.30	0.57	25.45	1.43	0.03	-0.01	99.07	71.44	2.8	68.8	28.4
032A_opx028	4	core	52.69	0.44	1.07	0.00	18.30	0.59	25.19	1.55	0.03	0.01	99.85	71.18	3.0	68.4	28.6
032A_opx029	3	outer mantle	53.11	0.37	1.01	0.02	18.23	0.53	25.24	1.36	0.03	-0.01	99.88	71.26	2.7	68.8	28.6
032A_opx030	3	outer mantle	53.69	0.29	0.76	0.01	18.33	0.53	25.33	1.45	0.04	0.02	100.45	71.21	2.8	68.6	28.6
032A_opx031	3	outer mantle	52.29	0.35	0.91	0.00	18.49	0.58	25.11	1.40	0.03	0.00	99.17	70.92	2.7	68.3	28.9
032A_opx032	2b	outer mantle	52.26	0.36	0.93	0.00	18.61	0.58	24.91	1.46	0.03	0.00	99.14	70.61	2.9	68.0	29.2
032A_opx033	1b	outer mantle	52.22	0.42	1.38	0.01	18.26	0.52	25.22	1.55	0.03	0.00	99.61	71.28	3.0	68.5	28.4
032A_opx034	1b	outer mantle	50.50	0.67	2.08	0.00	10.38	0.38	15.66	17.44	0.31	-0.01	97.44	72.97	36.6	45.8	17.6
032A_opx035	2b	outer mantle	52.81	0.40	0.93	0.01	18.60	0.55	24.79	1.44	0.05	0.00	99.58	70.48	2.8	67.9	29.3
Unit	**Population**	**Location**	**SiO2**	**TiO2**	**Al2O3**	**Cr2O3**	**FeO**	**MnO**	**MgO**	**CaO**	**Na2O**	**K2O**	**Total**	**Mg#**	**Wo**	**En**	**Fs**
alc																	
030B_opx002	1a	core	48.47	0.91	4.20	0.04	10.34	0.25	14.78	18.04	0.35	-0.01	97.36	71.98	38.5	43.9	17.5
030B_opx003	2a	core	51.90	0.43	1.35	-0.03	19.09	0.59	24.84	1.56	0.03	0.00	99.79	70.08	3.0	67.3	29.7
030B_opx004	2a	core	51.93	0.41	1.33	0.01	18.73	0.62	24.71	1.51	0.03	0.00	99.28	70.33	3.0	67.6	29.5
030B_opx006	2a	core	51.96	0.43	1.41	-0.02	18.52	0.52	24.87	1.70	0.04	0.01	99.45	70.71	3.3	67.8	28.9
030B_opx016	2a	core	52.16	0.42	1.56	0.00	18.44	0.58	24.76	1.55	0.04	-0.01	99.52	70.67	3.1	67.9	29.1
030B_opx007	2a	core	52.23	0.33	1.09	0.01	18.72	0.54	25.04	1.41	0.02	-0.01	99.38	70.62	2.8	68.1	29.2
030B_opx008	1b	core	52.78	0.35	1.01	0.01	18.14	0.56	25.23	1.48	0.02	0.01	99.57	71.38	2.9	68.7	28.4
030B_opx013	1a	core	50.36	0.81	2.22	-0.01	10.07	0.38	15.01	18.27	0.38	0.01	97.51	72.73	38.6	44.2	17.2
030B_opx015	2a	core	52.69	0.36	1.10	-0.01	18.26	0.58	25.12	1.49	0.02	-0.01	99.63	71.16	2.9	68.4	28.6
030B_opx009	2a	core	52.05	0.44	1.28	-0.01	18.94	0.58	24.59	1.79	0.04	-0.01	99.70	70.01	3.5	66.9	29.6
030B_opx010	2a	core	52.19	0.41	1.22	0.01	18.74	0.58	24.83	1.52	0.02	0.00	99.51	70.41	3.0	67.7	29.3
030B_opx011	2a	core	52.84	0.46	1.38	-0.01	18.62	0.62	24.84	1.52	0.03	0.00	100.32	70.51	3.0	67.7	29.3
030B_opx017	1a	core	51.46	0.49	2.23	-0.01	17.88	0.50	25.14	1.63	0.04	0.01	99.38	71.67	3.2	68.8	28.0
030B_opx012	2a	core	51.59	0.51	1.54	0.00	18.82	0.57	24.48	1.61	0.04	-0.01	99.16	70.04	3.2	67.2	29.6
030B_opx008	1b	rim	53.16	0.28	0.80	0.02	18.24	0.62	25.01	1.57	0.02	0.00	99.70	71.06	3.1	68.2	28.7
030B_opx002	1a	rim	50.35	0.84	1.65	0.02	12.10	0.33	15.57	16.36	0.38	0.00	97.60	69.76	34.3	45.4	20.2
030B_opx003	2a	rim	52.84	0.36	1.04	-0.01	18.21	0.58	25.30	1.49	0.03	-0.01	99.85	71.37	2.9	68.7	28.4
030B_opx004	2a	rim	52.51	0.34	1.04	0.00	18.45	0.57	25.06	1.53	0.05	0.00	99.57	70.92	3.0	68.2	28.8
030B_opx006	2a	rim	53.43	0.38	1.06	0.00	18.35	0.58	25.19	1.48	0.01	0.00	100.47	71.07	2.9	68.4	28.7
030B_opx016	2a	rim	52.54	0.31	0.82	0.00	18.39	0.59	25.25	1.38	0.04	0.01	99.33	71.15	2.7	68.6	28.7
030B_opx007	2a	rim	50.85	0.70	1.99	0.00	9.83	0.36	15.26	18.25	0.39	-0.01	97.62	73.51	38.5	44.8	16.7
030B_opx008	1b	rim	51.77	0.17	0.13	0.01	23.74	1.07	20.38	1.48	0.05	-0.01	98.80	60.56	3.0	57.7	39.3
030B_opx013	1a	rim	52.88	0.36	1.03	0.00	18.45	0.62	25.12	1.52	0.03	0.00	100.01	70.95	3.0	68.2	28.9
030B_opx015	2a	rim	32.52	0.69	1.09	0.00	9.47	0.32	15.43	17.98	0.36	-0.01	77.85	75.81	38.6	46.1	15.3
030B_opx009	2a	rim	52.89	0.32	0.85	0.01	18.30	0.58	25.46	1.41	0.04	0.00	99.86	71.41	2.7	68.8	28.4
030B_opx010	2a	rim	53.04	0.37	0.97	0.01	18.46	0.61	25.35	1.43	0.04	0.00	100.26	71.13	2.8	68.5	28.7
030B_opx011	2a	rim	52.40	0.36	1.03	0.00	18.01	0.55	25.03	1.50	0.03	0.01	98.93	71.36	3.0	68.6	28.4
030B_opx012	2a	rim	52.44	0.36	1.04	0.00	18.02	0.56	25.05	1.56	0.02	0.00	99.04	71.38	3.1	68.6	28.4
030B_opx017	1a	rim	52.75	0.55	2.08	-0.02	18.01	0.52	24.21	2.36	0.04	0.00	100.52	70.63	4.7	66.7	28.6
Unit	**Population**	**Location**	**SiO2**	**TiO2**	**Al2O3**	**Cr2O3**	**FeO**	**MnO**	**MgO**	**CaO**	**Na2O**	**K2O**	**Total**	**Mg#**	**Wo**	**En**	**Fs**
alc enclv 2 (opx)																	
030B_opx001	5	core	52.03	0.35	1.05	-0.01	18.60	0.59	24.99	1.45	0.03	0.01	99.10	70.73	2.8	68.1	29.1
030B_opx001	5	core	50.95	0.24	0.24	0.00	23.32	0.99	21.09	1.59	0.03	0.01	98.46	61.91	3.2	59.0	37.8

Same standard as clinopyroxene

iv. Table A6. Olivine EMPA Data

Unit	Pop	Loc	SiO2	Al2O3	Cr2O3	FeO	MnO	MgO	NiO	CaO	Total	Fo	Fa
alg													
032A_olv001	1	Core	36.29	0.00	0.00	29.10	0.56	33.05	0.05	0.14	99.20	66.94	33.06
032A_olv002	1	Core	36.11	0.00	0.00	29.40	0.58	33.04	0.03	0.13	99.31	66.71	33.29
032A_olv003	1	Core	36.46	0.03	0.00	29.93	0.52	32.60	0.03	0.14	99.72	66.01	33.99
032A_olv006	1	Core	36.00	0.01	0.01	29.49	0.56	33.15	0.04	0.13	99.39	66.71	33.29
032A_olv005	1	Core	35.47	0.01	0.00	30.40	0.59	31.88	0.02	0.14	98.52	65.15	34.85
032A_olv004	1	Core	35.89	0.01	0.01	29.81	0.58	32.82	0.02	0.13	99.27	66.24	33.76
032A_olv006	1	Core	35.96	0.00	-0.01	29.26	0.58	32.85	0.03	0.14	98.83	66.69	33.31
Unit	**Pop**	**Loc**	**SiO2**	**Al2O3**	**Cr2O3**	**FeO**	**MnO**	**MgO**	**NiO**	**CaO**	**Total**	**Fo**	**Fa**
alc enclv 1 (olv)													
030A2e_olv001	2a	Core	37.96	0.03	0.01	18.53	0.28	41.62	0.20	0.09	98.72	80.02	19.98
030A2e_olv002	2a	Core	38.22	0.01	0.01	17.11	0.29	42.69	0.22	0.13	98.68	81.65	18.35
030A2e_olv006	2a	Core	38.91	0.02	0.01	16.86	0.24	42.98	0.32	0.12	99.46	81.96	18.04
030A2e_olv004	2a	Core	38.45	0.03	0.01	16.89	0.26	42.97	0.30	0.13	99.04	81.94	18.06
030A2e_olv005	2a	Core	38.43	0.03	0.03	16.47	0.22	43.39	0.34	0.13	99.03	82.44	17.56
030A2e_olv007	2a	Core	38.28	0.02	0.02	17.41	0.25	42.62	0.21	0.15	98.96	81.36	18.64
030A2e_olv012	2a	Core	37.83	0.03	0.01	18.04	0.28	41.99	0.20	0.13	98.51	80.58	19.42
030A2e_olv011	2a	Core	37.84	0.01	0.00	19.04	0.26	41.55	0.17	0.12	98.99	79.55	20.45
030A2e_olv010	2a	Core	37.02	0.65	0.48	18.65	0.25	40.80	0.20	0.40	98.46	79.59	20.41
030A2e_olv032	2a	Core	38.51	0.03	0.01	17.23	0.25	42.66	0.21	0.14	99.04	81.53	18.47
030A2e_olv031	2a	Core	38.75	0.02	0.01	17.38	0.29	42.78	0.20	0.14	99.58	81.45	18.55
030A2e_olv022	2a	Core	38.29	0.10	0.10	16.81	0.20	42.87	0.28	0.15	98.80	81.97	18.03
030A2e_olv023	2b	Core	37.22	0.01	0.01	21.96	0.29	39.20	0.20	0.12	99.00	76.10	23.90
030A2e_olv001	2a	Rim	37.15	0.08	0.02	23.19	0.35	37.41	0.09	0.13	98.43	74.20	25.80
030A2e_olv002	2a	Rim	37.75	0.02	0.01	21.31	0.34	39.20	0.20	0.13	98.96	76.63	23.37
030A2e_olv006	2a	Rim	38.08	0.07	0.00	21.54	0.32	38.96	0.17	0.11	99.24	76.34	23.66
030A2e_olv004	2a	Rim	38.45	0.02	0.00	20.09	0.30	40.12	0.20	0.13	99.32	78.07	21.93
030A2e_olv005	2a	Rim	38.33	0.03	0.03	19.52	0.26	40.86	0.25	0.13	99.43	78.87	21.13
030A2e_olv007	2a	Rim	37.19	0.02	0.02	22.38	0.41	38.73	0.17	0.12	99.04	75.53	24.47
030A2e_olv012	2a	Rim	37.99	0.03	0.01	20.02	0.36	40.09	0.19	0.11	98.80	78.12	21.88
030A2e_olv011	2a	Rim	37.08	0.02	0.01	21.62	0.29	39.03	0.15	0.10	98.30	76.30	23.70
030A2e_olv010	2a	Rim	37.40	0.01	0.00	22.39	0.34	38.31	0.15	0.11	98.70	75.31	24.69
030A2e_olv032	2a	Rim	37.47	0.00	0.04	19.58	0.31	41.00	0.17	0.10	98.69	78.87	21.13
030A2e_olv031	2a	Rim	37.85	0.02	0.01	20.97	0.30	39.35	0.17	0.09	98.78	76.99	23.01
030A2e_olv022	2a	Rim	37.01	0.07	0.01	24.32	0.38	36.54	0.16	0.12	98.63	72.81	27.19
030A2e_olv023	2b	Rim	36.57	0.03	0.04	26.00	0.41	35.32	0.08	0.11	98.56	70.78	29.22

EMPA standard analyses (wt%) of USNM 2566

	Reported*	Analysed	+/-
SiO2	38.95	39.11	0.78
Al2O3		0.01	0.02
Cr2O3	0.02	0.03	0.01
ΣFeo	16.62	16.61	0.31
MnO	0.30	0.32	0.04
MgO	43.58	43.51	0.25
NiO		0.003	0.03
CaO		0.01	0.01
Total	99.47	99.61	0.84
			2sd, n=14

*Jarosewich, E., Nelen, J. A., and Norberg, J. A. (1980) Reference Samples for Electron Microprobe Analysis. Geostandards Newsletter 4, p. 43-47

IV. BSE images with EMPA locations

i. alg

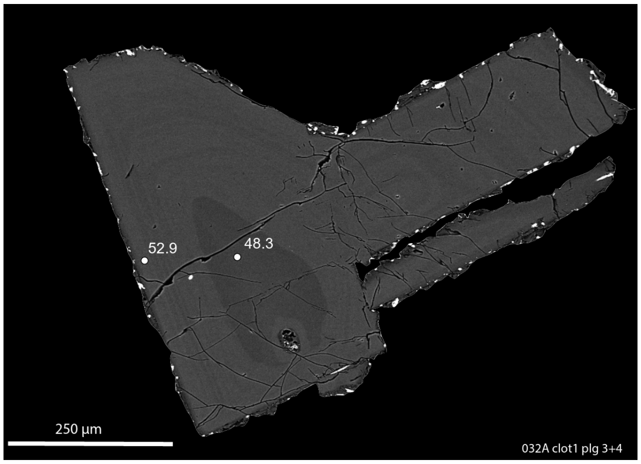

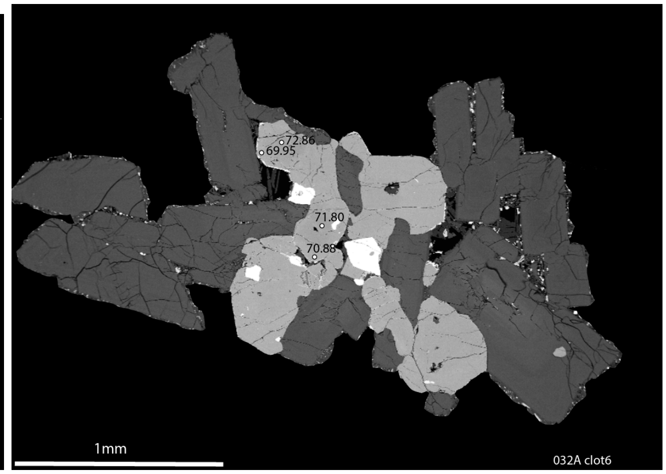

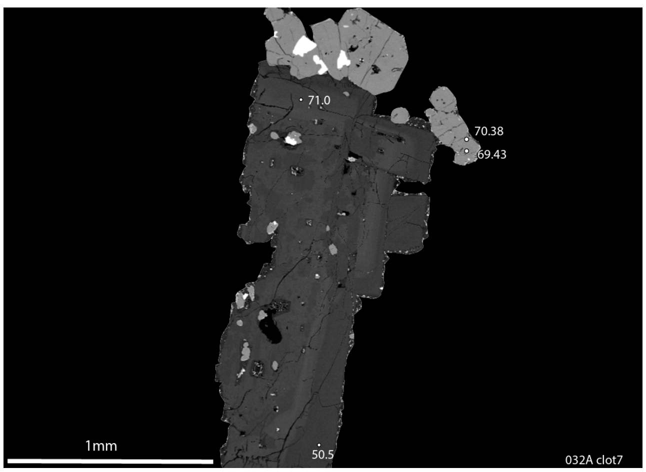

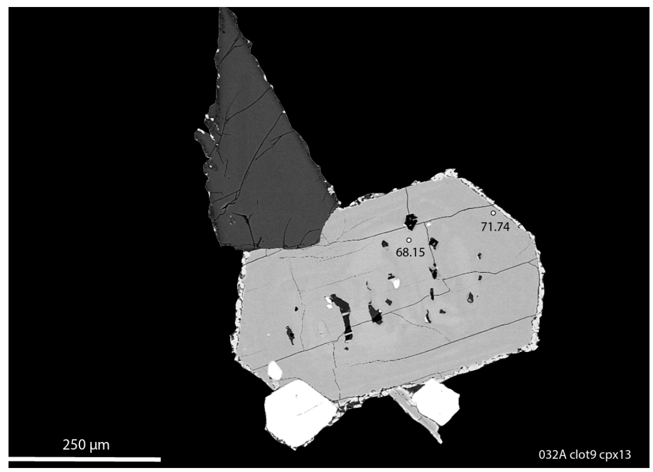

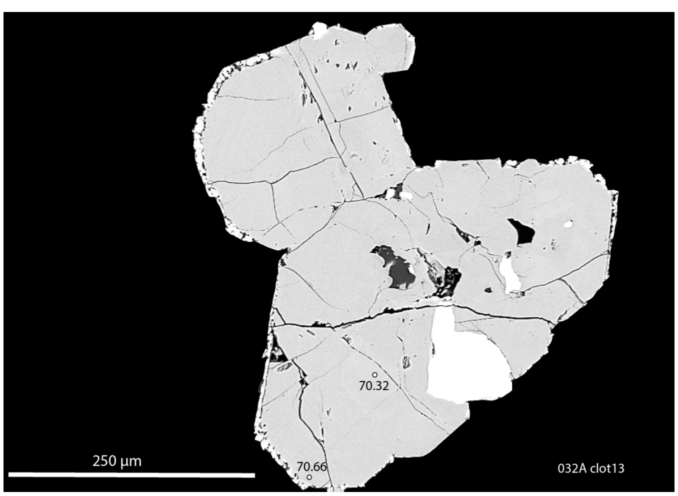

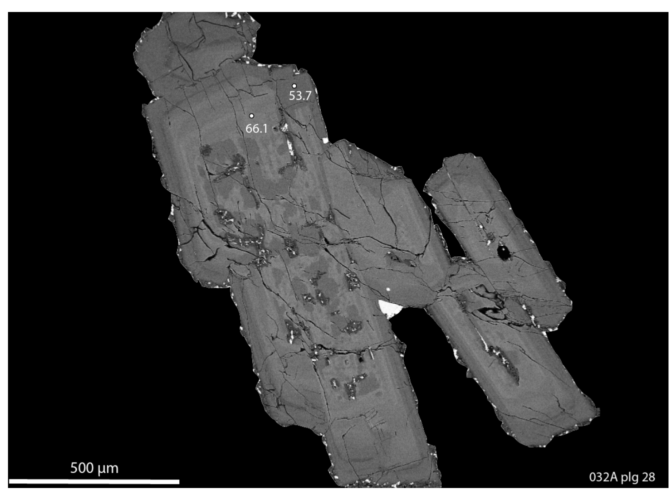

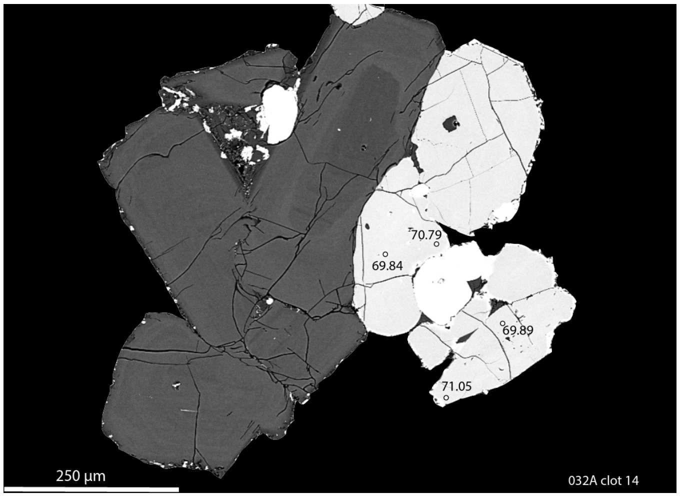
70.79
69.84
69.89
71.05
250 µm
032A clot 14

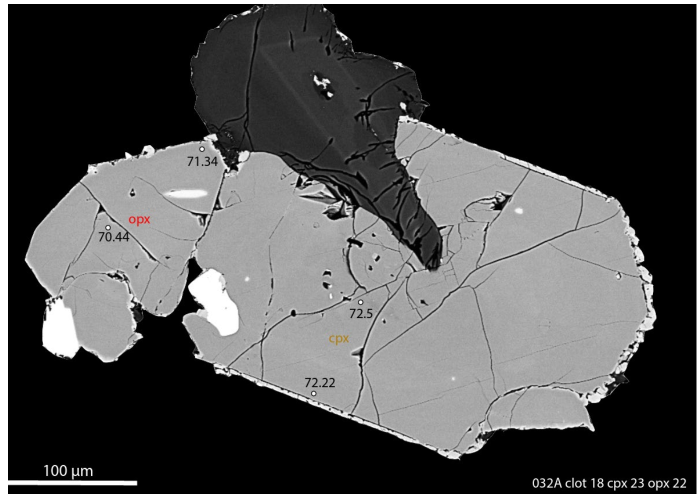
71.34
opx
70.44
72.5
cpx
72.22
100 µm
032A clot 18 cpx 23 opx 22

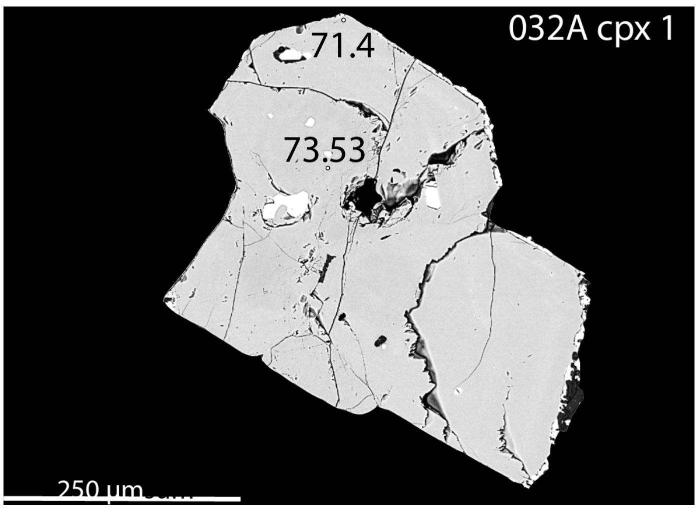
032A cpx 1
71.4
73.53
250 µm

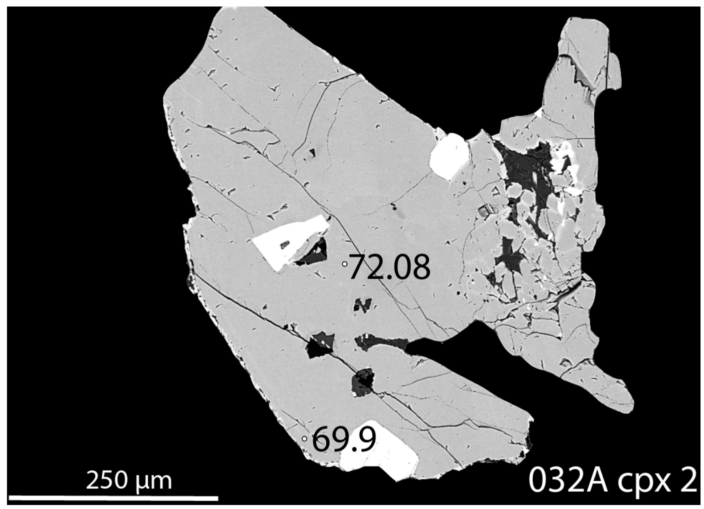
72.08
69.9
250 µm
032A cpx 2

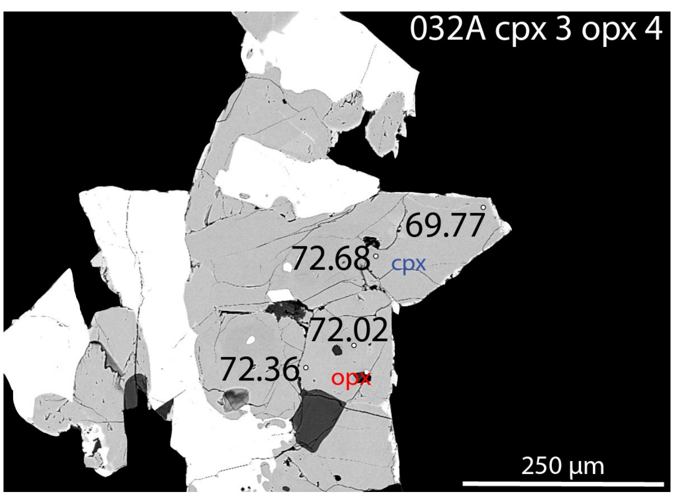
032A cpx 3 opx 4
69.77
72.68
cpx
72.02
72.36
opx
250 µm

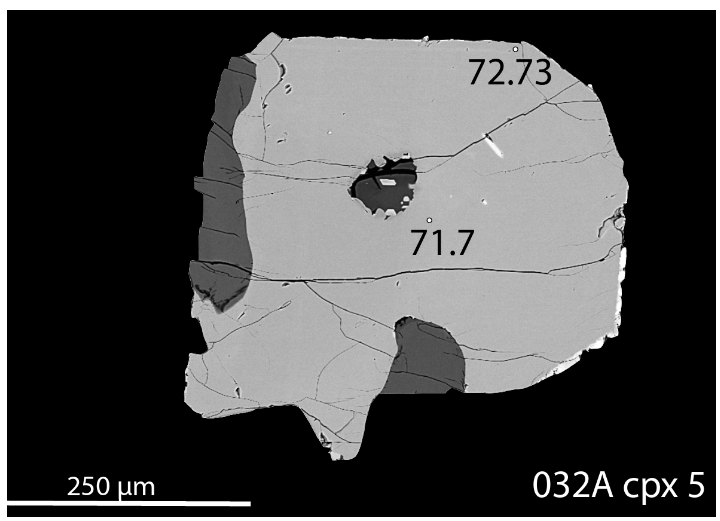
72.73
71.7
250 µm
032A cpx 5

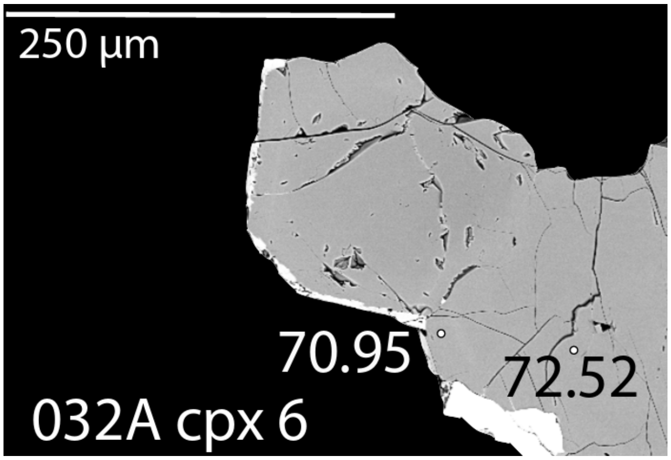
250 µm
70.95
72.52
032A cpx 6

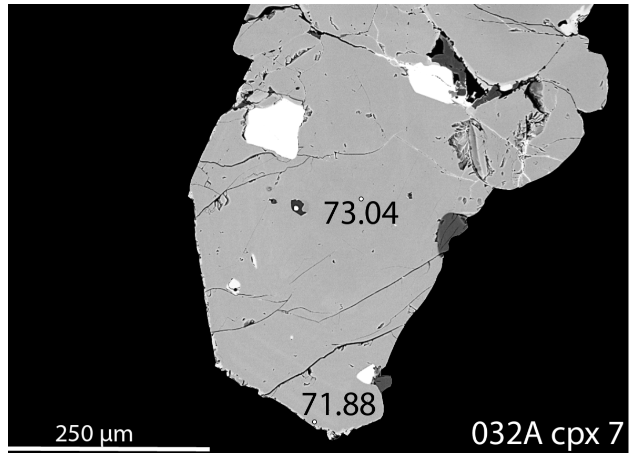
73.04
71.88
250 µm
032A cpx 7

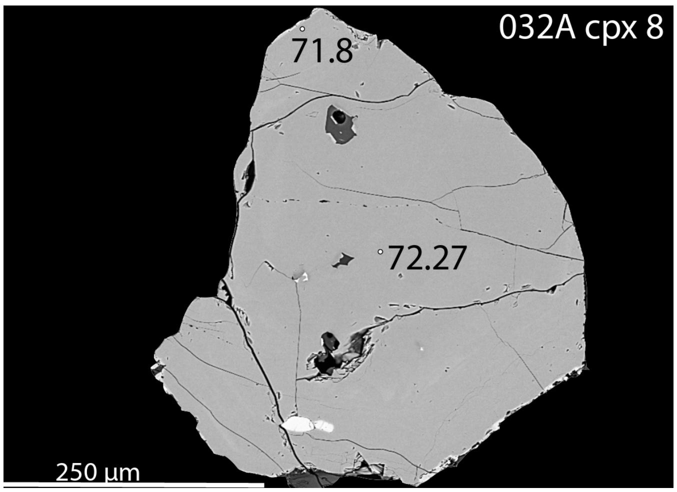
032A cpx 8
71.8
72.27
250 µm

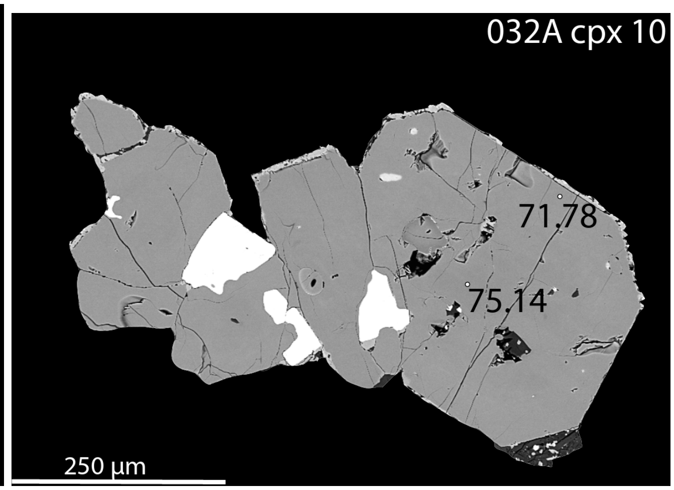
032A cpx 10
71.78
75.14
250 µm

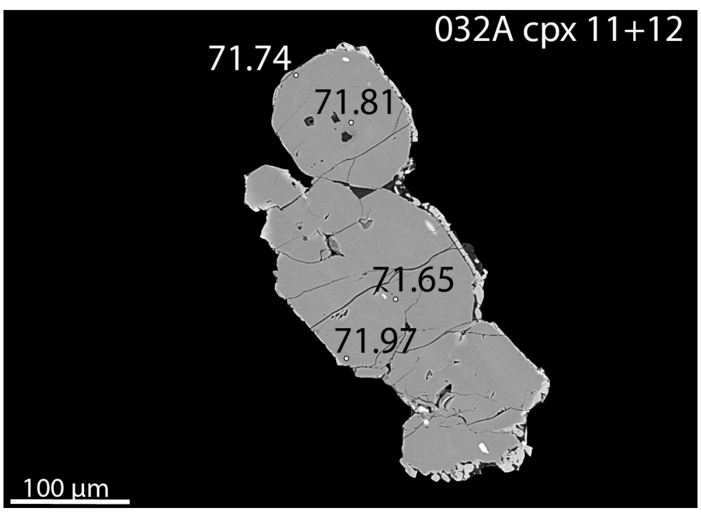
032A cpx 11+12
71.74
71.81
71.65
71.97
100 µm

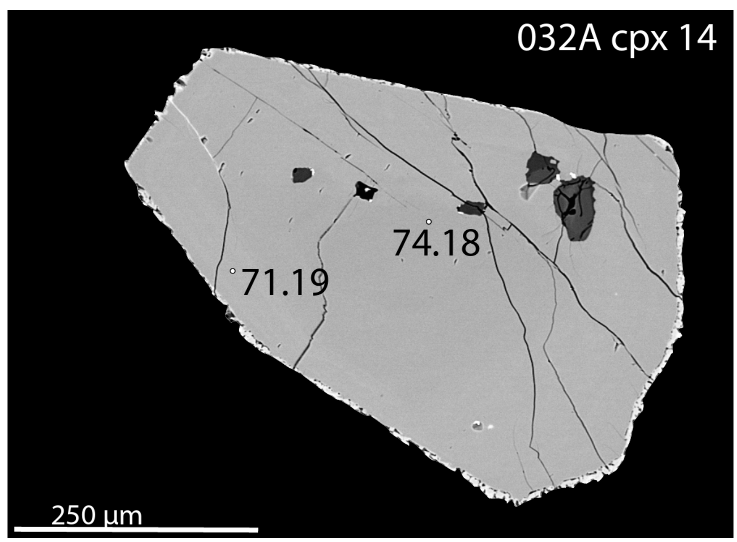
032A cpx 14
74.18
71.19
250 µm

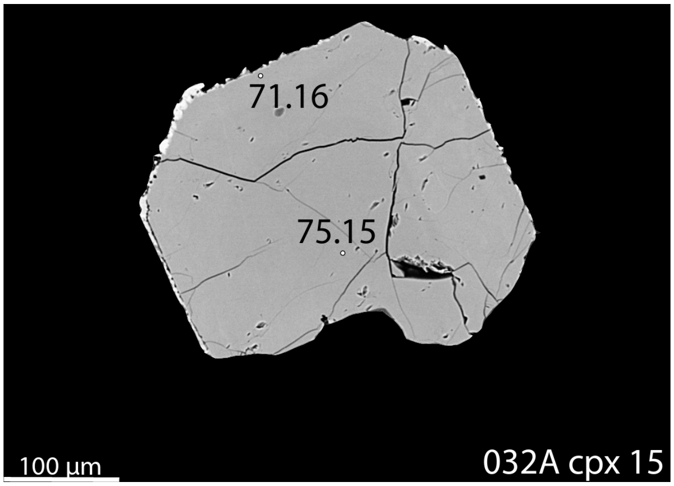
71.16
75.15
100 µm
032A cpx 15

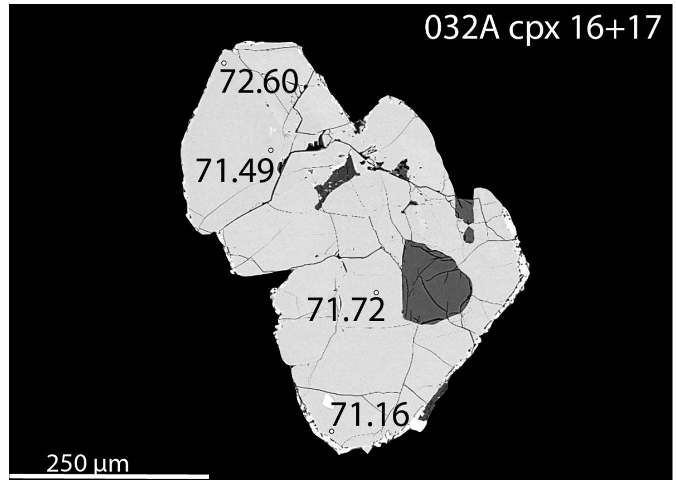
032A cpx 16+17
72.60
71.49
71.72
71.16
250 µm

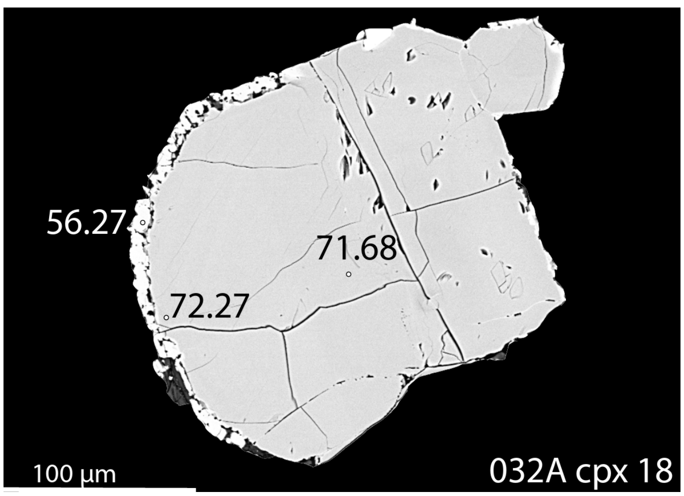
56.27
71.68
72.27
100 µm
032A cpx 18

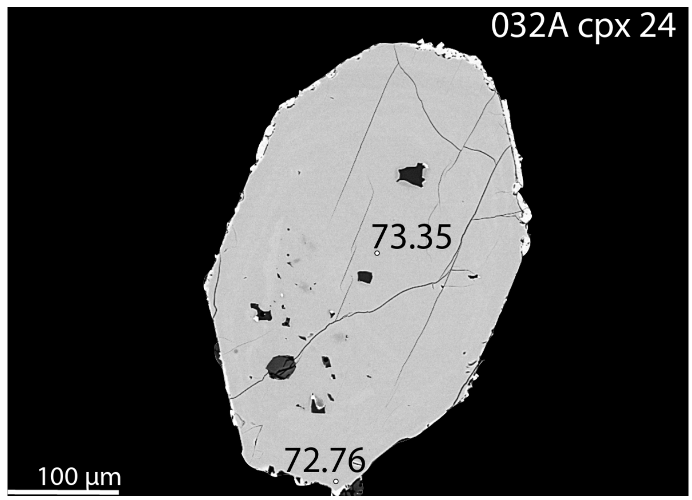
032A cpx 24
73.35
72.76
100 µm

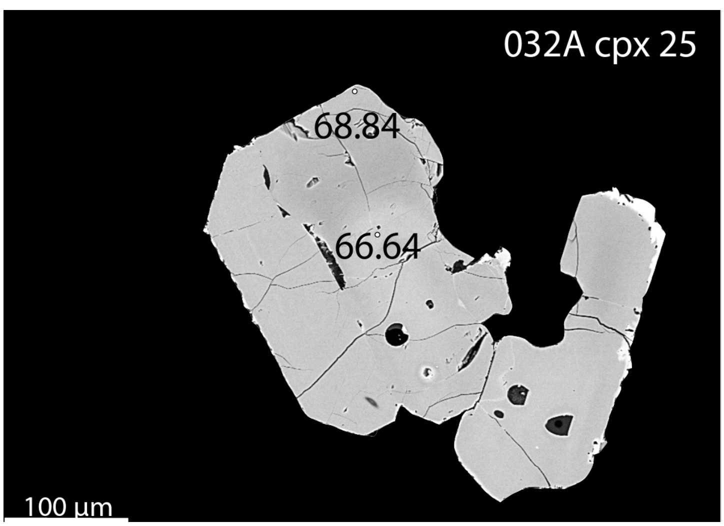
032A cpx 25
68.84
66.64
100 µm

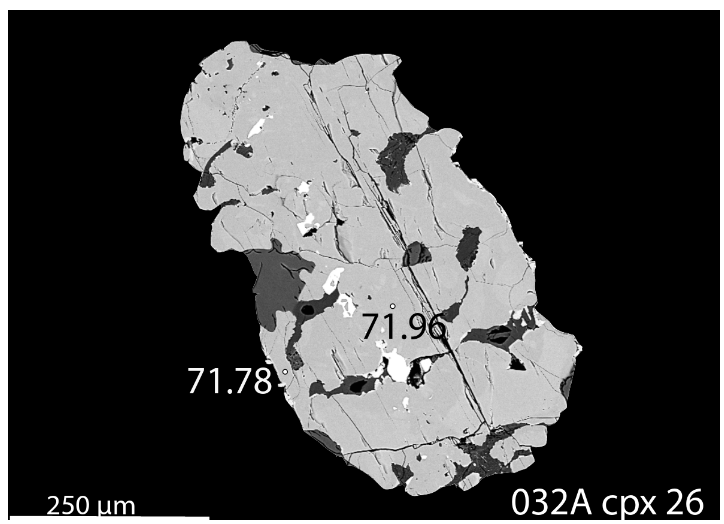
71.96
71.78
250 µm
032A cpx 26

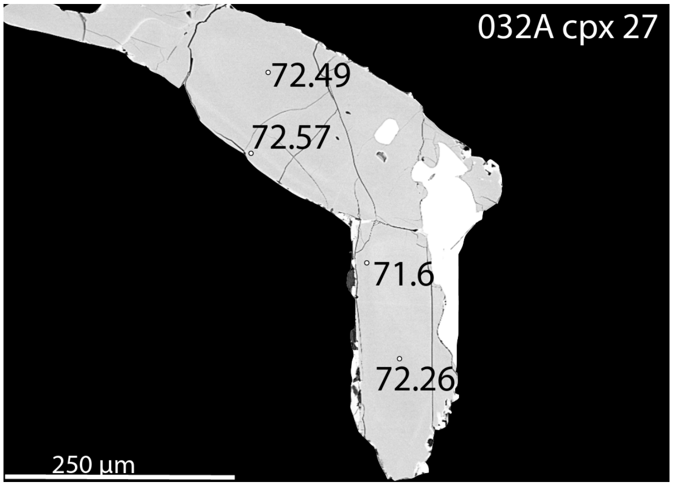
032A cpx 27
72.49
72.57
71.6
72.26
250 µm

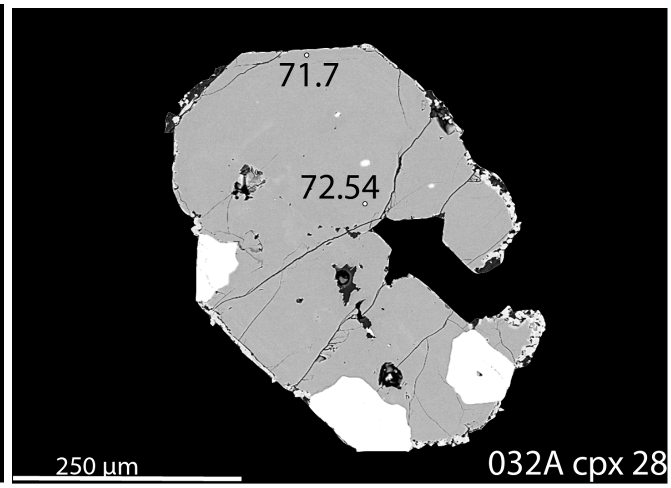
71.7
72.54
250 µm
032A cpx 28

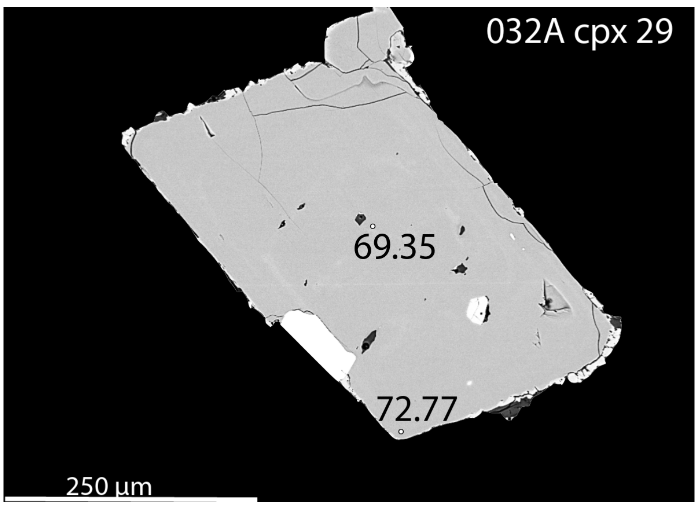
032A cpx 29
69.35
72.77
250 µm

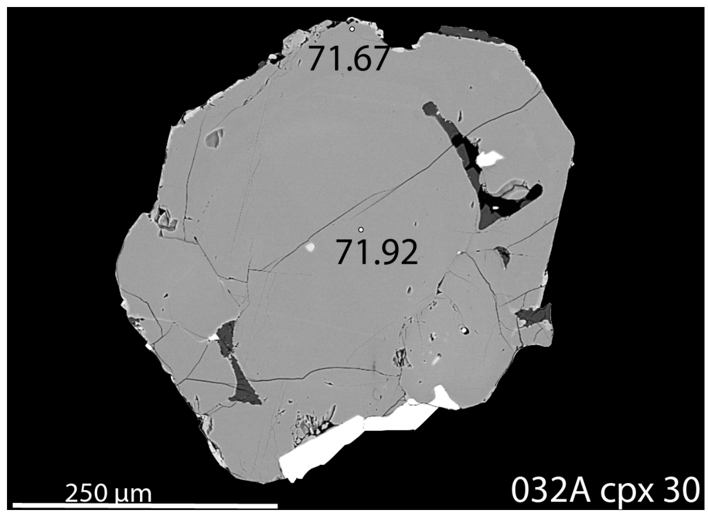
71.67
71.92
250 µm
032A cpx 30

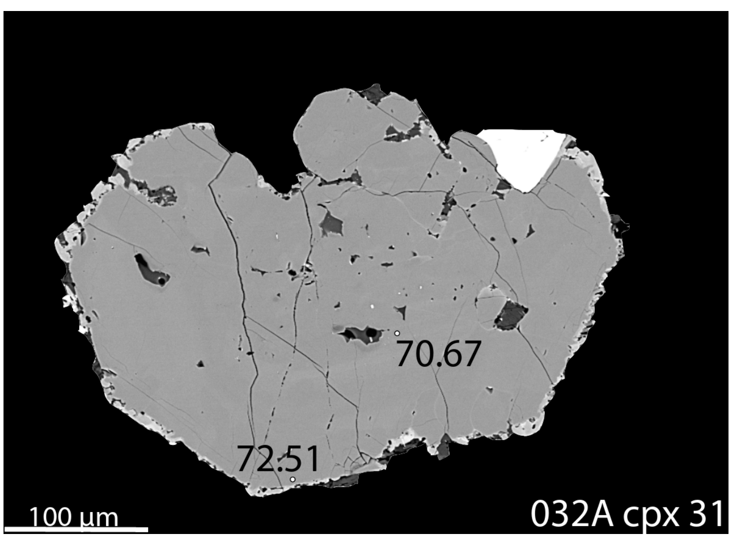
70.67
72.51
100 µm
032A cpx 31

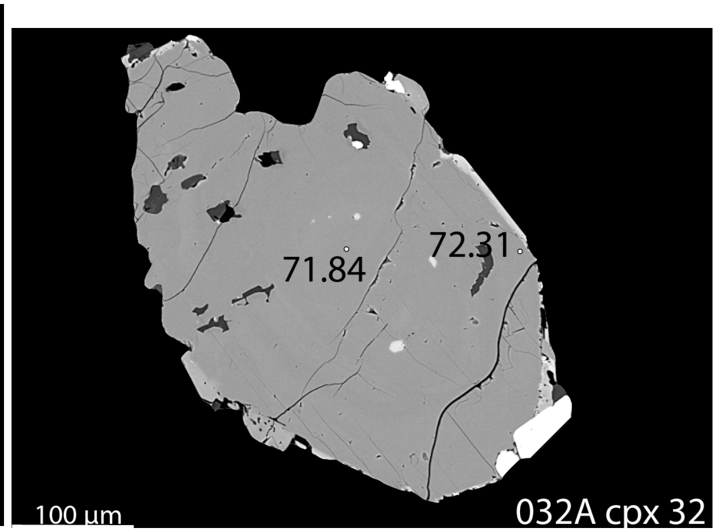
72.31
71.84
100 µm
032A cpx 32

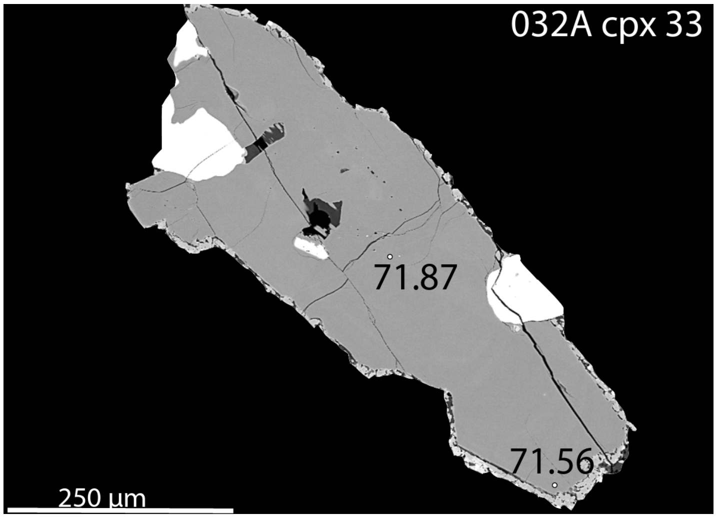
032A cpx 33
71.87
71.56
250 µm

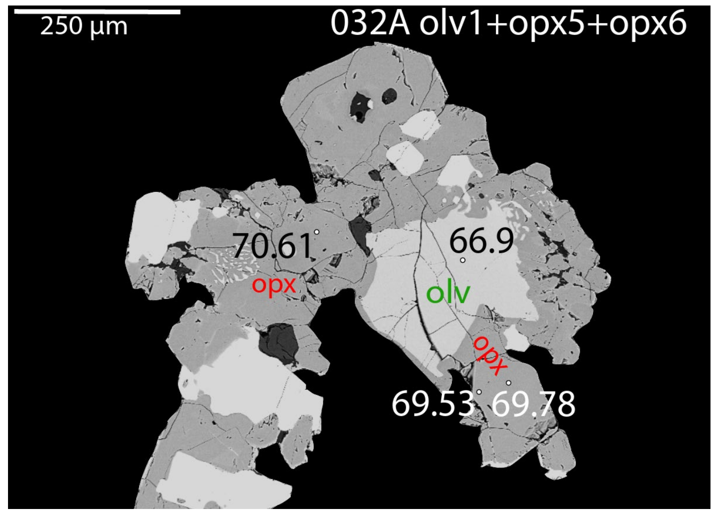
250 µm
032A olv1+opx5+opx6
70.61
opx
66.9
olv
opx
69.53
69.78

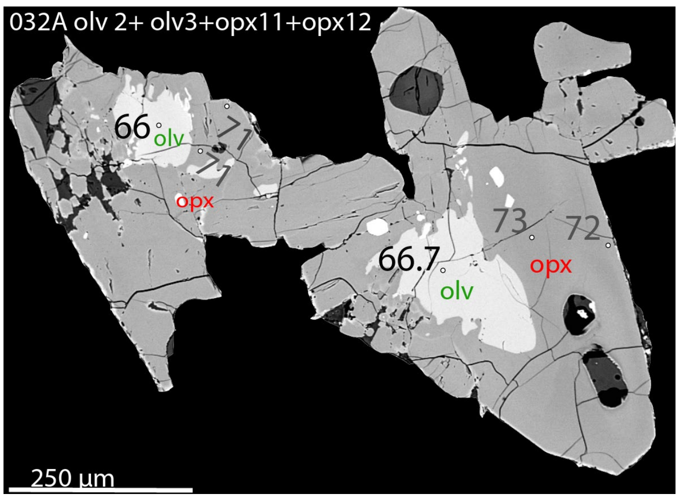
032A olv 2+ olv3+opx11+opx12
66
olv
71
71
opx
73
72
66.7
opx
olv
250 µm

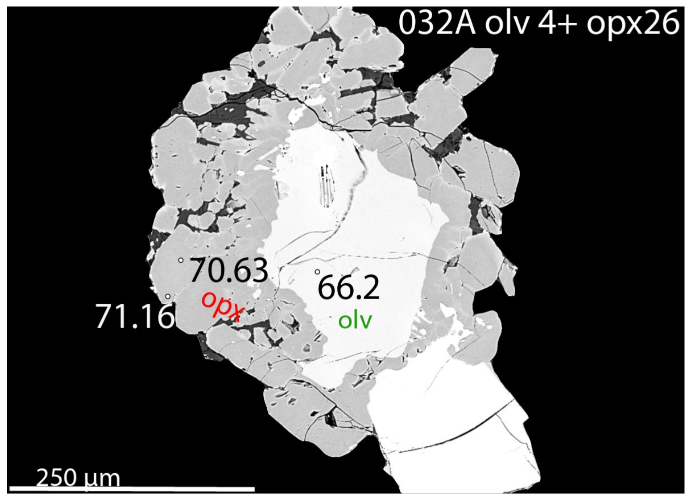
032A olv 4+ opx26
70.63
66.2
71.16
opx
olv
250 µm

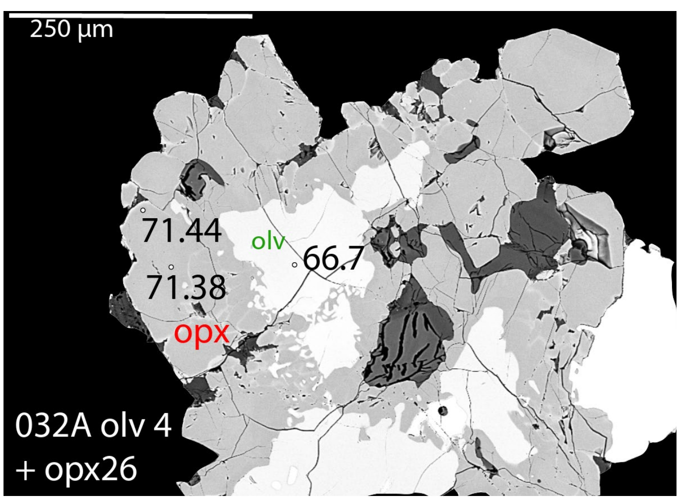
250 µm
71.44
olv
66.7
71.38
opx
032A olv 4
+ opx26

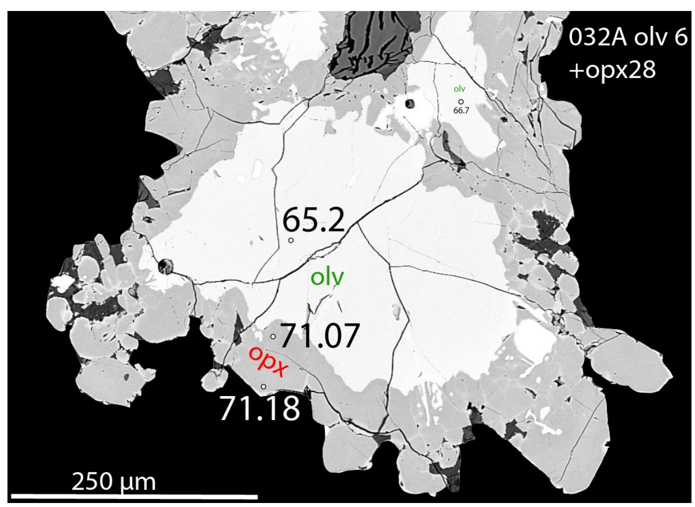
032A olv 6
+opx28
olv
66.7
65.2
olv
71.07
opx
71.18
250 µm

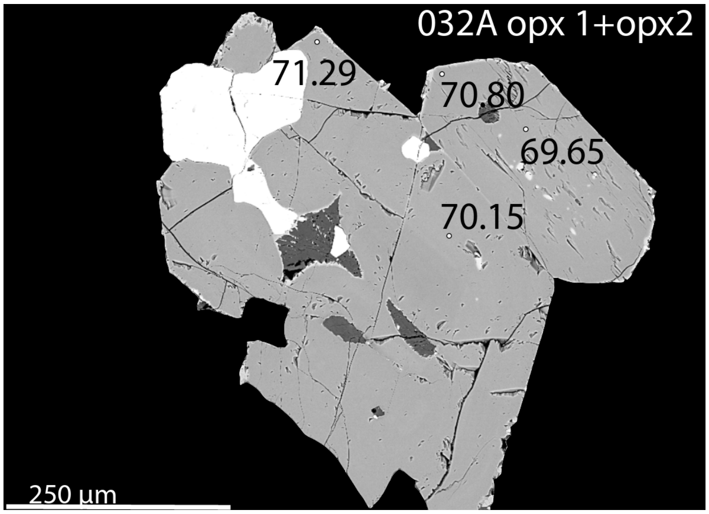
032A opx 1+opx2
71.29
70.80
69.65
70.15
250 µm

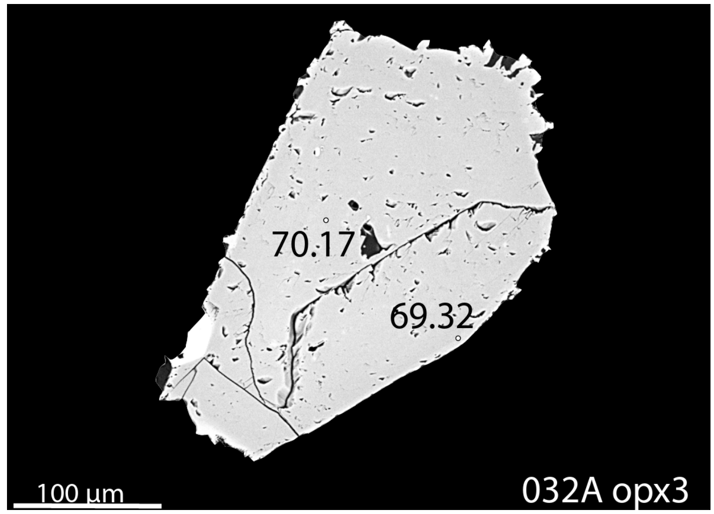
70.17
69.32
100 µm
032A opx3

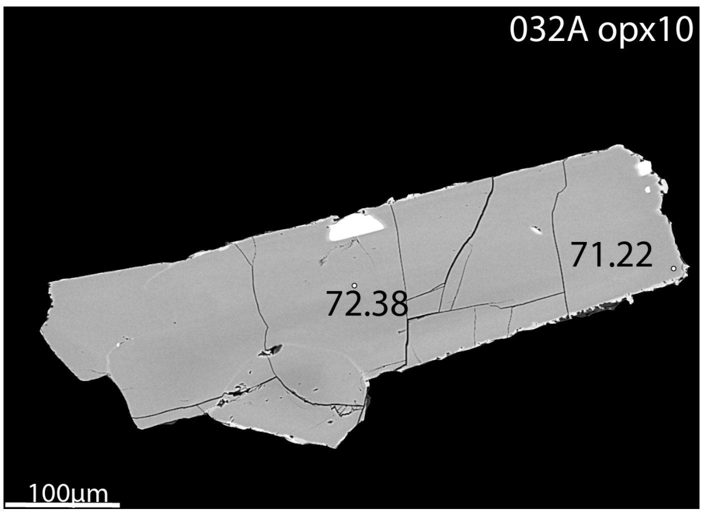
032A opx10
71.22
72.38
100µm

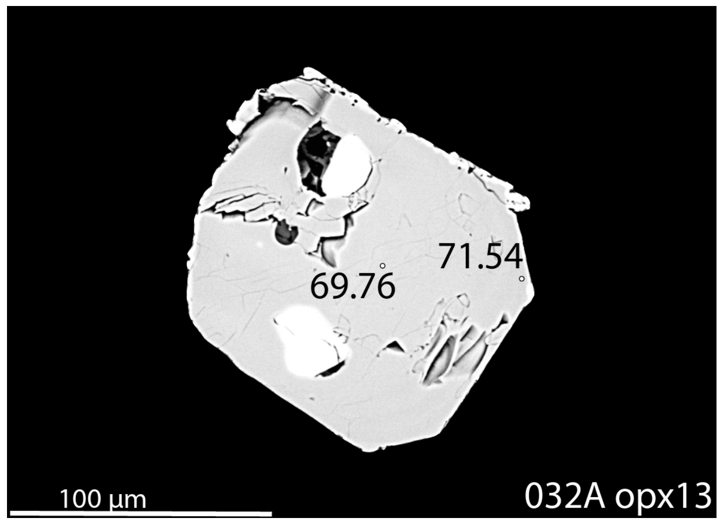
71.54
69.76
100 µm
032A opx13

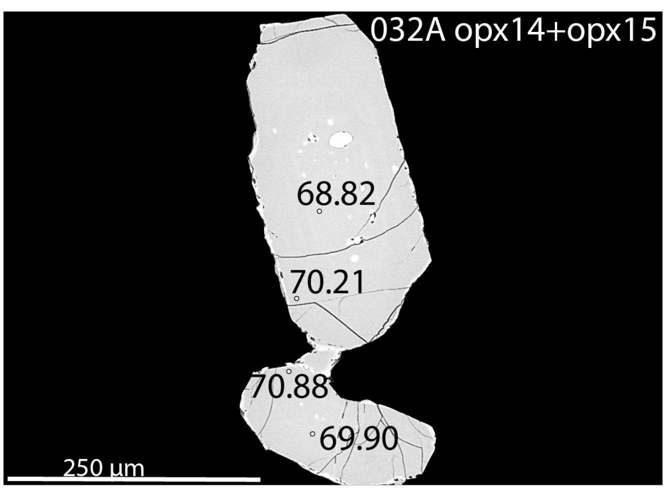
032A opx14+opx15
68.82
70.21
70.88
69.90
250 µm

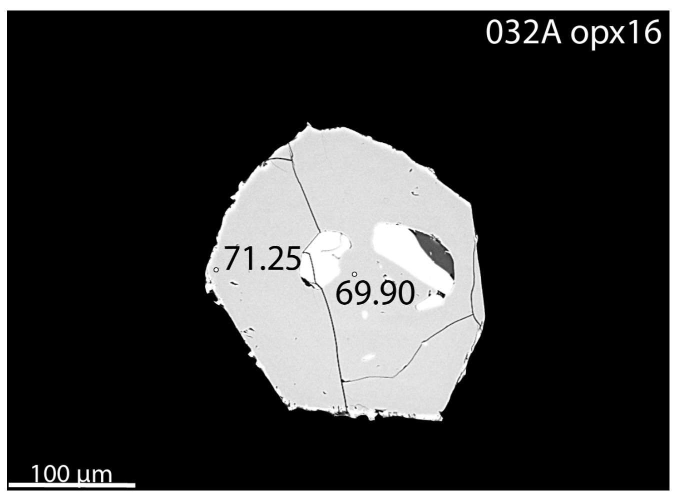
032A opx16
71.25
69.90
100 µm

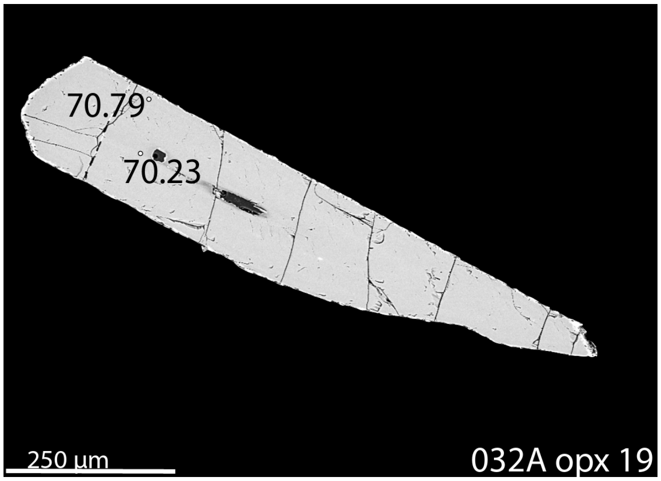
70.79
70.23
250 µm
032A opx 19

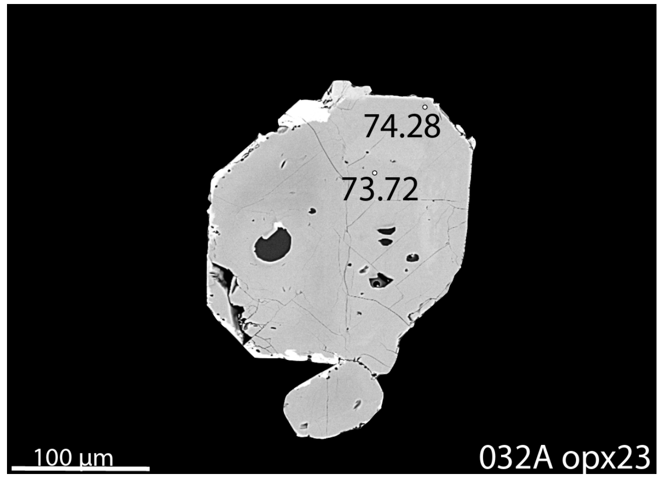
74.28
73.72
100 µm
032A opx23

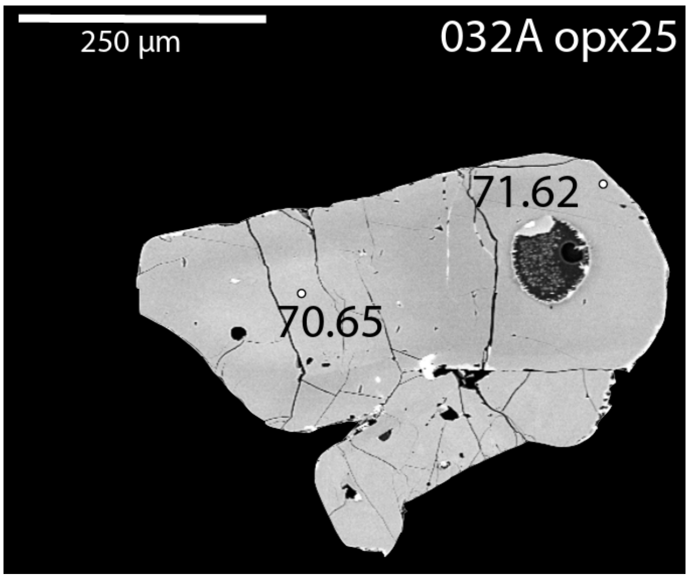
250 µm
032A opx25
71.62
70.65

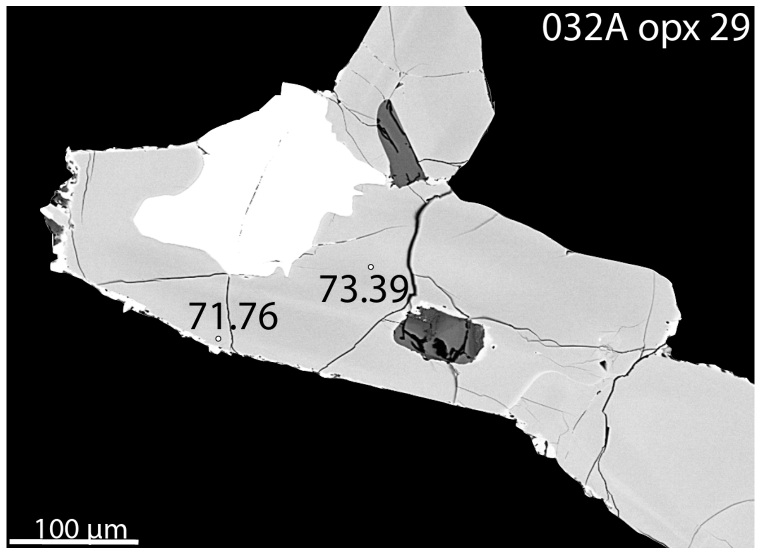
032A opx 29
73.39
71.76
100 µm

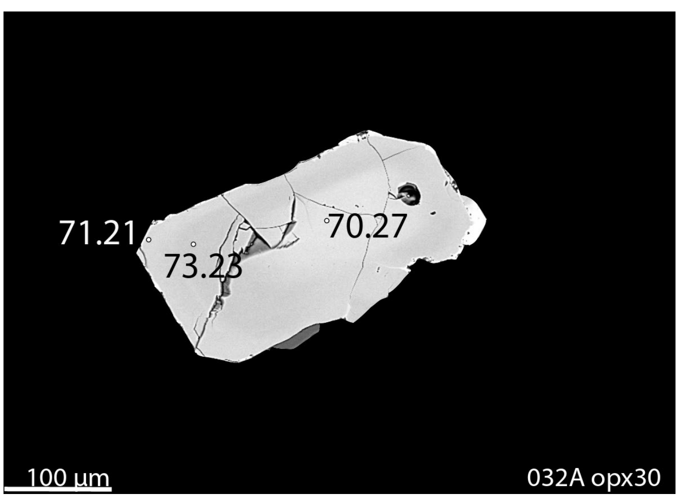
71.21
70.27
73.23
100 µm
032A opx30

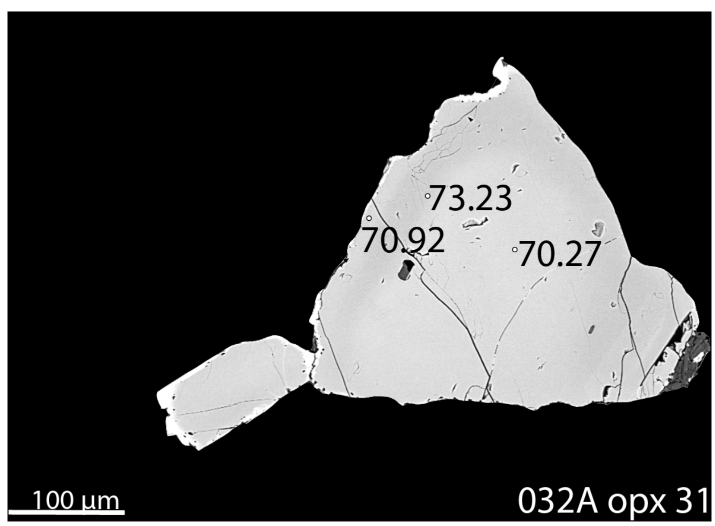
73.23
70.92
70.27
100 µm
032A opx 31

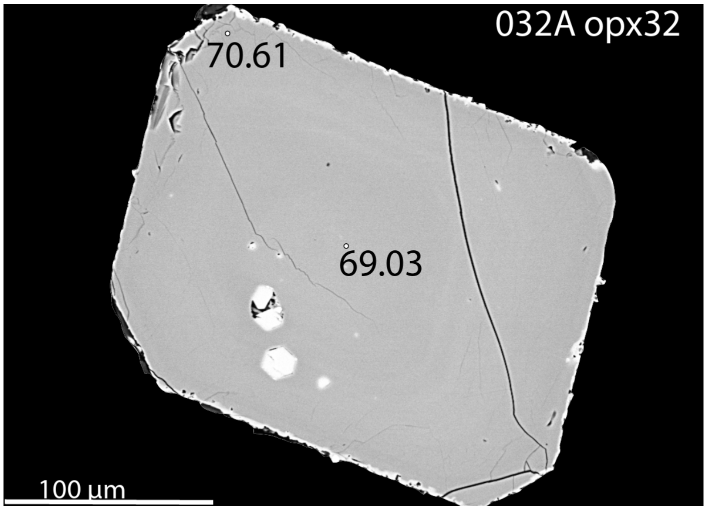
032A opx32
70.61
69.03
100 µm
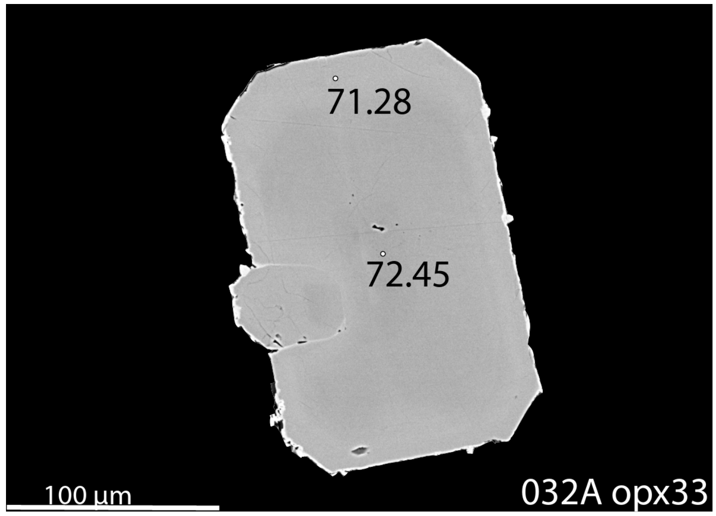
71.28
72.45
100 µm
032A opx33
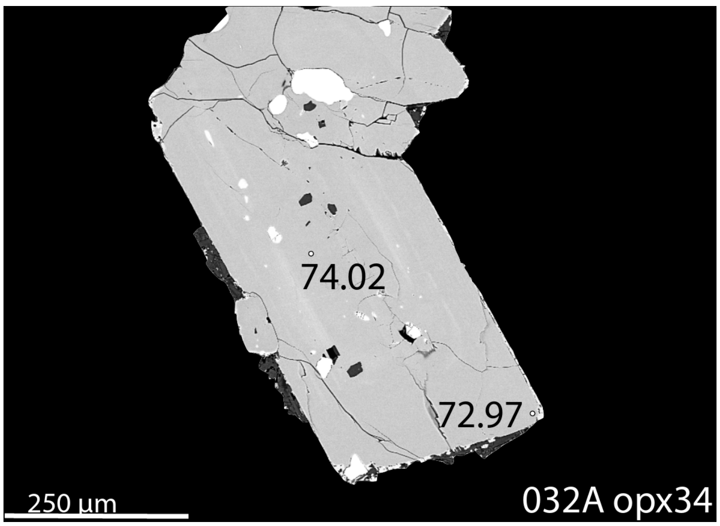
74.02
72.97
250 µm
032A opx34
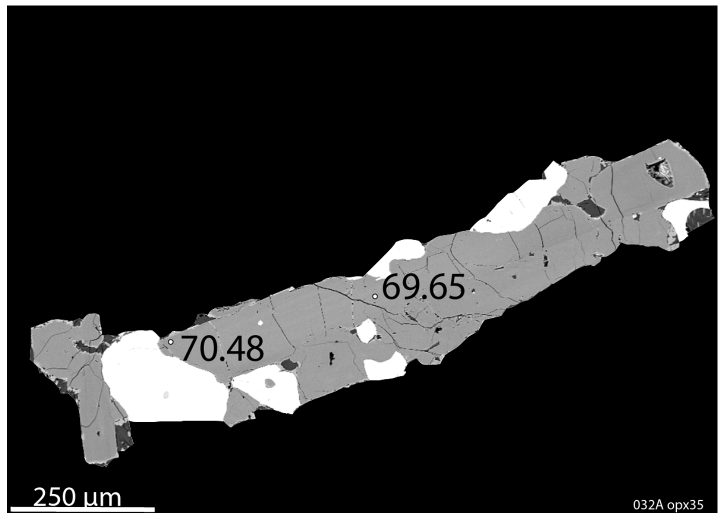
69.65
70.48
250 µm
032A opx35
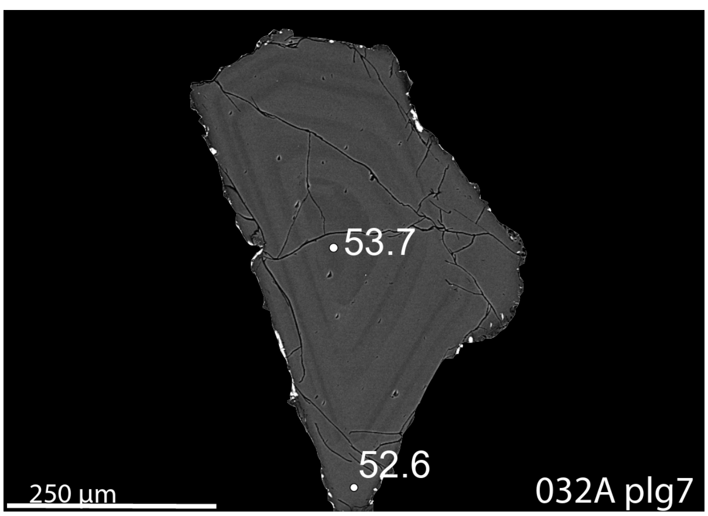
53.7
52.6
250 µm
032A plg7
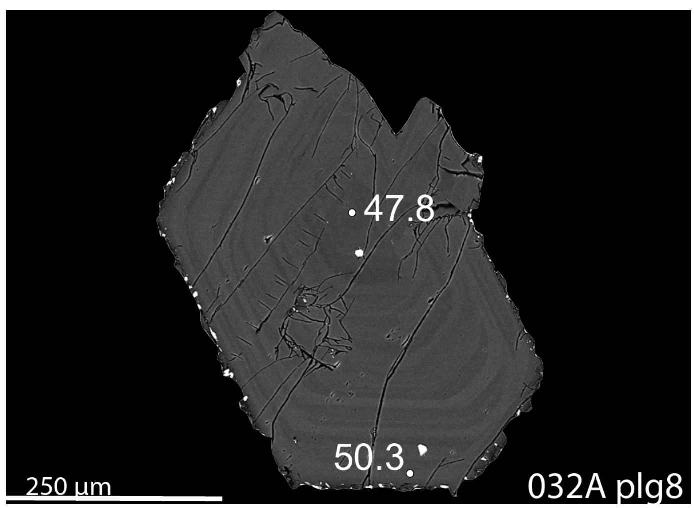
47.8
50.3
250 µm
032A plg8

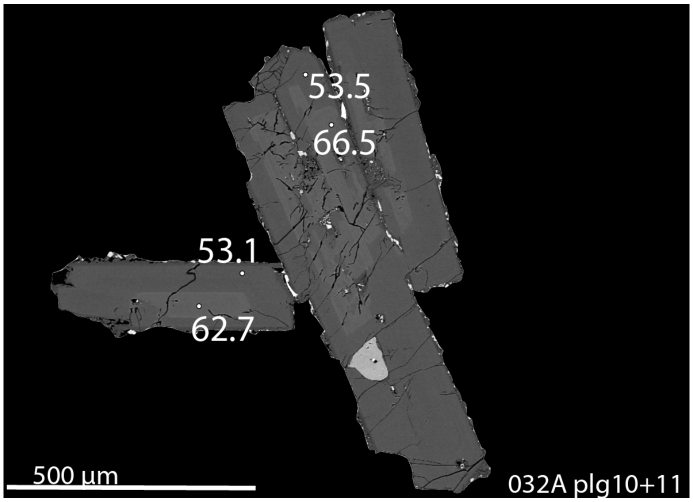
53.5
66.5
53.1
62.7
500 µm
032A plg10+11

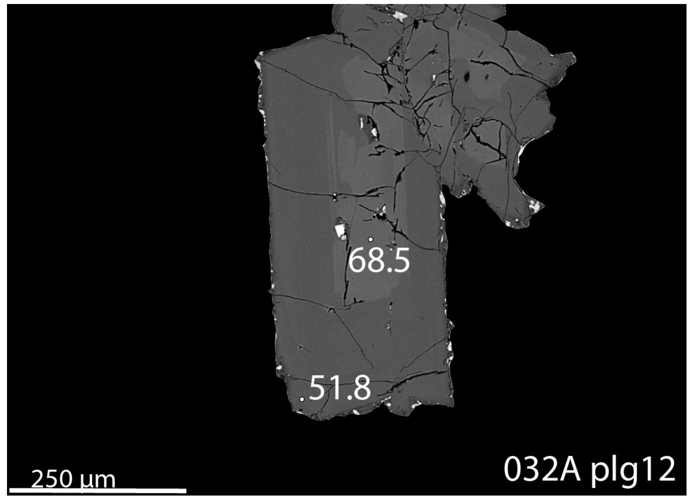
68.5
51.8
250 µm
032A plg12

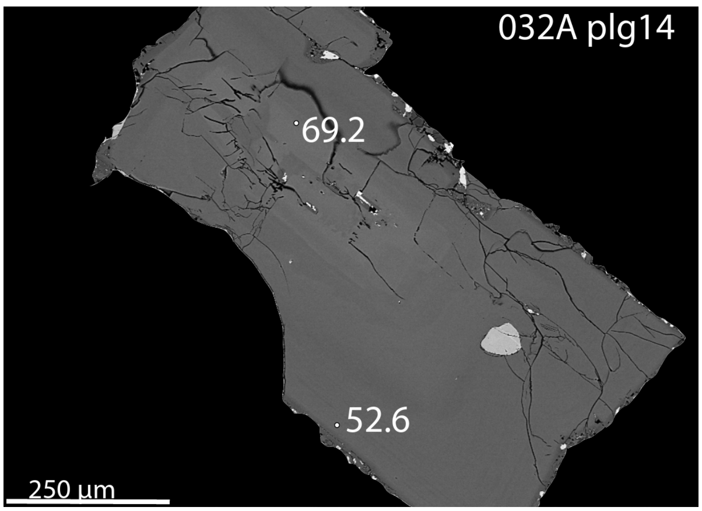
032A plg14
69.2
52.6
250 µm

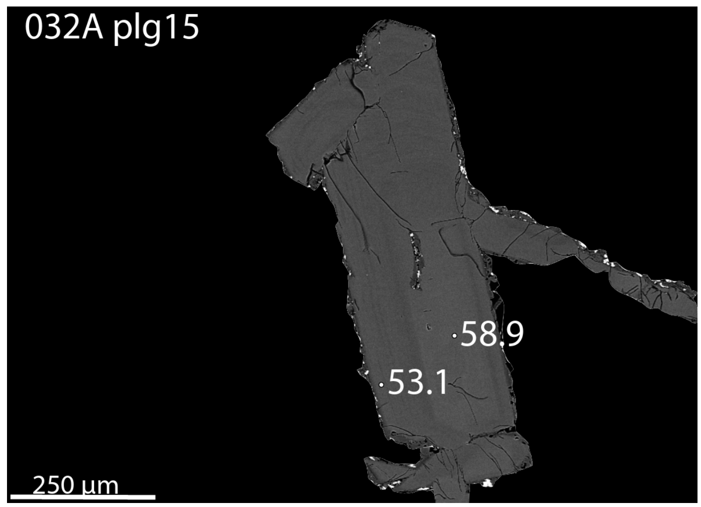
032A plg15
58.9
53.1
250 µm

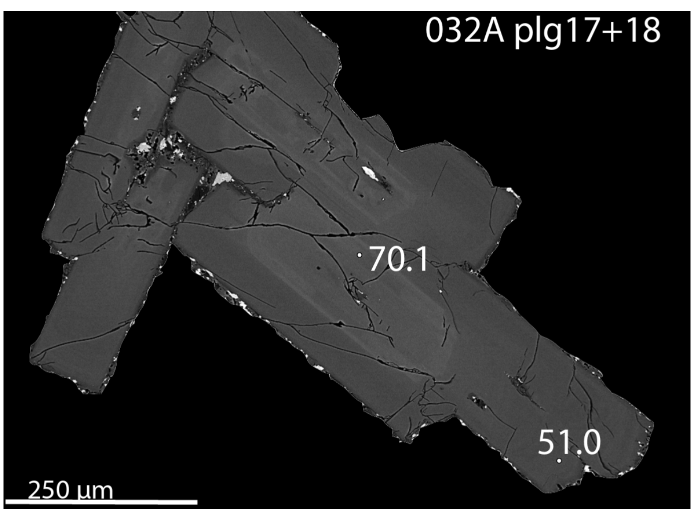
032A plg17+18
70.1
51.0
250 µm

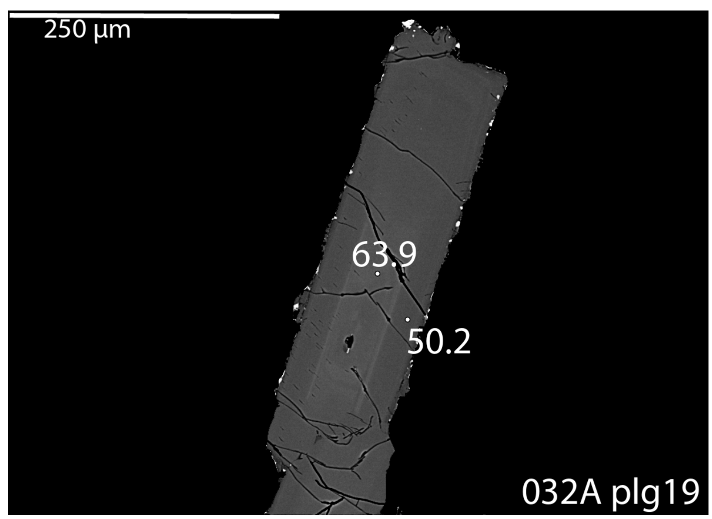
250 µm
63.9
50.2
032A plg19

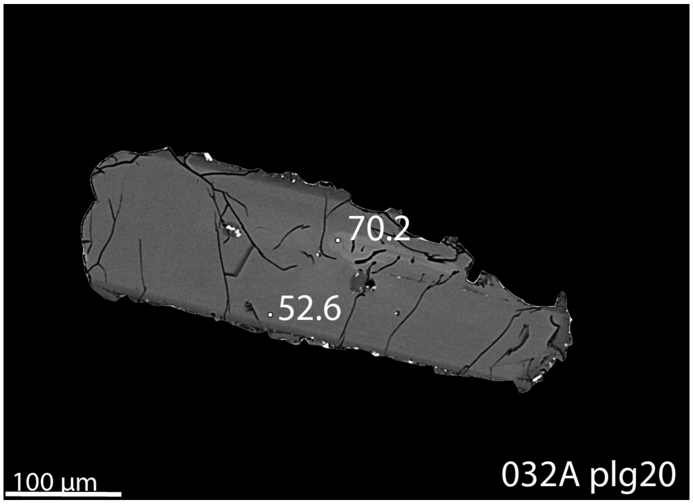
70.2
52.6
100 µm
032A plg20

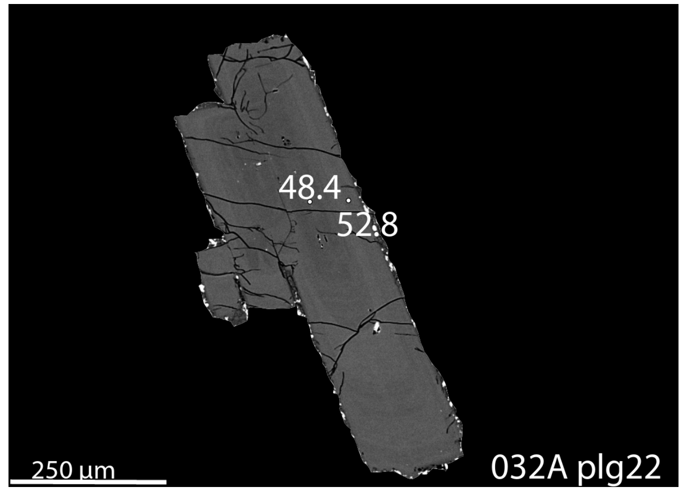
48.4
52.8
250 µm
032A plg22

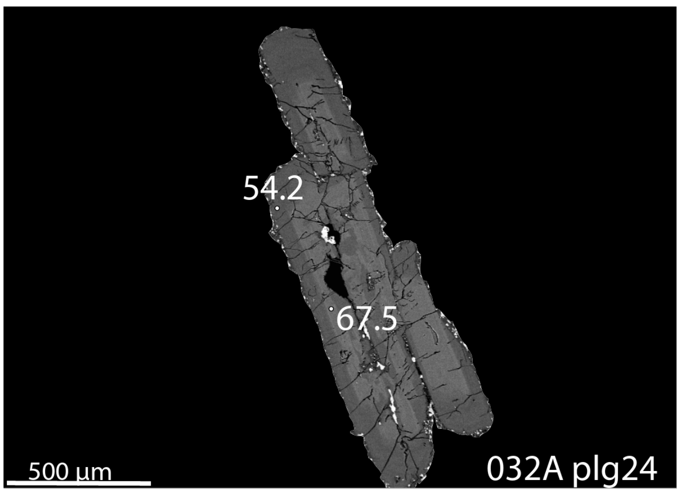
54.2
67.5
500 µm
032A plg24

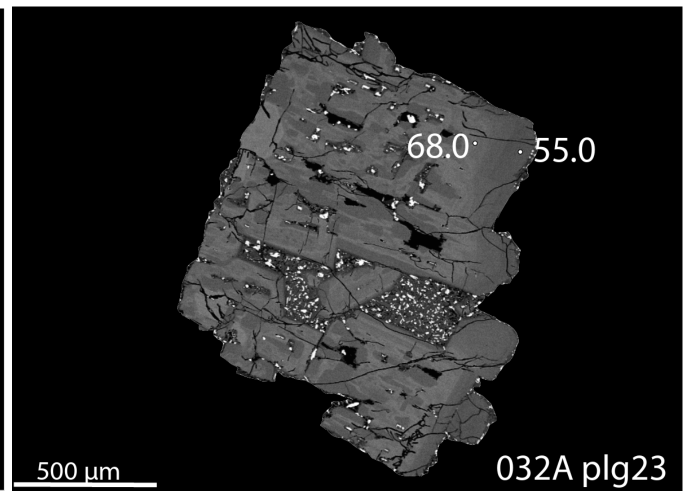
68.0
55.0
500 µm
032A plg23

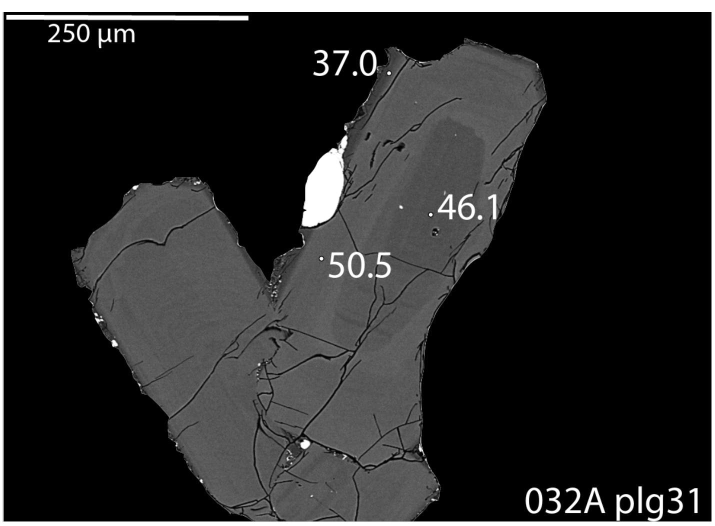
250 µm
37.0
46.1
50.5
032A plg31

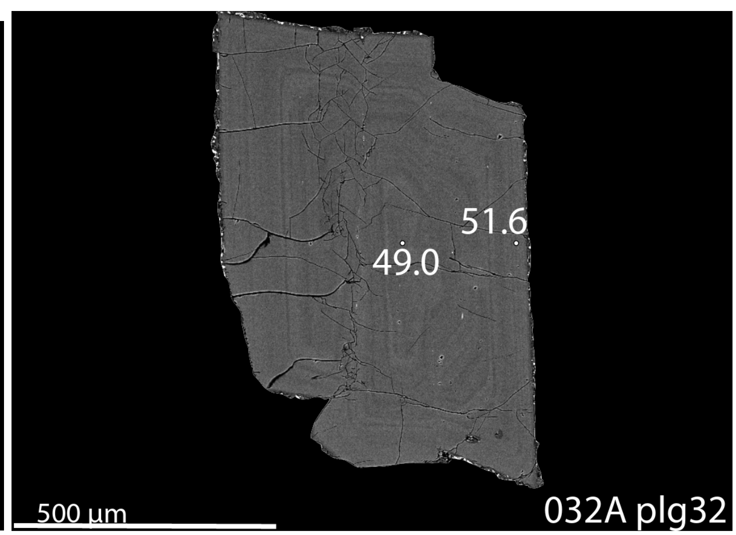
51.6
49.0
500 µm
032A plg32

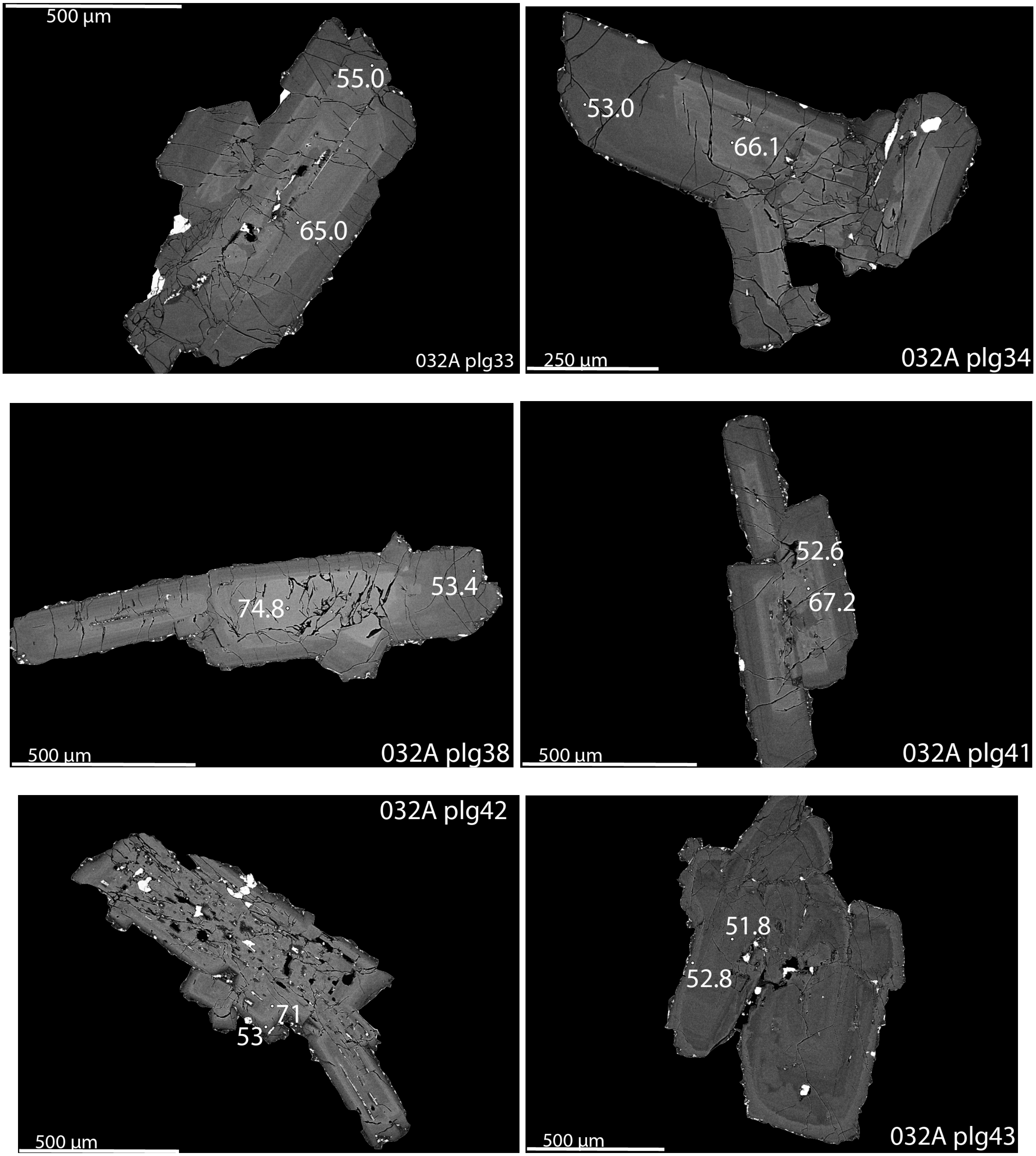
500 µm
55.0
65.0
032A plg33
53.0
66.1
250 µm
032A plg34
74.8
53.4
500 µm
032A plg38
52.6
67.2
500 µm
032A plg41
032A plg42
71
53
500 µm
51.8
52.8
500 µm
032A plg43

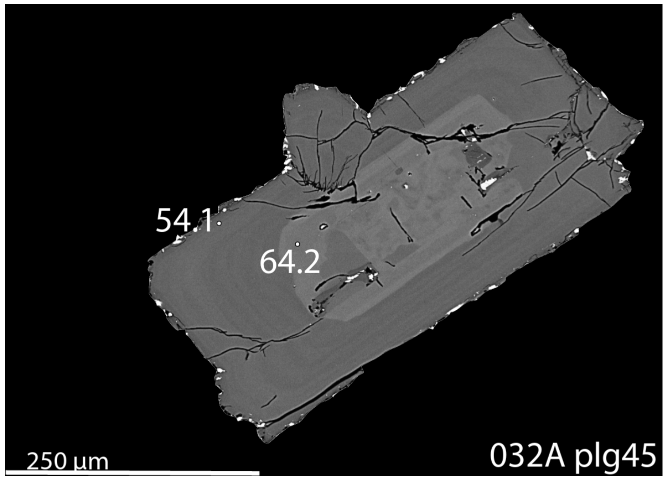
54.1
64.2
250 µm
032A plg45

ii. alc

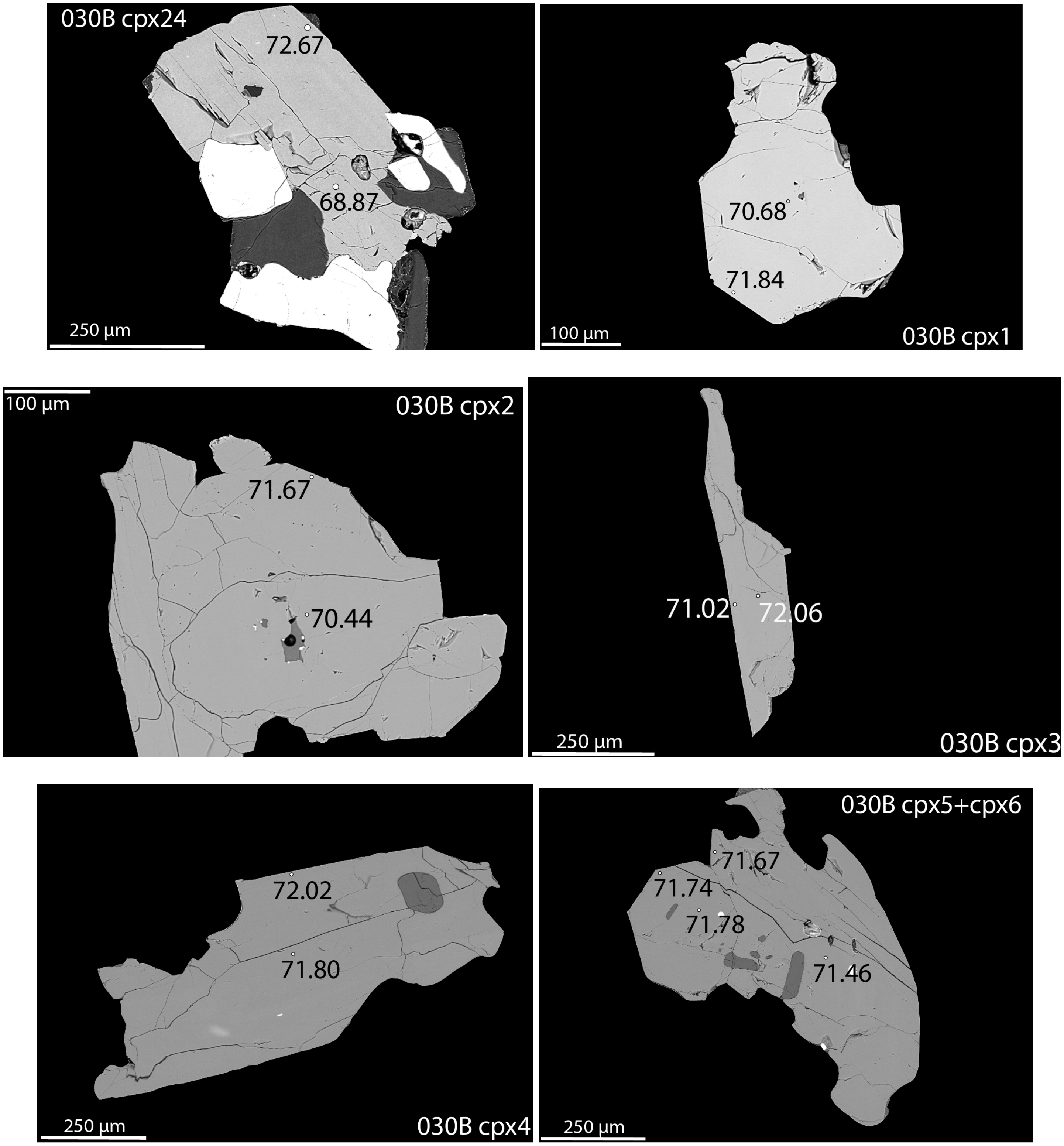
030B cpx24
72.67
68.87
250 µm
70.68
71.84
100 µm
030B cpx1
100 µm
030B cpx2
71.67
70.44
71.02
72.06
250 µm
030B cpx3
72.02
71.80
250 µm
030B cpx4
030B cpx5+cpx6
71.67
71.74
71.78
71.46
250 µm

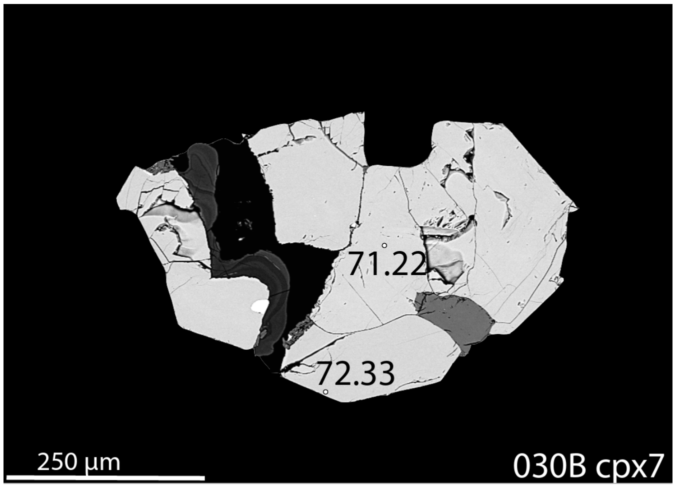
71.22
72.33
250 µm
030B cpx7

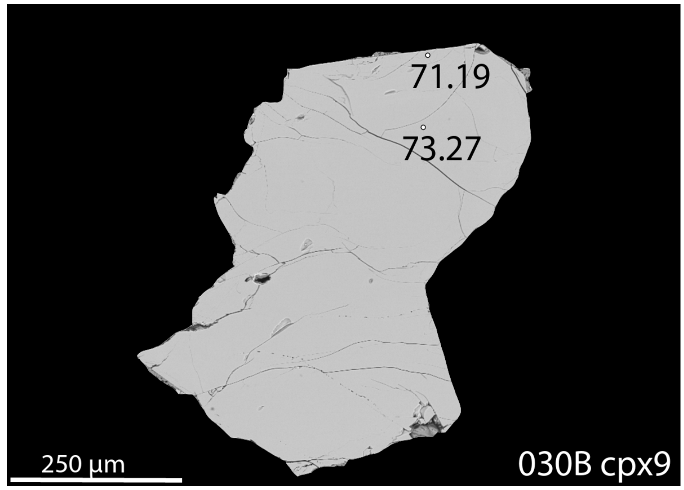
71.19
73.27
250 µm
030B cpx9

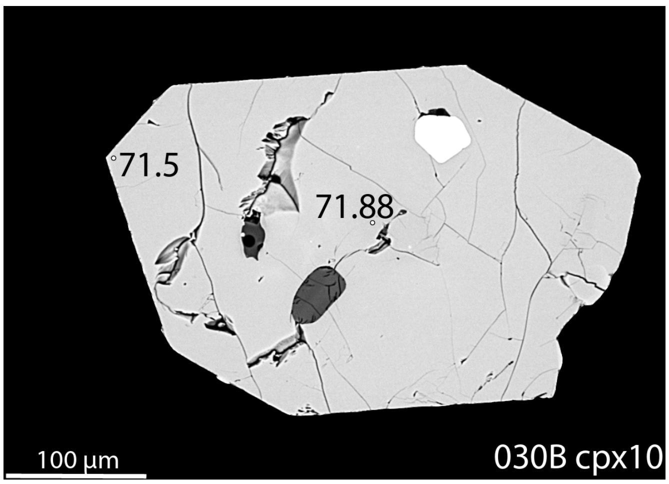
71.5
71.88
100 µm
030B cpx10

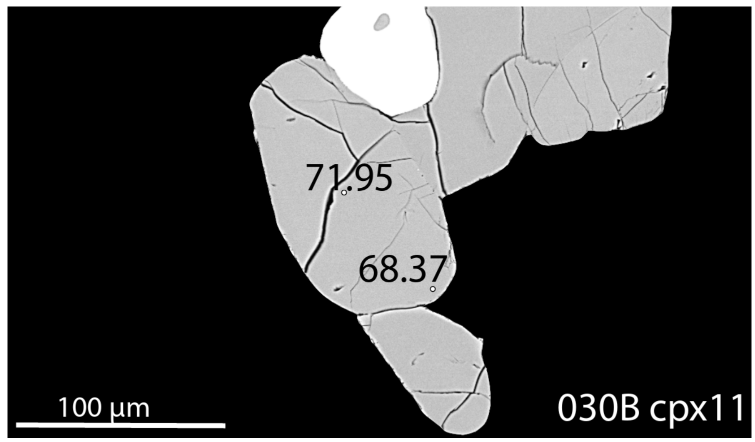
71.95
68.37
100 µm
030B cpx11

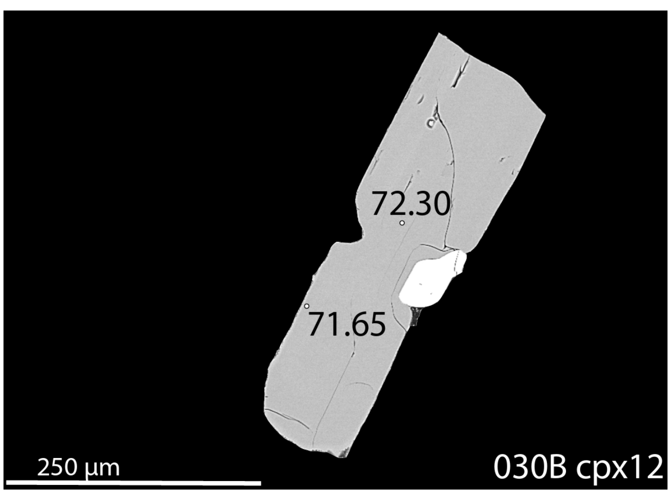
72.30
71.65
250 µm
030B cpx12

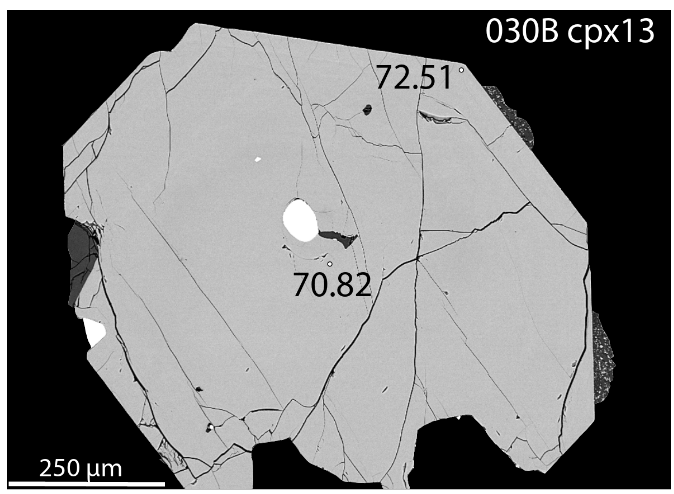
030B cpx13
72.51
70.82
250 µm

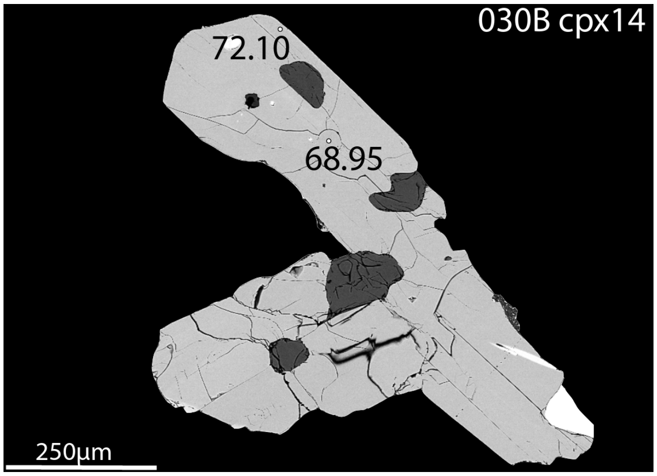
030B cpx14
72.10
68.95
250µm

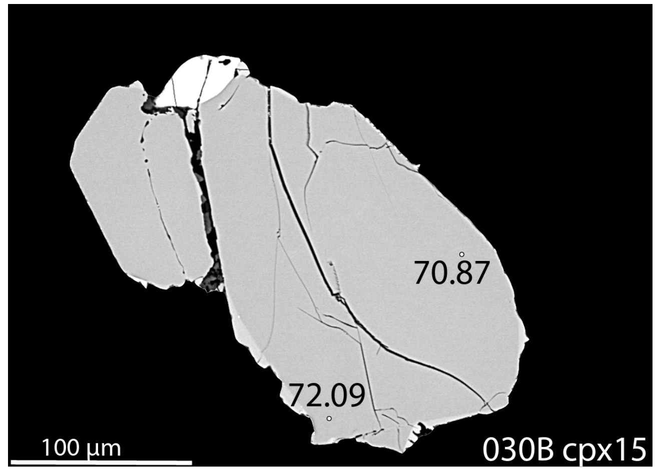
70.87
72.09
100 µm
030B cpx15

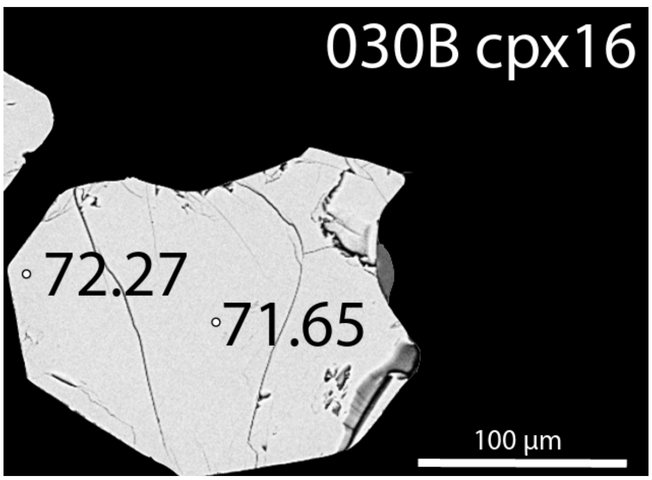
030B cpx16
72.27
71.65
100 µm

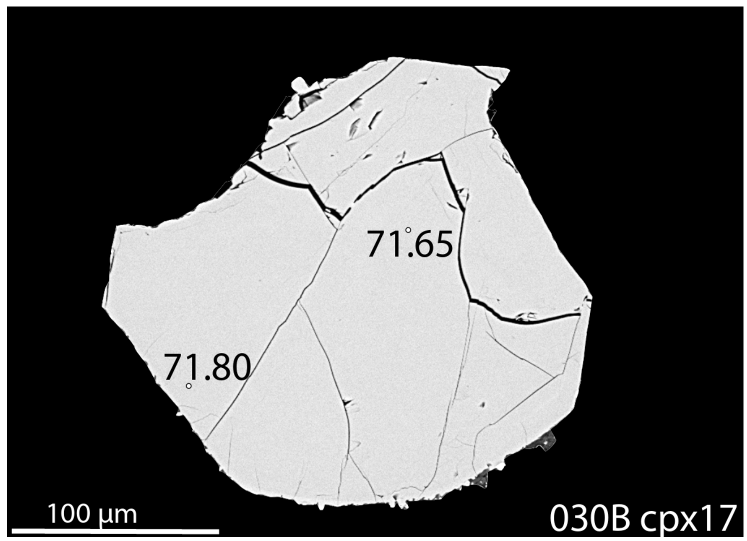
71.65
71.80
100 µm
030B cpx17

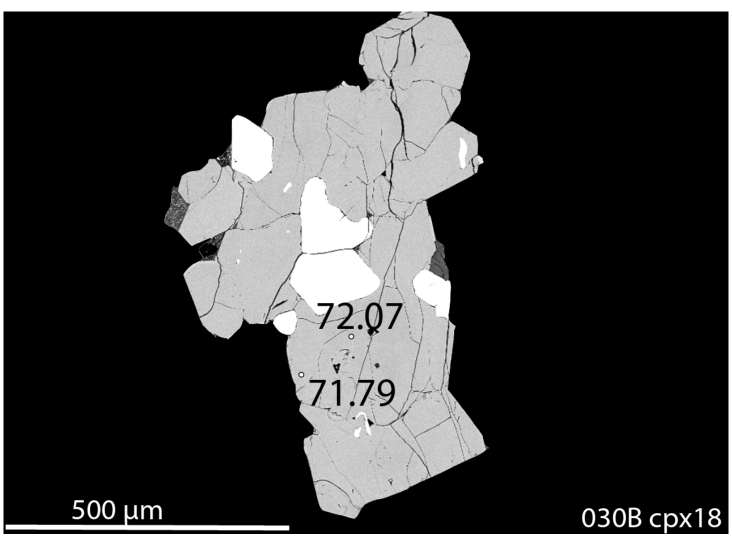
72.07
71.79
500 µm
030B cpx18

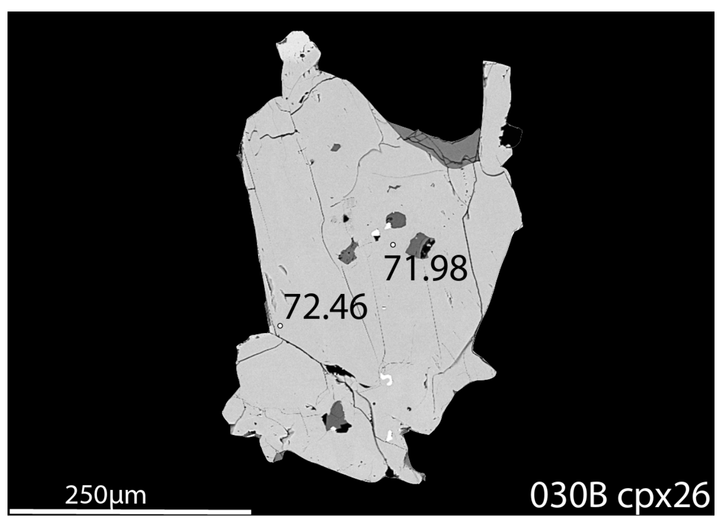
71.98
72.46
250µm
030B cpx26

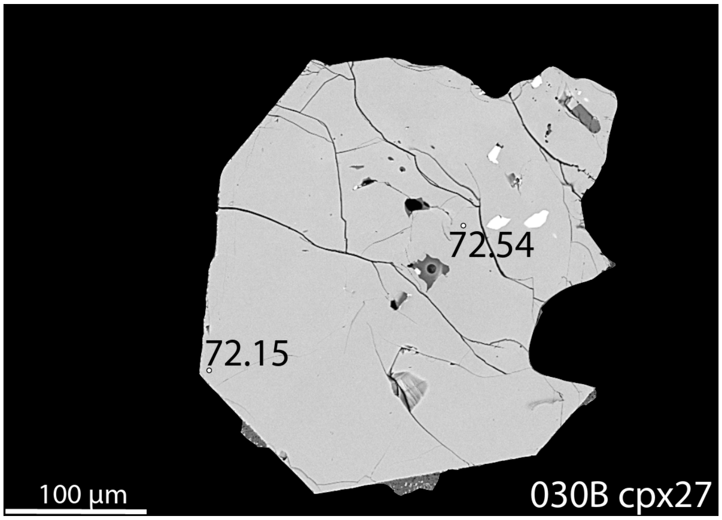
72.54
72.15
100 µm
030B cpx27

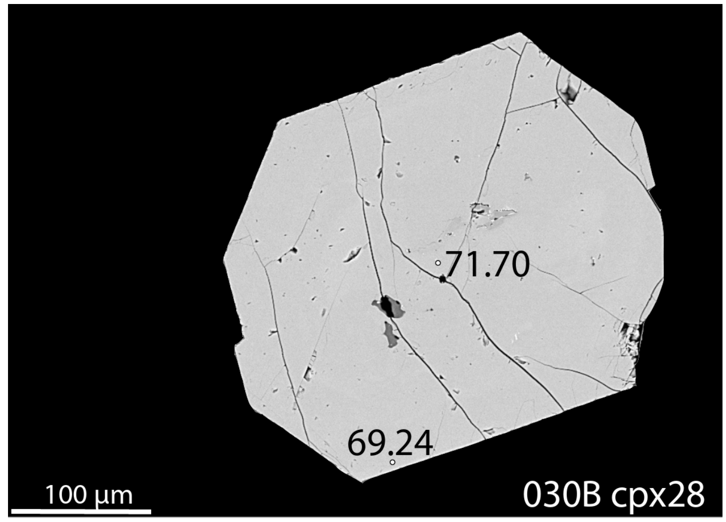
71.70
69.24
100 µm
030B cpx28

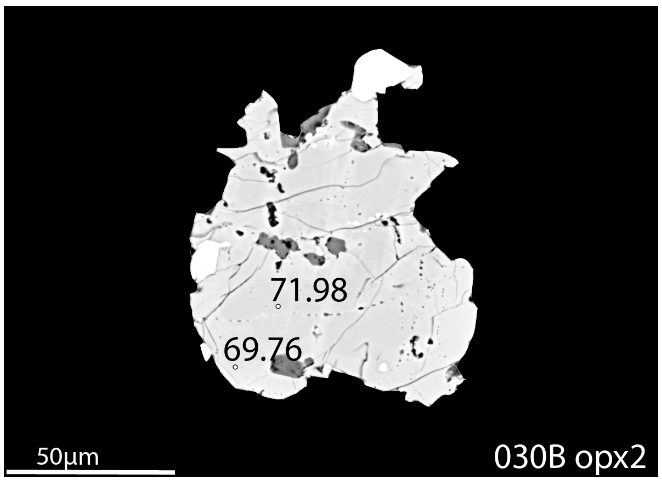
71.98
69.76
50µm
030B opx2

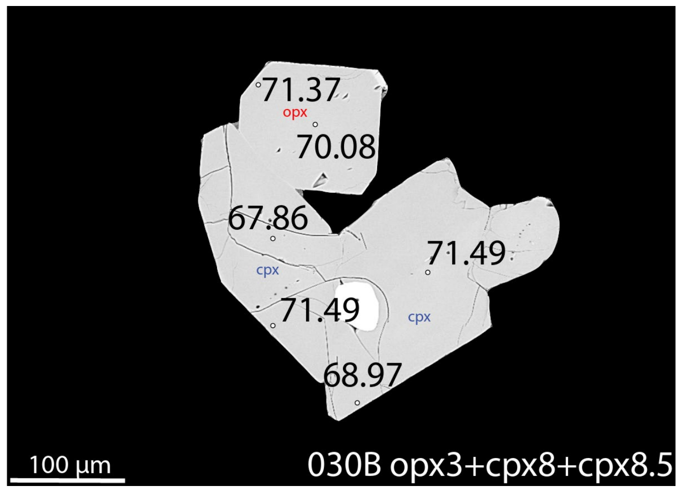
71.37
opx
70.08
67.86
71.49
cpx
71.49
cpx
68.97
100 µm
030B opx3+cpx8+cpx8.5

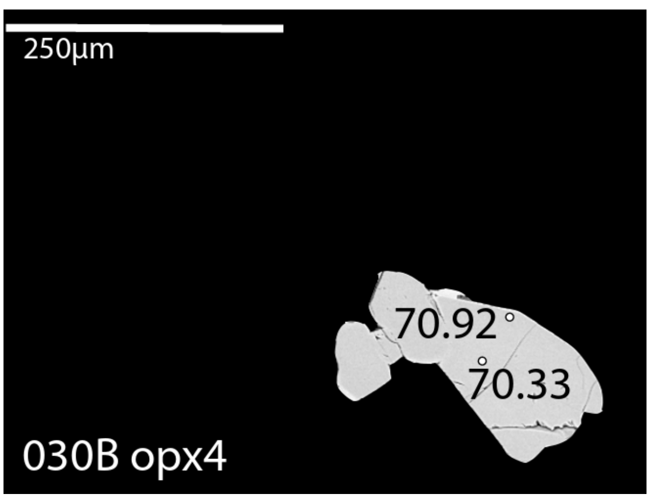
250µm
70.92
70.33
030B opx4

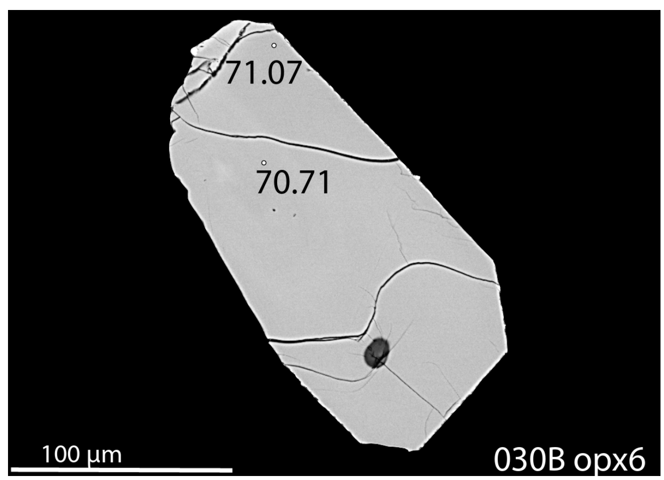
71.07
70.71
100 µm
030B opx6

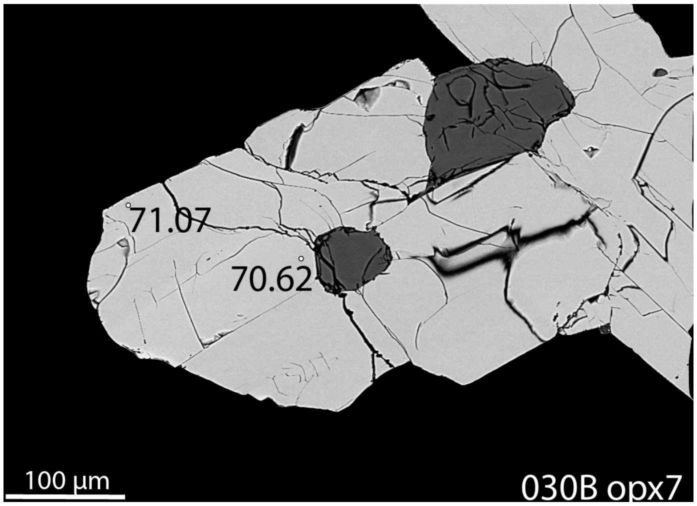
71.07
70.62
100 µm
030B opx7

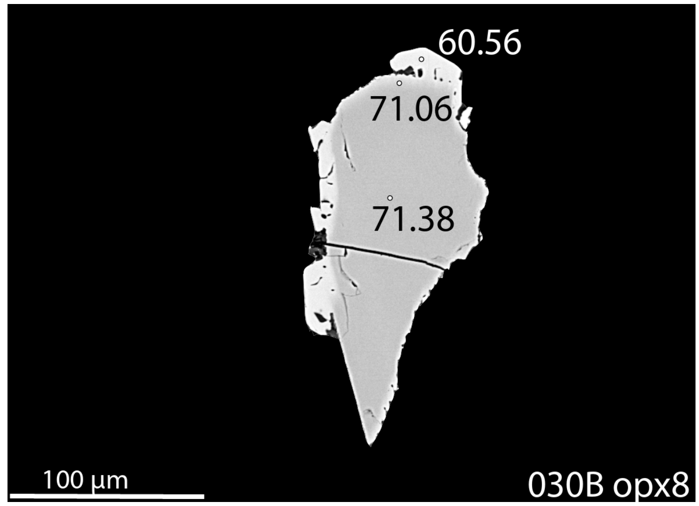
60.56
71.06
71.38
100 µm
030B opx8

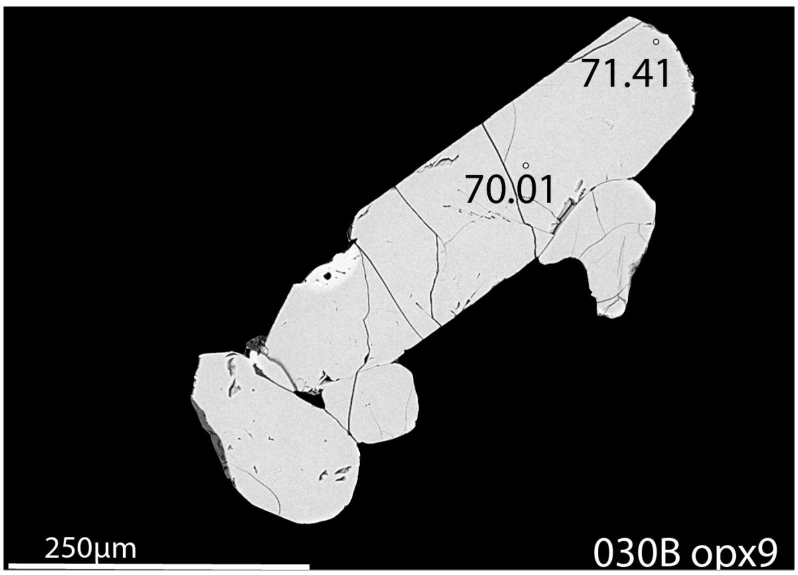
71.41
70.01
250µm
030B opx9

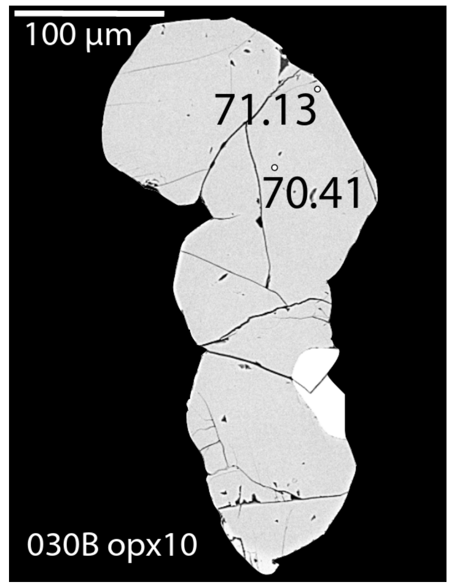
100 µm
71.13
70.41
030B opx10

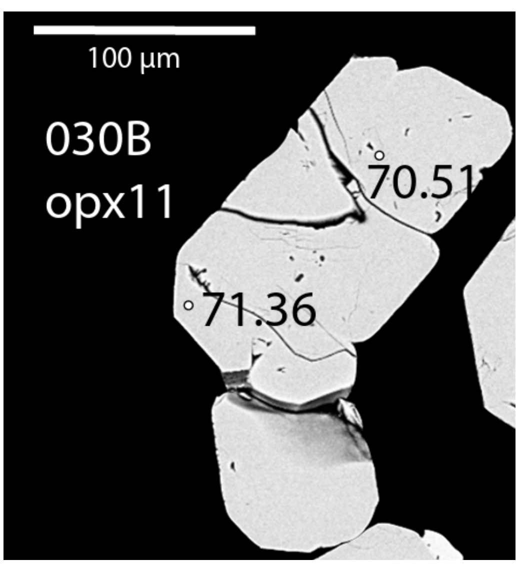
100 µm
030B
opx11
70.51
71.36

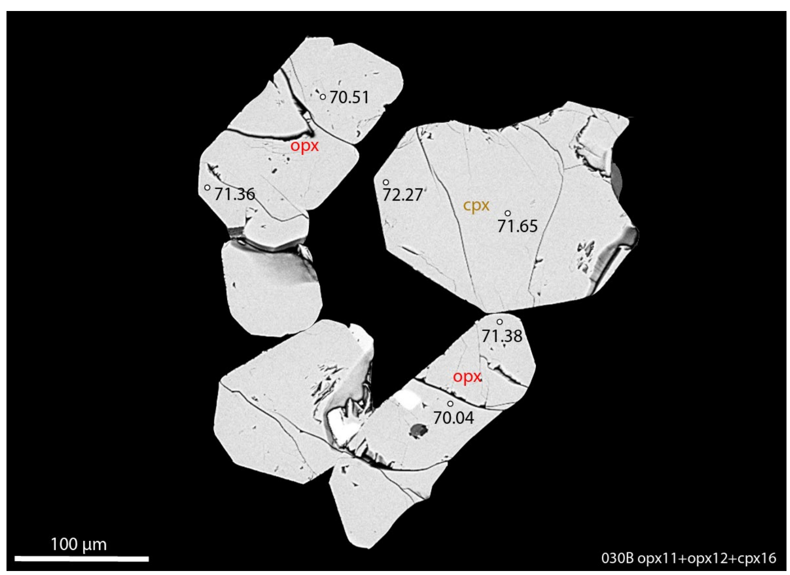
70.51
opx
71.36
72.27
cpx
71.65
71.38
opx
70.04
100 µm
030B opx11+opx12+cpx16

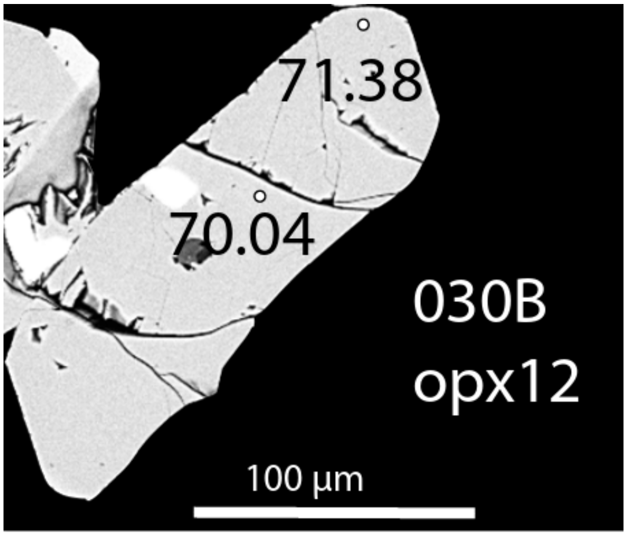
71.38
70.04
030B
opx12
100 µm

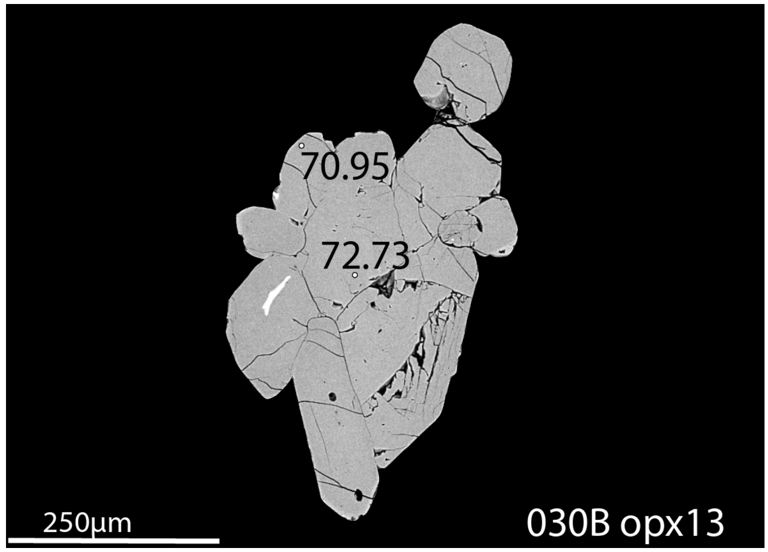
70.95
72.73
250µm
030B opx13

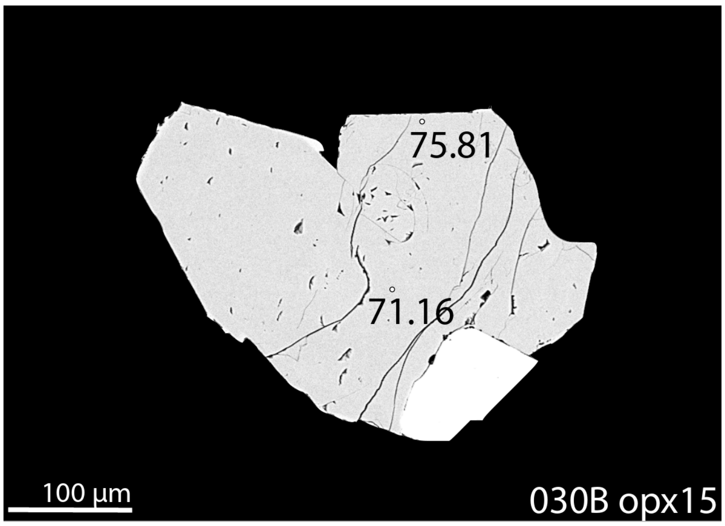
75.81
71.16
100 µm
030B opx15

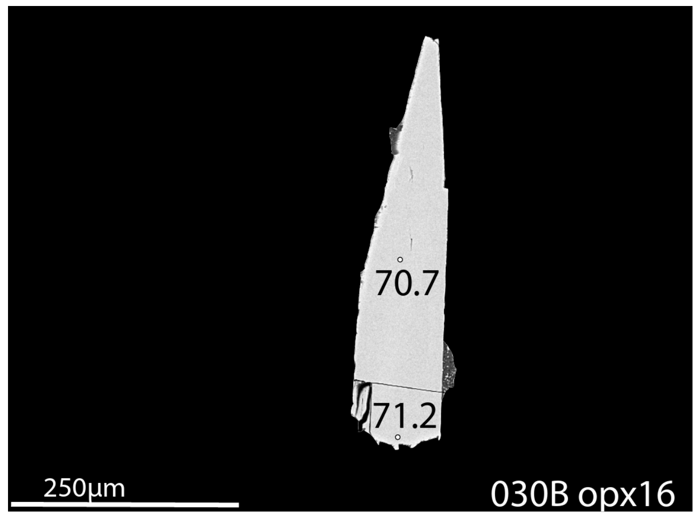
70.7
71.2
250µm
030B opx16

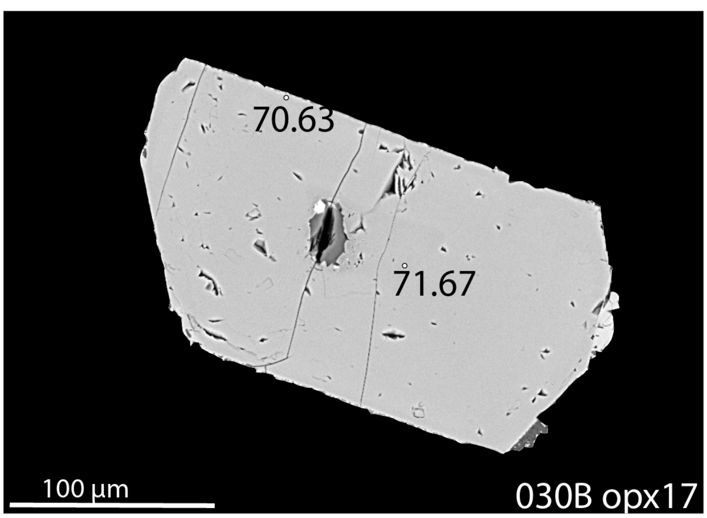
70.63
71.67
100 µm
030B opx17

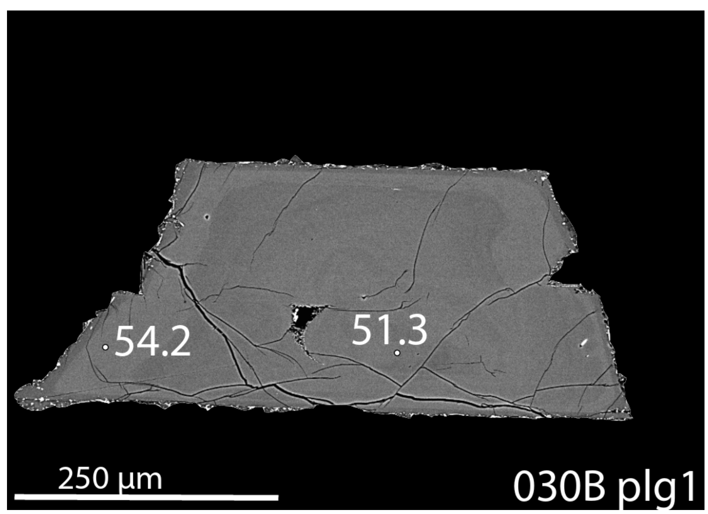
54.2
51.3
250 µm
030B plg1

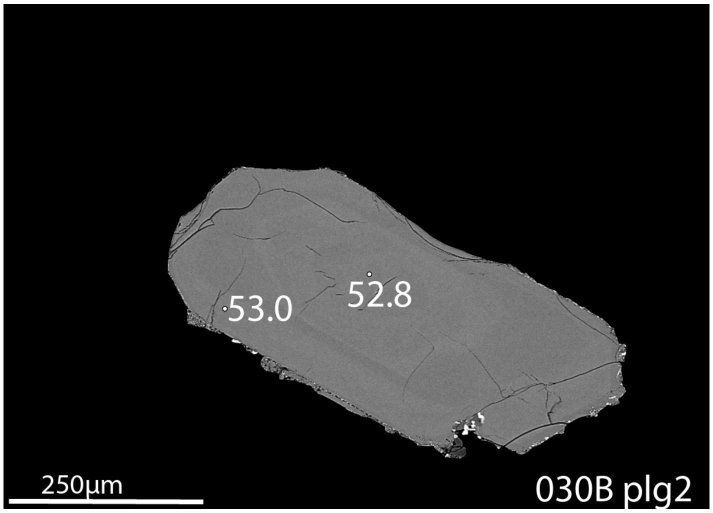
53.0
52.8
250μm
030B plg2

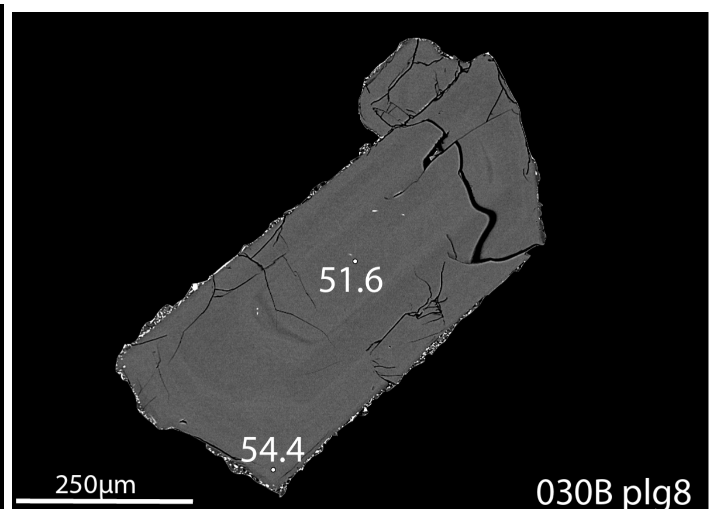
51.6
54.4
250μm
030B plg8

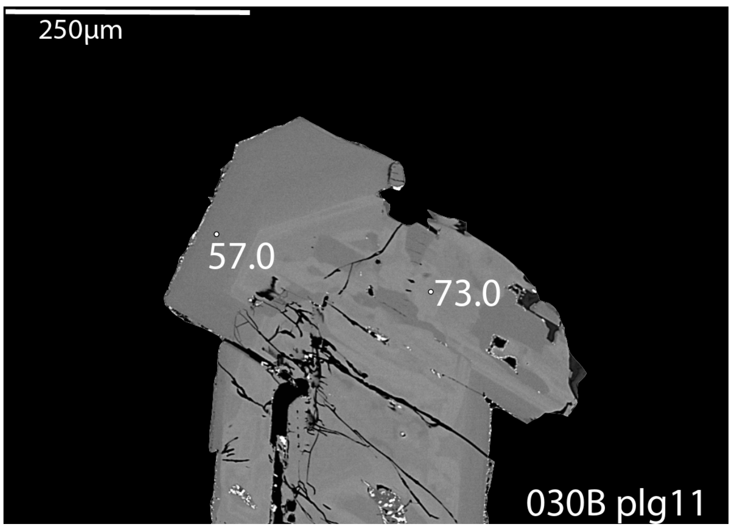
250μm
57.0
73.0
030B plg11

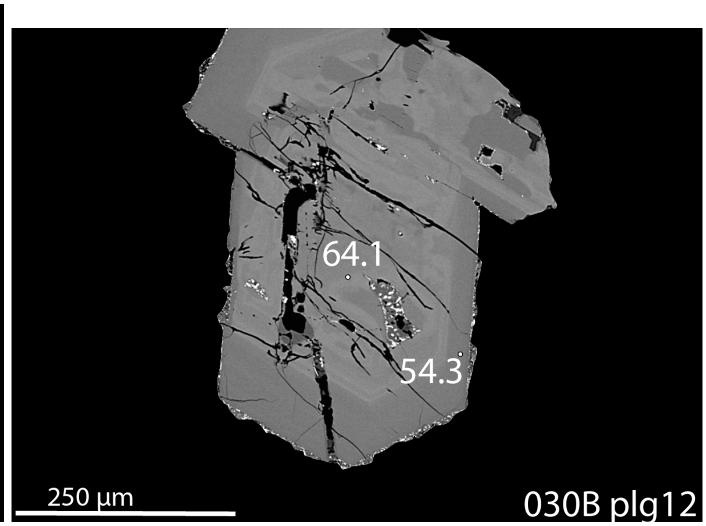
64.1
54.3
250 μm
030B plg12

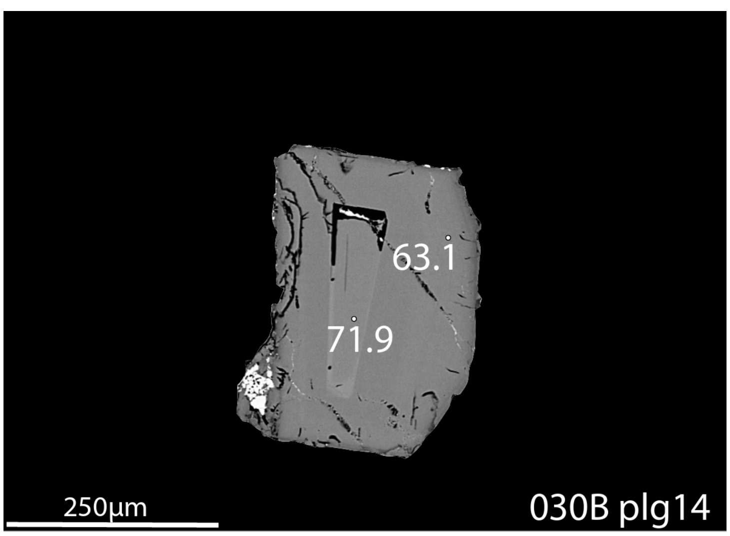
63.1
71.9
250μm
030B plg14

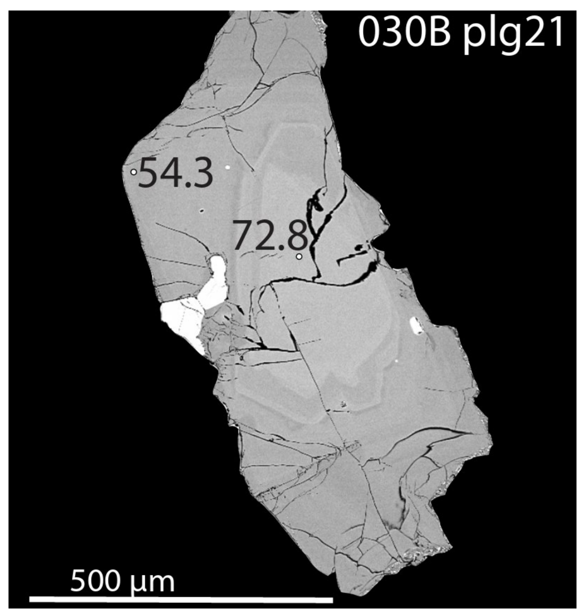
030B plg21
54.3
72.8
500 μm

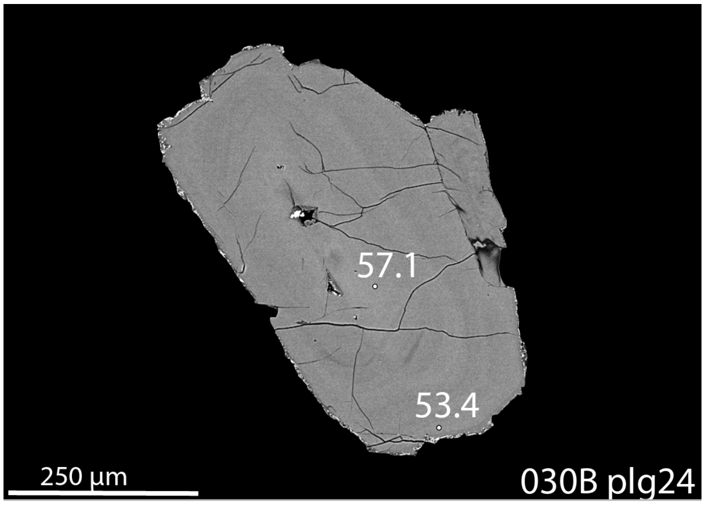
57.1
53.4
250 µm
030B plg24

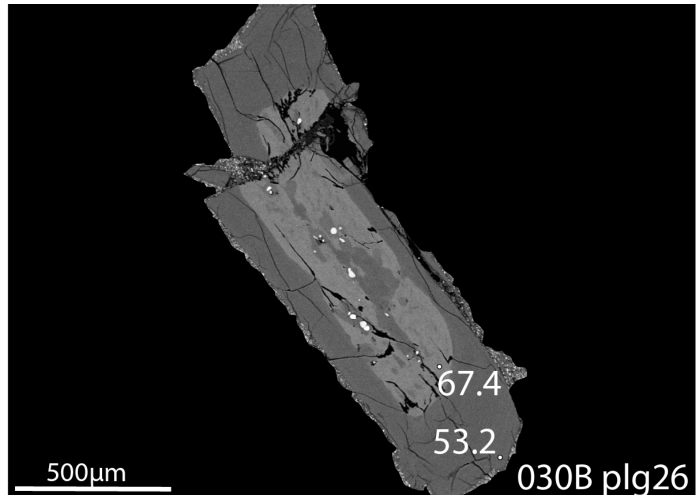
67.4
53.2
500µm
030B plg26

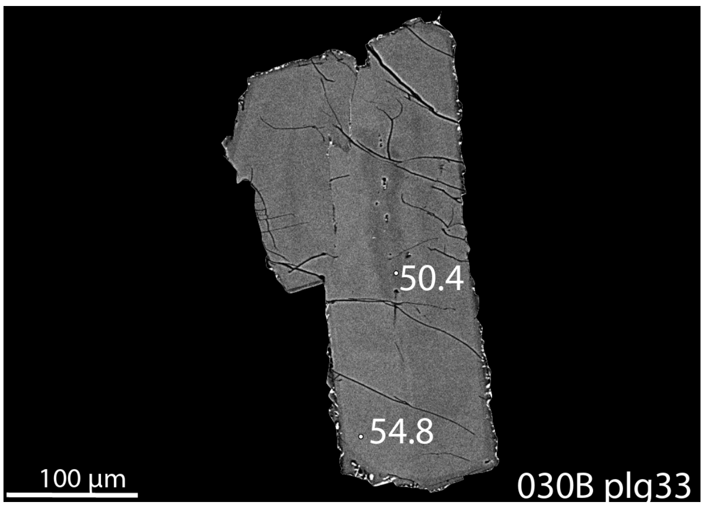
50.4
54.8
100 µm
030B plg33

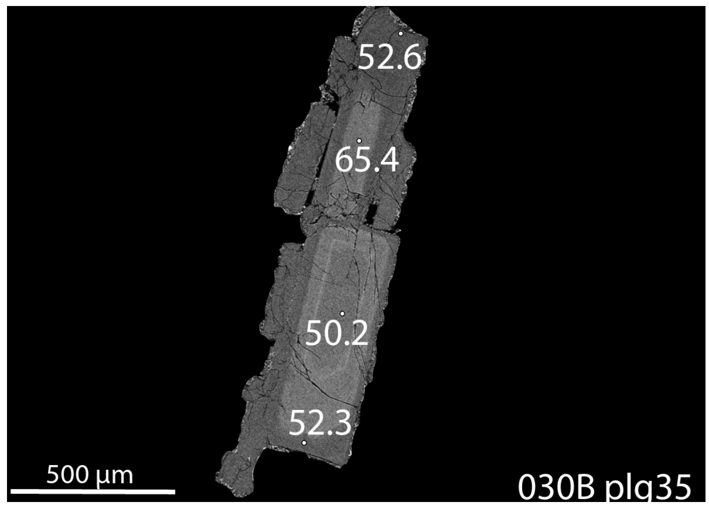
52.6
65.4
50.2
52.3
500 µm
030B plg35

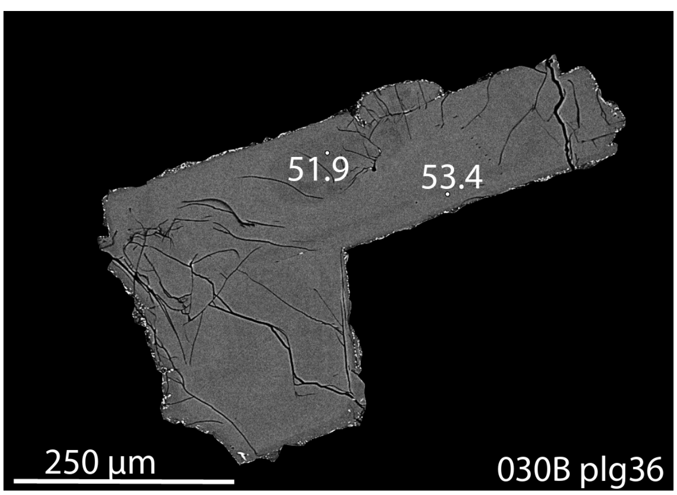
51.9
53.4
250 µm
030B plg36

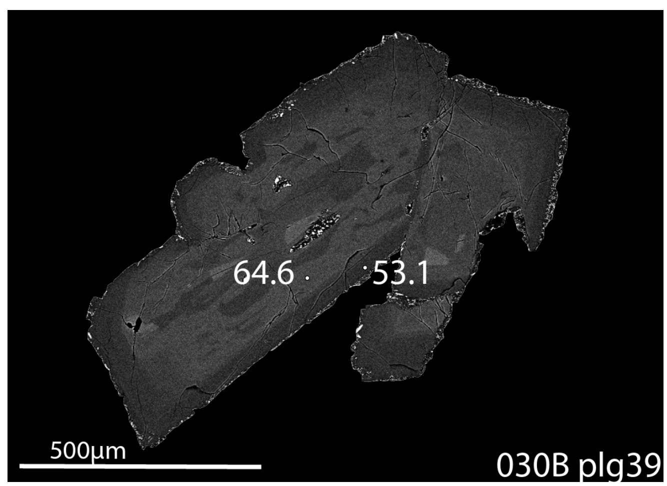
64.6
53.1
500µm
030B plg39

iii. alc- olivine bearing enclave (Type I)

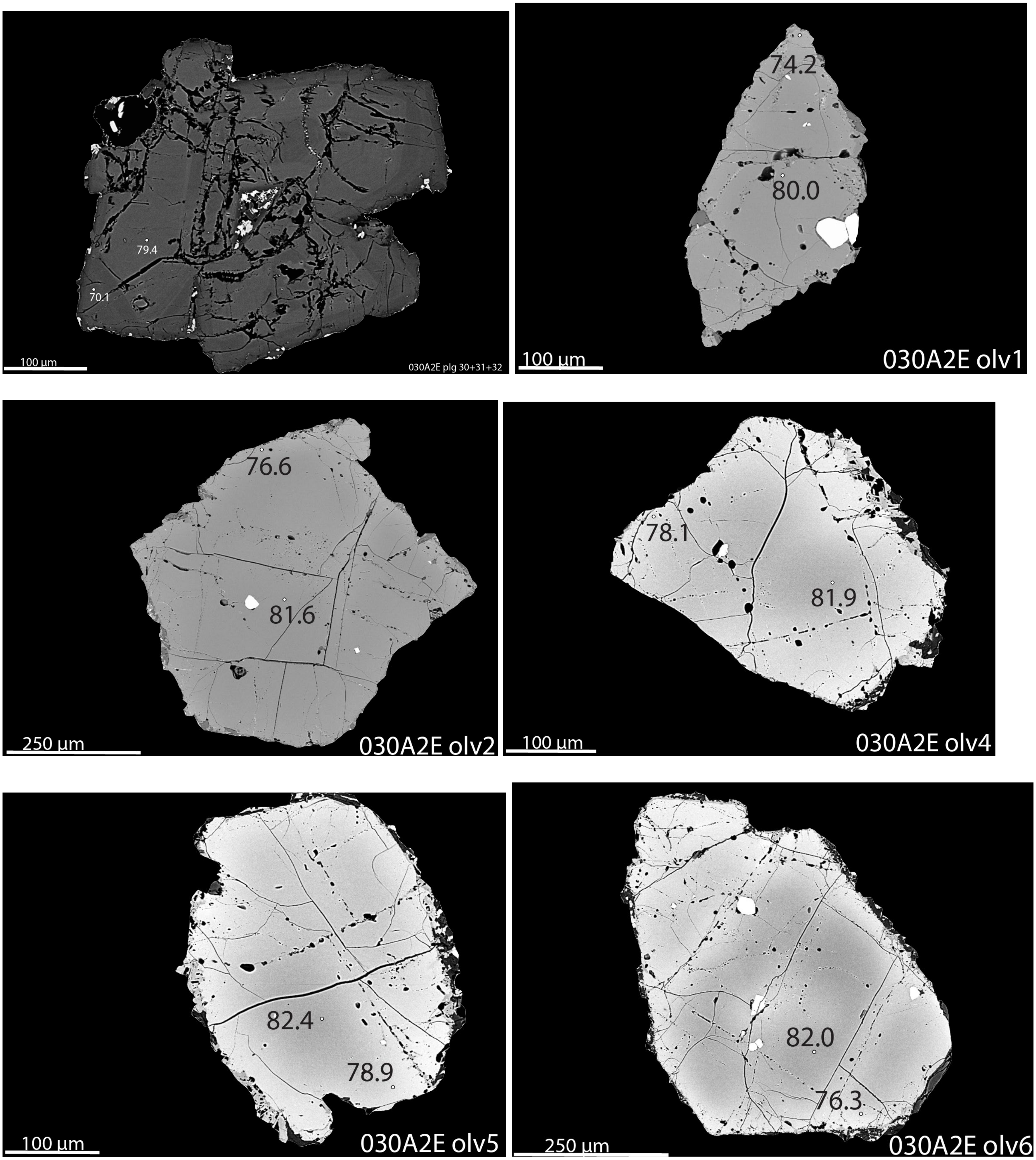

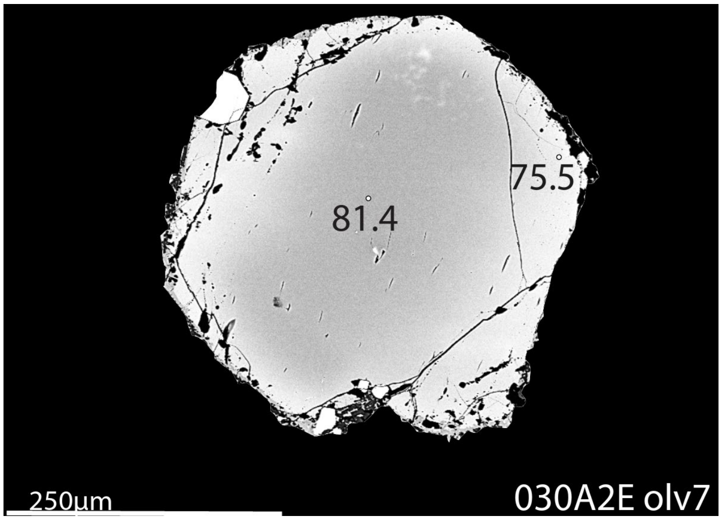
75.5
81.4
250µm
030A2E olv7

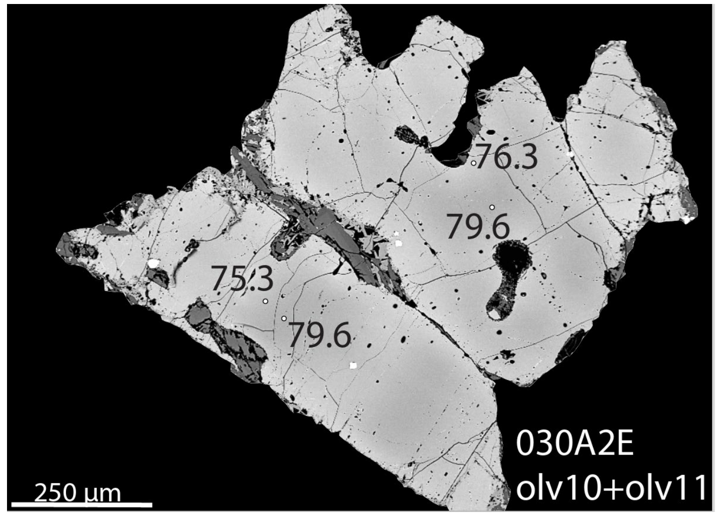
76.3
79.6
75.3
79.6
030A2E
olv10+olv11
250 µm

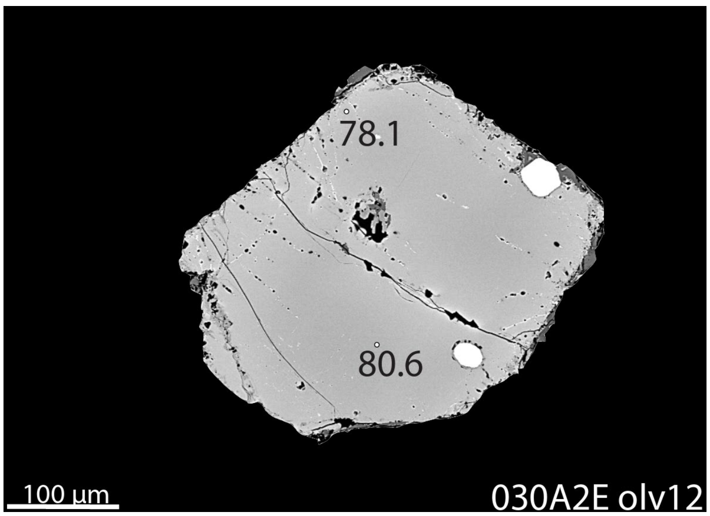
78.1
80.6
100 µm
030A2E olv12

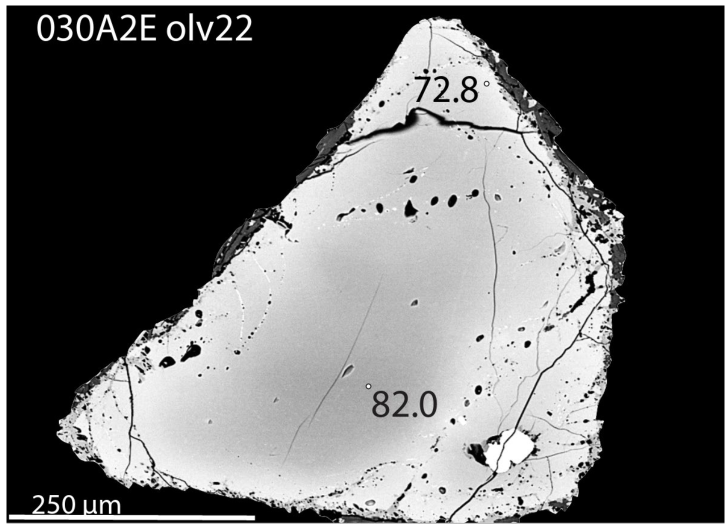
030A2E olv22
72.8
82.0
250 µm

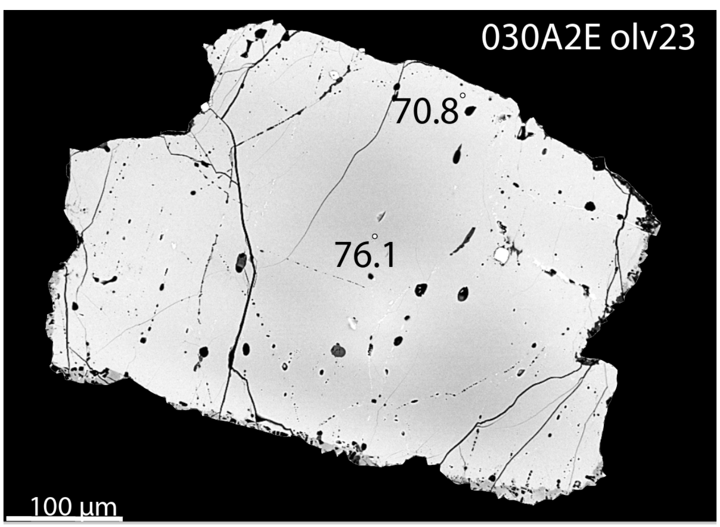
030A2E olv23
70.8
76.1
100 µm

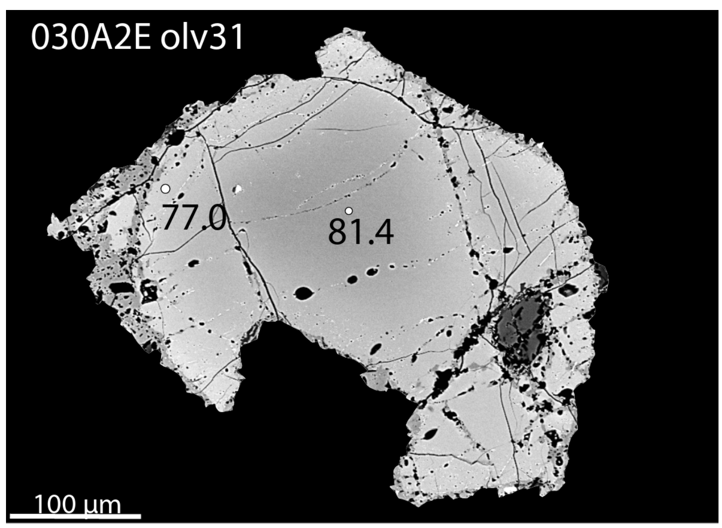
030A2E olv31
77.0
81.4
100 µm

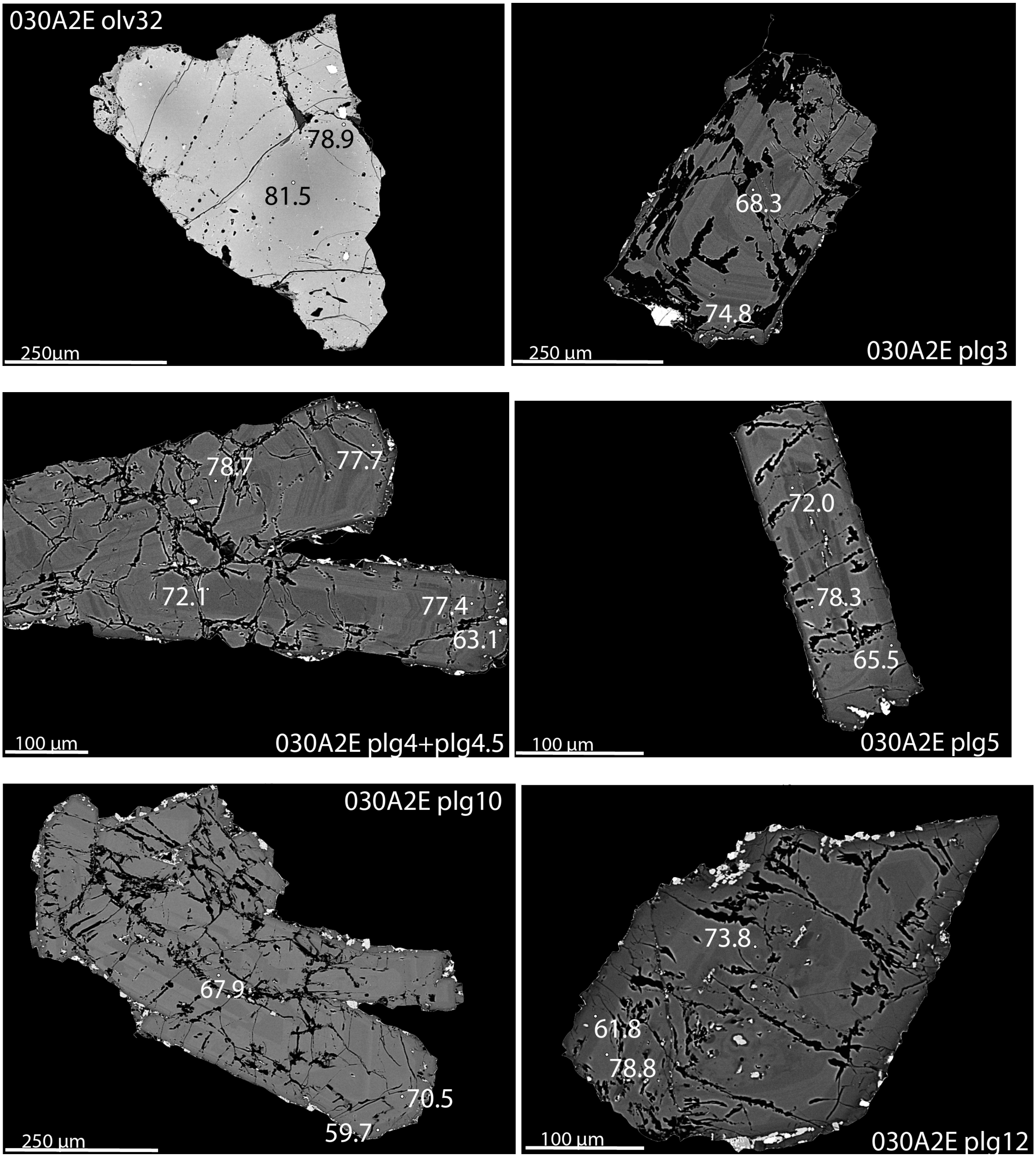
030A2E olv32
78.9
81.5
250µm
68.3
74.8
250 µm
030A2E plg3
78.7
77.7
72.1
77.4
63.1
100 µm
030A2E plg4+plg4.5
72.0
78.3
65.5
100 µm
030A2E plg5
030A2E plg10
67.9
70.5
59.7
250 µm
73.8
61.8
78.8
100 µm
030A2E plg12

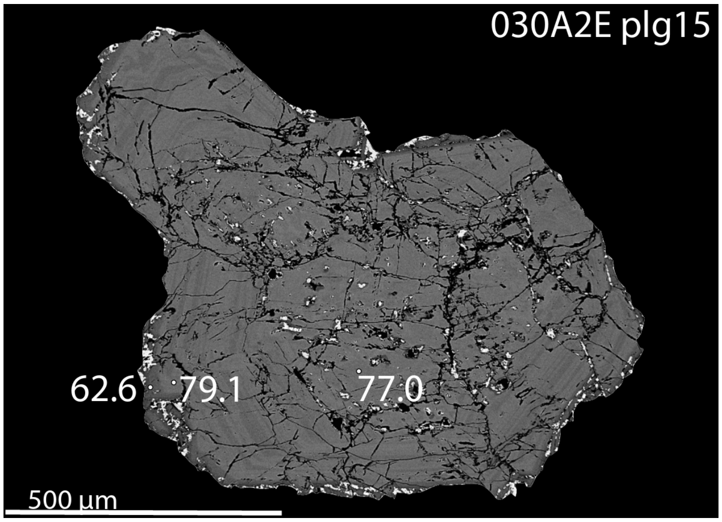
030A2E plg15
62.6
79.1
77.0
500 µm

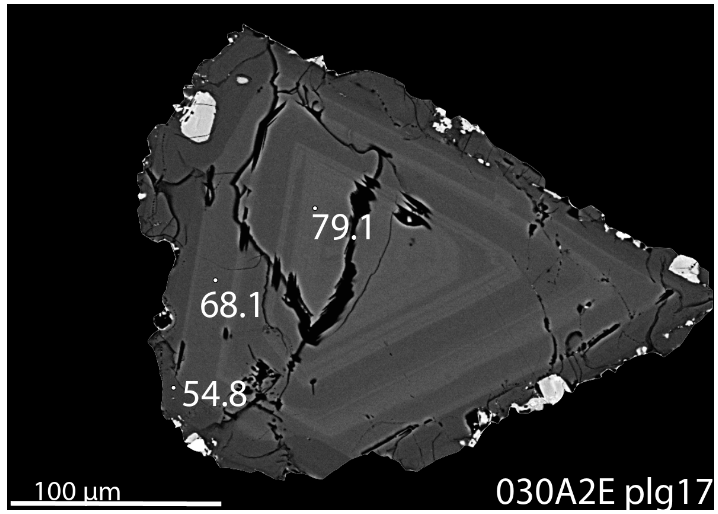
79.1
68.1
54.8
100 µm
030A2E plg17

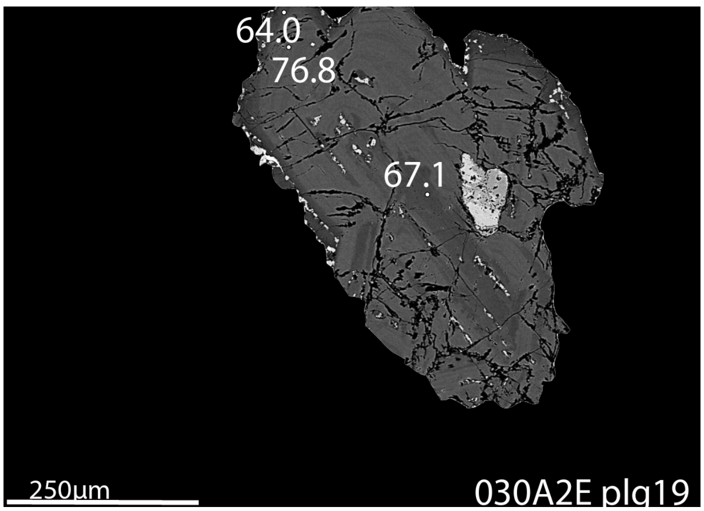
64.0
76.8
67.1
250µm
030A2E plg19

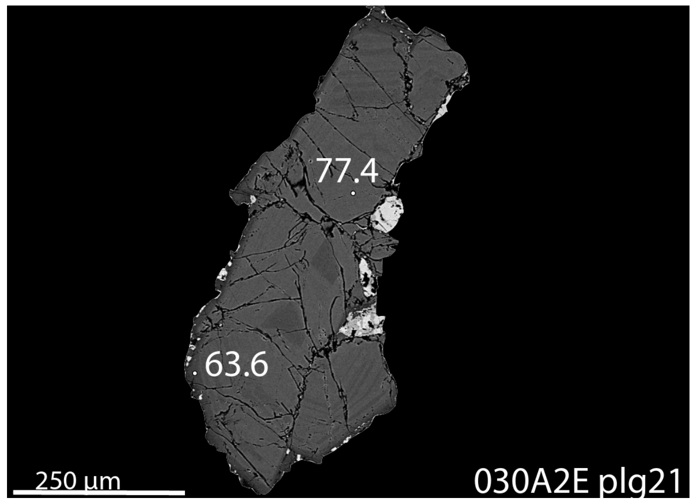
77.4
63.6
250 µm
030A2E plg21

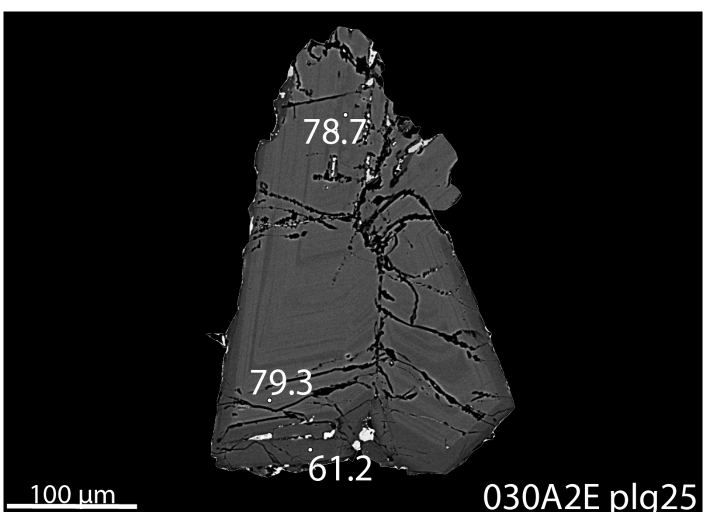
78.7
79.3
61.2
100 µm
030A2E plg25

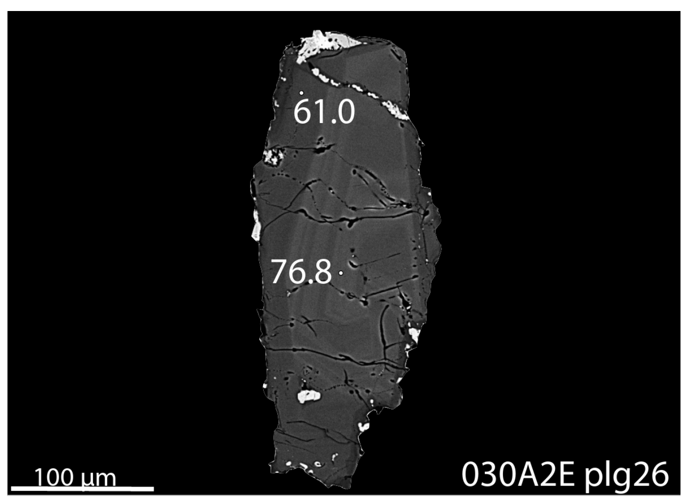
61.0
76.8
100 µm
030A2E plg26

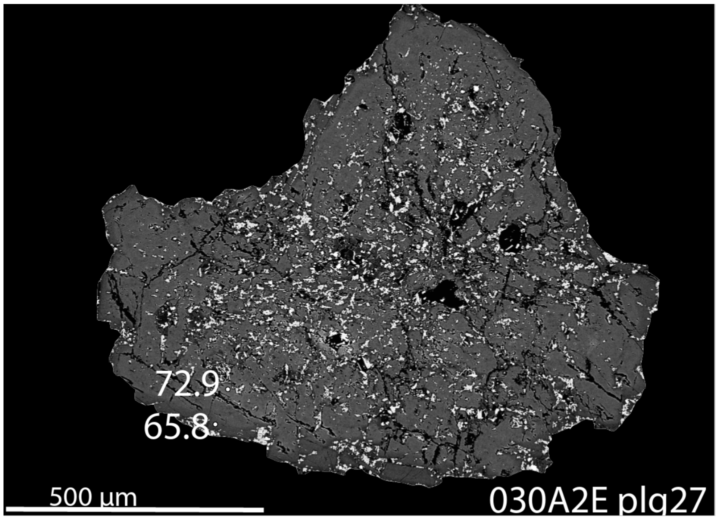
72.9
65.8
500 µm
030A2E plg27

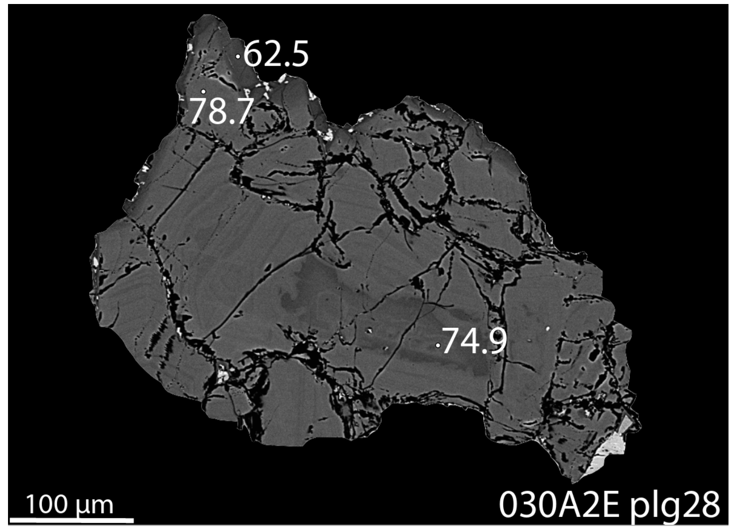
62.5
78.7
74.9
100 µm
030A2E plg28

iv. alc- orthopyroxene bearing enclave (Type II)